

الجمهورية الجزائرية الديمقراطية الشعبية

PEOPLE'S DEMOCRATIC REPUBLIC OF ALGERIA

وزارة التعليم العالي والبحث العلمي

MINISTRY OF HIGHER EDUCATION AND SCIENTIFIC RESEARCH

جامعة أبي بكر بلقايد - تلمسان -

University Aboubakr Belkaïd – Tlemcen –

Faculty of Sciences of Nature and Life, Earth Sciences and Universe



THESIS

Presented for obtaining the DOCTORAL degree in Sciences

In: Geology

Speciality: Geodynamics of sedimentary basins

By : MENZOUL Bouabdellah

Topic

Sedimentology and ichnology of the Numidian Formation in the Ouarsenis Mountains, northwestern Algeria

Publicly defended, on 20/05/2023, before the jury composed of:

Mr. BOUANANI Abderrezak	Professor	University of Tlemcen	Chairman
Mr. ADACI Mohamed	Lecturer	University of Tlemcen	Supervisor 1
Mr. UCHMAN Alfred	Professor	Jagiellonian University	Supervisor 2
Mr. BENYOUCEF Madani	Professor	University of Mascara	Examiner
Mr. BENDELLA Mohamed	Professor	University of Oran 2	Examiner
Mr. BENSALAH Mustapha	Professor	University of Tlemcen	Guest of honor

Academic year: 2022–2023

Abstract

The Numidian Formation in the Ouarsenis Mountains, NW Algeria consists of siliciclastic deposits intercalated with hemipelagic mudstones in the four sections studied, located in the Theniet El Haad and Chlef regions. The latter includes two main informal lithostratigraphic units: (1) the lower unit (mud-dominated); (2) the upper unit (sand-dominated). The lower unit delivers rare agglutinated foraminifers, such as *Glomospira* sp., *Ammodiscus* sp., *Paratrochamminoides* sp., *Haplophragmoides* sp., *Trochamminoides* sp., and *Recurvoides* sp. In contrast, investigations for dinoflagellate cysts from the lower and upper units of the sections studied gave positive results. Both units yielded rich although taxonomically impoverished, dinoflagellate cyst assemblages associated with other aquatic palynomorphs. Biostratigraphic interpretation of the assemblages from the interval studied is difficult and imprecise so far, but it suggests a time span from the late Paleogene to early Miocene.

Eight lithofacies have been distinguished, including, structureless sandstone (F1), normally-graded, medium- to very coarse-grained sandstone (F2), inversely-graded pebbly sandstone to parallel stratified sandstone (F3), medium- to fine-grained sandstone (F4), and mudclast conglomerates (F5), soft-sediment deformed sandstone/siltstone (F6), mudstone with siltstone and sandstone (F7), and varicoloured marly mudstone (F8). These lithofacies yielded three main facies associations, including (1) FA1 sand-rich facies association deposited in the channel-fill setting. It occurs in the upper part of all the studied sections; (2) FA2 mudstone and sandstone alternations facies association, corresponding to channel margin, channel-levee-overbank, crevasse-splays, and lobes. This facies association occurs occasionally in the lower and the upper units of the studied sections; (3) FA3 mud-rich facies association deposited on the basin-floor or slope-apron settings, which were cut by narrow, sparse channels, occurring in the lower unit of all the studied sections except for the Forêt des Cèdres section.

Twenty-two ichnogenera have been determined, with the dominance of post-depositional ichnotaxa (62%), and predepositional ichnotaxa (38%). They commonly occur in fine-grained, thin-bedded sandstones (representing facies F4), mostly in facies associations FA2 and FA3. Ichnological analysis associated with sedimentary data indicate a deep-sea environment with typical trace fossil assemblages attributed to the *Nereites* ichnofacies, including its three main ichnosubfacies, i.e. (1) the *Ophiomorpha rudis* ichnosubfacies recorded within FA1, originated in channel and levee-overbank environments; (2) the *Paleodictyon* ichnosubfacies occurs in facies F4, deposited probably in channel-margin or channel-levee-overbank settings; (3) The *Nereites* ichnosubfacies is recorded in FA2, which were probably deposited in the basin-floor environment, specifically in crevasse splays or small lobes characterized by occasional turbiditic flows associated with pelagic and hemipelagic sedimentation.

The method of provenance analysis in conjunction with data on palaeocurrent orientation is applied here to constrain the source rock of the Numidian Formation sediments. Analysis of the palaeoflow data based on measurements of sole marks does not show a single orientation of the palaeocurrent. However, the major orientation based on orientation of flute casts and frondescant marks is more consistent and ranges from the south-east to the east. 205 zircon grains were separated from two representative samples (KMS-b29 and KRS-b01) to perform U/Pb geochronology and morphological description. CL images of zircon grains and Th/U ratio show abundant grains of magmatic origin and less abundant zircon grains indicating metamorphic origin. Three main groups of zircon ages were characterized: (1) 563–992 Ma indicating the Neoproterozoic; (2) 1007–1527 Ma indicating the Mesoproterozoic; (3) 1684–2470 Ma indicating the Paleoproterozoic, with a few zircon grains indicating the Neoproterozoic and Mesoproterozoic. These zircon ages indicate the Eburnean and the Panafrican orogenies without evidence of the Hercynian and Alpine orogenies. The above-mentioned characteristics of the zircon grains analysed, associated with palaeoflow data, point toward an African origin of the deposits studied.

المخلص

يتكون التكوين النوميدي في جبال وارسينيس ، شمال غرب الجزائر من رواسب فتاتية مقسمة مع أحجار طينية نصف عميقة في المقاطع الأربعة التي تمت دراستها، وتقع في منطقتي ثنية الحد والشلف. يتضمن الأخير وحدتين رئيسيتين للطبقات الصخرية غير الرسمية: (1) الوحدة السفلية (التي يهيمن عليها الطين) ؛ (2) الوحدة العلوية (التي يغلب عليها الرمل). تتوفر الوحدة السفلية على كمية قليلة من المنخربات، مثل *Glomospira sp* و *Ammodiscus sp* و *Paratrochamminoides sp* و *Haplophragmoides sp* و *Trochamminoides sp* و *Recurvoides sp*. في المقابل، أعطت التحقيقات لكيسات الدينوفلاجيلات من الوحدات السفلية والعلوية للأقسام المدروسة نتائج إيجابية. أسفرت كلتا الوحدتين عن تجمعات كيس دينوفلاجيلات غنية على الرغم من أنها فقيرة تصنيفياً مرتبطة بأشكال مائية أخرى. يعتبر تفسير البيوستراتيغرافي للتجمعات من الفترة المدروسة صعباً وغير دقيق حتى الآن، لكنه يشير إلى فترة زمنية من أواخر العصر الباليوجيني إلى أوائل العصر الميوسيني.

تم تمييز ثمانية سحنات حجرية، بما في ذلك ، الحجر الرملي غير المنظم (F1)، الحجر الرملي متوسط الحبيبات الخشنة جداً (F2)، الحجر الرملي المرصوف بالحصى المتدرج عكسياً إلى الحجر الرملي الطبقي المتوازي (F3)، الحجر الرملي متوسط إلى ناعم الحبيبات (F4)، وتكتلات الطين (F5)، والحجر الرملي / الحجر الطيني الناعم (F6)، والحجر الطيني مع الحجر الطيني والحجر الرملي (F7)، والحجر الطيني الكلسي متعدد الألوان (F8). أسفرت دراسة السحنات عن ثلاث روابط رئيسية للسحنات، بما في ذلك (1) اتحاد السُحف الغنية بالرمل FA1 المودعة في إعداد ملء القناة. يحدث في الجزء العلوي من جميع الأقسام المدروسة؛ (2) اتحاد سحنات الأحجار الطينية والحجر الرملي FA2، المقابلة لهامش القناة، وسد القناة، والصفة العلوية، والشقوق المتصدعة، والفصوص. يحدث هذا الارتباط للوجه من حين لآخر في الوحدات السفلية والعلوية للأقسام المدروسة؛ (3) ترسب رابطة السحنات الغنية بالطين FA3 على إعدادات أرضية الحوض أو المنحدرات، والتي تم قطعها بواسطة قنوات ضيقة ومتفرقة، والتي تحدث في الوحدة السفلية لجميع الأقسام المدروسة باستثناء قسم غابة الارز.

تم تحديد اثنين وعشرين من الكائنات الحية الدقيقة، مع هيمنة *ichnotaxa* ما بعد الترسيب (62%)، و *ichnotaxa* قبل الترسيب (38%). وجدت عادةً في الأحجار الرملية ذات الحبيبات الدقيقة والرقيقة (F4)، ومعظمها في تجمع السحنات FA2 و FA3. يشير التحليل الأيكنولوجي المرتبط بالبيانات الرسوبية إلى بيئة أعماق البحار مع مجموعات أحفورية نموذجية تُعزى إلى النيريتس، بما في ذلك اصنافه الثلاثة المتمثلة في: (1) *Ophiomorpha rudis ichnosubfacies* المتواجدة في FA1، والتي نشأت في بيئات القناة والسدود؛ (2) تحدث الأسماك الفرعية *Paleodictyon ichnosubfacies* في الوجه F4، والتي ربما ترسبت في إعدادات هامش القناة أو القناة - السدود - فوق الصفة؛ (3) سُجِّلَت *Nereites ichnosubfacies* في FA2 ، والتي من المحتمل أن تكون قد ترسبت في بيئة قاع الحوض، وتحديدًا في شقوق الصدع أو الفصوص الصغيرة التي تتميز بتدفقات عكر عرضية مرتبطة بالترسيب السطحي.

تم تطبيق طريقة تحليل المصدر جنباً إلى جنب مع البيانات حول اتجاه التيار القديم لتقييد صخور المصدر لرواسب التكوين النوميدي. لا يُظهر تحليل بيانات اتجاه التيار القديم بناءً على قياسات الهياكل الرسوبية اتجاهًا واحدًا للتيار القديم. ومع ذلك ، فإن الاتجاه الرئيسي القائم على اتجاه الفلوت وعلامات السعف أكثر اتساقًا ويتراوح من الجنوب الشرقي إلى الشرق. تم فصل 205 حبة من الزركون من عينتين تمثيليتين (KMS-b29 و KRS-b01) لأداء التحليل الكيميائي U/Pb والوصف المورفولوجي. تُظهر صور CL لحبوب الزركون ونسبة Th/U حبات وفيرة من أصل صهاري وحبوب زركون أقل وفرة تشير إلى أصل متحولة. تميزت ثلاث مجموعات رئيسية من أعمار الزركون: (1) 992-563 مليون مما يشير إلى الحياة الحديثة؛ (2) 1527-1007 مليون سنة تشير إلى عصر الميزوبروتروزويك؛ (3) 2470 - 1684 مليونًا يشير إلى العصر القديم، مع وجود عدد قليل من حبيبات الزركون التي تشير إلى العصر الحديث والوسطى. تشير عصور الزركون هذه إلى أجناس إبورن وبانافريكان بدون دليل على تكوينات الهرسينيان وجبال الألب. تشير الخصائص المذكورة أعلاه لحبوب الزركون التي تم تحليلها، والمرتبطة ببيانات اتجاه التيار القديم، إلى أصل أفريقي للرواسب المدروسة.

Résumé

La Formation Numidienne dans les Monts de l'Ouarsenis, au Nord-Ouest de l'Algérie, est constituée de dépôts siliciclastiques intercalés avec des argilites hémipélagiques dans les quatre coupes étudiées, situées dans les régions de Theniet El Haad et de Chlef. Ces derniers comprennent deux principales unités lithostratigraphiques informelles : (1) l'unité inférieure (dominée par les argiles) ; (2) l'unité supérieure (dominée par les grès). L'unité inférieure a livré de rares foraminifères agglutinés, tels que *Glomospira* sp., *Ammodiscus* sp., *Paratrochamminoides* sp., *Haplophragmoides* sp., *Trochamminoides* sp., et *Recurvoides* sp.. En revanche, les recherches de kystes de dinoflagellés dans les unités inférieure et supérieure des coupes étudiées ont donné des résultats positifs manifesté par des assemblages riches, bien que taxonomiquement appauvris, associés à d'autres palynomorphes aquatiques. L'interprétation biostratigraphique de ces assemblages est difficile et imprécise jusqu'à présent, mais elle suggère une période allant de la fin du Paléogène au début du Miocène.

Huit lithofaciès ont été distingués, dont un grès massif (F1), un grès à grains moyens à très grossiers, à granoclassement normal (F2), un grès caillouteux à granoclassement négatif à un grès à stratification parallèle (F3), grès à grains moyens à fins (F4), et conglomérats à mudclastes (F5), grès/siltite déformé (F6), Alternance d'argilite avec siltite et grès (F7), et argiles marneux versicolores (F8). Ces lithofaciès ont donné lieu à trois principales associations de faciès, dont (1) l'association de faciès riche en sable FA1 déposée en remplissage de chenaux. Il est présent dans la partie supérieure de toutes les coupes étudiées ; (2) l'association de faciès FA2, alternances d'argile silteuse et de grès, correspondant au dépôt de la bordure de chenal, au débordement du chenal, aux crevasses-splay et/ou lobes. Cette association de faciès se rencontre occasionnellement dans les unités inférieures et supérieures des coupes étudiées ; (3) l'association de faciès FA3, riche en boue déposée sur le fond du bassin ou sur le talus continental, qui ont été coupées par des chenaux étroits et épars, présente dans l'unité inférieure de toutes les coupes étudiées, à l'exception de la coupe de la Forêt des Cèdres.

Vingt-deux ichnogenres ont été déterminés, avec une dominance des ichnotaxons post-dépositionnels (62%), et des ichnotaxons pré-dépositionnels (38%). Ils sont généralement présents dans les grès à grains fins et à lits minces (représentant le faciès F4), principalement dans les associations de faciès FA2 et FA3. Les analyses ichnologiques associées aux données sédimentologiques indiquent un environnement de mer profonde avec des assemblages typiques de traces fossiles attribués à l'ichnofaciès *Nereites*, y compris ses trois principaux ichno-sous-faciès, notamment : (1) l'ichno-sous-faciès *Ophiomorpha rudis*, enregistré dans le faciès F1, provenant d'environnements de chenaux et de levées; (2) l'ichno-sous-faciès *Paleodictyon* enregistré dans le faciès F4, déposé dans des environnements de marges de chenaux ou de levées; (3) L'ichno-sous-faciès *Nereites* est enregistré dans FA2, qui a probablement été déposé dans l'environnement du fond de bassin, spécifiquement dans des crevasses-splay ou de petites lobes caractérisés par des flux turbiditiques occasionnels associés à une sédimentation pélagique et hémipélagique.

La méthode d'analyse de provenance avec les données du paléocourant est appliquée ici pour contraindre la roche mère des sédiments de la formation Numidienne. L'analyse des données du paléocourant basée sur les mesures prises sur des structures sédimentaires de base de banc ne montre pas une orientation unique du paléocourant. Cependant, l'orientation principale basée sur les flutes casts et les frondescant marks est plus cohérente et va du Sud-est à l'Est. 205 grains de zircon ont été séparés de deux échantillons représentatifs (KMS-b29 et KRS-b01) pour effectuer des analyses géochronologiques U/Pb et une description morphologique. Les images CL des grains de zircon et le rapport Th/U montrent des grains abondants d'origine magmatique et des grains de zircon moins abondants indiquant une origine métamorphique. Trois groupes principaux d'âges de zircon ont été caractérisés : (1) 563-992 Ma indiquant le Néoprotérozoïque ; (2) 1007-1527 Ma indiquant le Mésoprotérozoïque ; (3) 1684-2470 Ma indiquant le Paléoprotérozoïque, avec quelques grains de zircon indiquant le Néoarchéen et le Mésoarchéen. Ces âges de zircon indiquent les orogénèses éburnéenne et panafricaine sans preuve sur les orogénèses hercynienne et alpine. Les caractéristiques susmentionnées des grains de zircon analysés, associées aux données de paléocourant, pointent vers une origine africaine des dépôts étudiés.

LIST OF CONTENTS

1. INTRODUCTION	
1.1. MOTIVATION AND OBJECTIVES	2
1.2. PRESENTATION OF THE NUMIDIAN FORMATION	2
1.3. GEOLOGICAL SETTING	3
1.4. OVERVIEW ON THE STUDY AREA	6
1.5. PREVIOUS RESEARCH	9
1.5.1. The recognition and stratigraphy of the Numidian Formation	9
1.5.2. Provenance of the Numidian Formation material	10
1.6. MATERIAL AND METHODS	11
1.6.1. Field work	11
1.6.2. Laboratory analysis	11
1.7. ORGANIZATION OF THE THESIS	13
 2. LITHOSTRATIGRAPHY & REMARKS ON BIOSTRATIGRAPHY	
2.1. INTRODUCTION	15
2.2. DESCRIPTION OF THE STUDIED SECTIONS	16
2.2.1. KEF RZAMA SECTION	16
2.2.1.1. The lower unit	16
2.2.1.2. The upper unit	17
2.2.2. AIN GHANEM SECTION	19
2.2.2.1. The lower unit	19
2.2.2.2. The upper unit	19
2.2.3. KEF MAIZ SECTION	21
2.2.3.1. The lower unit	21
2.2.3.2. The upper unit	21
2.2.4. FORÊT DES CÈDRES SECTION	23
2.3. PARTIAL CONCLUSIONS	25
 3. SEDIMENTOLOGY	
3.1. INTRODUCTION	27
3.2. LITHOFACIES	27
3.2.1. Structureless sandstone (F1)	27
3.2.2. Normally-graded, medium- to very coarse-grained sandstone (F2)	30
3.2.3. Inversely-graded pebbly sandstone to parallel stratified sandstone (F3)	33

LIST OF CONTENTS

3.2.4. Medium- to fine-grained sandstone (F4)	34
3.2.5. Conglomerates rich in mudstone clasts (F5)	36
3.2.6. Strongly deformed sand/siltstones (F6)	36
3.2.7. Mudstones with intercalated sand/silt/mudstones (F7)	37
3.2.8. Marly mudstones (F8)	38
3.3. DESCRIPTION OF THE STUDIED SECTIONS	44
3.3.1. Forêt des Cèdres section	44
3.3.2. Kef Maiz section	44
3.3.3. Kef Rzama section	44
3.3.4. Ain Ghanem section	45
3.4. Facies associations	51
3.4.1. Sand-rich channel-fills (FA1)	51
3.4.2. Mudstone and sandstone alternations from channel margins, channel/ levee/ overbank systems, and crevasse-splays (FA2)	51
3.4.3. Basin floor mudstones (FA3)	52
3.5. PARTIAL CONCLUSIONS	54
4. ICHNOLOGY & PALAEOENVIRONMENT	
4.1. INTRODUCTION	56
4.2. SYSTEMATIC DESCRIPTION OF TRACE FOSSILS	56
4.2.1. Circular and elliptical structures	56
4.2.2. Spiral structures	57
4.2.3. Simple and branched structures	57
4.2.4. Winding and meandering structures	68
4.2.5. Branched winding and meandering structures	74
4.2.6. Spirals and networks	76
4.2.7. Spreite structures	77
4.3. DISTRIBUTION OF TRACE FOSSILS	81
4.4. DISCUSSION	83
4.4.1. ICHNOFACIES AND DEPOSITIONAL SYSTEM	83
4.4.2. COMPARISONS	89
4.5. PARTIAL CONCLUSIONS	90
5. SEDIMENT PROVENANCE ANALYSIS	
5.1. INTRODUCTION	93

LIST OF CONTENTS

5.2. METHODS	93
5.3. SAMPLING LOCALITIES AND DESCRIPTION OF SAMPLES	95
5.4. RESULTS	97
5.4.1. PALAEOCURRENT DATA	97
5.4.1.1. INTERPRETATION	98
5.4.2. ZIRCON DATA	98
5.4.2.1. ZIRCON TEXTURES	98
5.4.2.2. U-Pb ZIRCON AGES	99
5.4.3. DISCUSSION	103
5.5. PARTIAL CONCLUSIONS	104
6. GENERAL CONCLUSIONS	107
7. REFERENCES	111

LIST OF FIGURES

- Fig. 1.** (A) Location of the study area with indication of the principal Alpine domains in the western Mediterranean (after Durand-Delga, 1969, modified); (B) Location of the main Numidian Formation outcrops in the Mediterranean (Hoyer, 1989) **3**
- Fig. 2.** Palaeogeographic reconstruction from the Paleocene to the late Burdigalian with simplified cross-section of the Maghrebian Basin. (A) Paleogene (60–55 Ma); (B) Late Oligocene–Early Miocene (25–21 Ma); (C) Late Burdigalian–Langhian (17–14 Ma) (Leprêtre et al., 2018, modified). **5**
- Fig. 3.** Chronostratigraphy of the main Numidian successions in the Mediterranean (Guerrera, 2012, modified) **6**
- Fig. 4.** (A) Location of the Ouarsenis Mountains; (B) Map showing the location of the Ouarsenis Mountains (modified from Benhamou, 1996 after Perrodon, 1957) **7**
- Fig. 5.** Geological map showing the main studied sections (interpretative Geological Map of Algeria 1: 200 000, N°: NI-31-XX/NI-31-XXI/ NJ-31-II/ NJ-31-III, ANRH, 2008) **8**
- Fig. 6.** Map showing the distribution of the main Numidian outcrops in the Ouarsenis Mountains **15**
- Fig. 7.** Key for the Figures 9, 11, 13, 15 **16**
- Fig. 8.** Panoramic view of the Kef Rzama section showing the lower and upper units **17**
- Fig. 9.** Lithological column of the Kef Rzama section with indication of the numbering of beds and sedimentary structures **18**
- Fig. 10.** Panoramic view of the Ain Ghanem section, showing the lower unit, varicoloured marly mudstone, and the upper unit (sand-dominated) **19**
- Fig. 11.** Lithological column of the Ain Ghanem section with indication of the numbering of beds and sedimentary structures **20**
- Fig. 12.** Panoramic view showing the lower and upper units of the Kef Maiz section **21**
- Fig. 13.** Lithological column of the Kef Maiz section with indication of the numbering of beds and sedimentary structures **22**
- Fig. 14.** Panoramic view of the Forêt des Cèdres section (A) The lower part, (B) Succession of medium-to thick-bedded sandstone in the middle part of the section **23**
- Fig. 15.** Lithological column of the Forêt des Cèdres section with indication of the numbering of beds and sedimentary structures **24**
- Fig. 16.** Photomicrographs of thin section analysis in cross polarized. (A) Subangular to angular quartz grains associated with rare feldspars (F), Muscovite (M), sparite cement (S), Kef Maiz section; (B) Quartz rich thin section including glauconite (G), and zircon

LIST OF FIGURES & TABLES

grains (z), Forêt des Cèdres section; (C) Polycrystalline quartz grains (PQ), Forêt des Cèdres section; (D) Coarse cracked quartz grain (Q) with zircon crystal (Z), Forêt des Cèdres section; (E) Tourmaline crystal (T), Forêt des Cèdres section; (F) Muscovite (M), Forêt des Cèdres section **28**

Fig. 17. Photographs of the main described lithofacies. (A) Massif sandstone bed (F1), Forêt des Cèdres section; (B) Massif sandstone bed (F1), Ain Ghanem section; (C), (F) Conglomerates rich in mudstone clasts (F5), upper unit of Kef Rzama section; (D), (E), (G) Inversely-graded pebbly sandstone to parallel stratified sandstone (F3), upper unit of the Kef Rzama section; (H) Reverse grading in F3, upper unit of Kef Rzama section; (I), (J) Normal grading (F2) from the upper unit of the Ain Ghanem section **29**

Fig. 18. Photographs of some sole marks from the sections studied. (A), (B) Groove casts within F2, Forêt des Cèdres section; (C) Casts of mud ripples within F2, Forêt des Cèdres section; (D) Flute casts associated with flute-loaded within F2, Forêt des Cèdres section; (E) Small-size flute casts within F4, Forêt des Cèdres section **31**

Fig. 19. Photographs of other sole marks from the sections studied. (A), (B) Casts of longitudinal scours (ridge and furrow structures) within F2, upper part of the Ain Ghanem section; (C), (D) Gutter casts within F2, Forêt des Cèdres section; (E), (F), (G), (H) Frondescant mark casts, F2 sandstone, Forêt des Cèdres section **32**

Fig. 20. Photographs of the Curved flute structure; (A), (B) panoramic photographs of the curved flute structure, Forêt des Cèdres section; (C) structure obtained experimentally by Dżułyński (1965) described as asymmetrical flute **33**

Fig. 21. Photographs of soft-sediment deformation structures from the sections studied. (A), (B) Fluid-escape structures (dish structures) within F1, upper unit of the Kef Maiz section; (C), (D) Fluid-escape structures, F2, lower unit of the Ain Ghanem section; (E), (F) Load casts, F1, Forêt des Cèdres section **35**

Fig. 22. Photographs showing some soft-sediment deformation structures with incomplete intervals of Bouma sequences within the studied sections. (A), (B) Deformed bed (F6), the lower unit of the Ain Ghanem section; (C), (D) Ball-and-pillow structures within F6, the Forêt des Cèdres section; (E) Incomplete Bouma sequence (F2), the upper unit of the Kef Maiz section; (F) Incomplete Bouma sequence (F2), the lower unit of the Ain Ghanem section **38**

Fig. 23. Photographs of the lower unit of the studied sections; (A) Varicoloured marly mudstone, F8, lower unit of the Ain Ghanem section; (B) Soft-sediment deformed sandstone, F6, lower unit of the Kef Maiz section **39**

Fig. 24. Lithological column of the Forêt des Cèdres section. Both sections show numbering of beds, trace fossils and sedimentary structures **46**

Fig. 25. Lithological column (part 01) of the Kef Maiz section with indication of the numbering of beds, trace fossils and sedimentary structures **47**

- Fig. 26.** Lithological column (part 02) of the Kef Maiz section with indication of the numbering of beds, trace fossils and sedimentary structures **48**
- Fig. 27.** Lithological column of the Kef Rzama section with indication of the numbering of beds, trace fossils and sedimentary structures **49**
- Fig. 28.** Lithological column of the Ain Ghanem section with indication of the numbering of beds, trace fossils and sedimentary structures **50**
- Fig. 29.** Elliptical, simple and branched structures from the Numidian Formation in the Ouarsenis Mountains, NW Algeria. (A) *Planolites montanus* (*Plm*) and *?Palaeophycus* isp. (*P*), hypichnial full reliefs; (B) *Lockeia* isp. (*Lo*) and *Helminthoidichnites* isp. (*He*), hypichnial full and semi-reliefs, respectively; (C) *Lockeia* isp. (*Lo*) and *Planolites montanus* (*Plm*), hypichnial full reliefs; (D) *?Planolites* isp. (*Pl*) and *Thorichnus* isp. (*Th*), hypichnial full and semi-reliefs, respectively; (E) *Siphonichnus* isp. (*Si*), full relief manifested on the lower bedding surfaces and *Thorichnus* isp. (*Th*), preserved in hypichnial semi-relief; (F) *Spirophycus* isp. (arrowed), hypichnial semi-relief; (G), (I), (J) *Spirophycus bicornis* (arrowed), hypichnial semi-reliefs; (H) *Halimedides* isp. (*Ha*) and *Palaeophycus* isp. (*P*), hypichnial semi-reliefs; (K) *Oravaichnium* isp. (*Or*), *?Arthrophycus tenuis* (*Art*), and *Planolites beverleyensis* (*Plb*), hypichnial full reliefs **58**
- Fig. 30.** Simple and branched structures, including a single ichnotaxon of network structures, from the Numidian Formation in the Ouarsenis Mountains, NW Algeria. (A), (B) *Ophiomorpha rudis* (arrowed), hypichnial full relief; (C) *?Planolites* isp., hypichnial full relief; (D) *Planolites beverleyensis* (*Plb*), hypichnial full relief; *Oravaichnium* isp. (*Or*), hypichnial semi-relief; *Paleodictyon strozzii* (*Pas*) hypichnial semi-relief; (E) *Palaeophycus striatus* (*Ps*), hypichnial full relief; *Helminthoidichnites* isp. (*He*), hypichnial semi-relief; (F) *Palaeophycus tubularis* (*Pt*), hypichnial full relief; (G) *Planolites beverleyensis* (*Plb*), hypichnial full relief; wash-out *?Planolites* isp. (*Pl*), hypichnial semi-relief; (H), (I) *?Parataenidium* isp. (arrowed), epichnial semi-relief **64**
- Fig. 31.** Simple and branched structures from the Numidian Formation in the Ouarsenis Mountains, NW Algeria. (A) *Phycodes* isp. (arrowed), hypichnial semi-relief; (B), (C) *Thalassinoides* isp. (arrowed), larger form, hypichnial semi-relief; (D), (E), *Thalassinoides* isp. (arrowed), smaller form, hypichnial full relief; (F), (G), (H) *Tubulichnium rectum* (*Tr*) (arrowed), hypichnial semi-relief; (H) with *Ophiomorpha rudis* (*Opr*), hypichnial full relief **66**
- Fig. 32.** Simple structures from the Numidian Formation in the Ouarsenis Mountains, NW Algeria. (A) *Tubulichnium mediterraneum*, endichnial full relief; (B) *T. mediterraneum* within marly mudstone in the lower unit of the Ain Ghanem section. (C) micrograph showing the cross section of the trace fossil in thin section, showing two main zones: (1) the internal zone filled with micrite, including quartz grains, some microfossils and shell fragments; (2) the external zone (envelope) made up of stacking pellets, without any internal structure, dominated by iron oxides, brown to dark brown in colour **69**
- Fig. 33.** Winding and meandering structures with one single network structure, from the Numidian Formation in the Ouarsenis Mountains, NW Algeria. (A), (B) *Helminthopsis* isp. (*Hel*), hypichnial semi-relief; *Paleomeanderson rude* (*Plr*), hypichnial semi-relief;

LIST OF FIGURES & TABLES

- Paleodictyon strozzii* (Pas), hypichnial semi-relief; *Helminthoidichnites* isp. (He), hypichnial semi-relief; (C), (D) *Cosmorhaphé sinuosa* (Cs), hypichnial semi-relief; (C) *C. lobata* (Cl), hypichnial semi-relief; (E) *Helminthoidichnites* isp. (He), hypichnial semi-relief; *Gordia arcuata* (Ga), hypichnial semi-relief; (F), (G) *Gordia arcuata* (arrowed), hypichnial semi-relief; (H), (I) *Nereites* isp. (arrowed), epichnial semi-relief **72**
- Fig. 34.** Spreite, meandering, branched, and network structures from the Numidian Formation in the Ouarsenis Mountains, NW Algeria. (A) *Phycosiphon incertum* (Ph), epichnial semirelief; *Helminthoidichnites* isp. (He), hypichnial semi-relief; *Oravaichnium* isp. (Or), hypichnial semi-relief; (B) *Scolicia strozzii*, hypichnial semi-relief; (C) *Taenidium* isp. (Ta), epichnial semi-relief; *Chondrites* isp. (Cn), epichnial full relief; *Zoophycos* isp. (Z), epichnial semi-relief; (D) (E), (F), *Gyrochorte* isp. (Gy), epichnial semi-relief; (E) *Zoophycos* isp. (Z), epichnial semi-relief; (G), (H), *Lophoctenium* isp. (Lo), epichnial semi-relief; (G) *Ophiomorpha rudis* (Opr), hypichnial full relief; (I) *Megagraption irregulare* (arrowed), hypichnial semi-relief **75**
- Fig. 35.** Spreite, network, branched, and meandering structures from the Numidian Formation in the Ouarsenis Mountains, NW Algeria. (A) *Rutichnus* isp., hypichnial full relief; (B) *Squamodictyon tectiforme*, hypichnial semi-relief; (C), (D) *Diplocraterion* isp., endichnial full relief; (E), (F), (G) *Zoophycos* isp., small forms; (H), (I), (J) *Zoophycos* isp. (Z), large forms; (J) *Gyrochorte* isp. (Gy), epichnial semi-relief **80**
- Fig. 36.** Vertical distribution of the distinguished ichnofacies in the studied sections with regard to lithostratigraphic subdivision (for explanation of lithofacies see Fig. 7) **87**
- Fig. 37.** Simplified schematic block diagram showing the distribution of ichnofacies in the study area **88**
- Fig. 38.** Photographs of the beds analysed for zircon dating. (A), (B) Photographs of the sample KMS-bed 29, the Kef Maiz section; (A), (B) Photographs of the sample KRS-bed-01, the Kef Rzama section **95**
- Fig. 39.** Lithological columns with indication of sedimentary structures and the analysed samples for the U-Pb zircon dating **96**
- Fig. 40.** Palaeocurrent rose diagrams from the study area. (A) Data measured from the Forêt des Cèdres section; (B) Data measured from the Ain Ghanem section; (C) Data measured from the Kef Rzama section **98**
- Fig. 41.** CL images showing the main zircon textures in the study area. (A), (B) zircons with unperturbed zoning, sample KMS-B29; (C), (F), sample KRS B01; (D), (E), (H), sample KRS B01; (G), sample KMS-B29 **99**
- Fig. 42.** U-Pb concordia and probability diagrams of zircon ages from the sample KMS-B29, the Kef Maiz section. (A) Histogram of probability density plots of zircon ages; (B) U-Pb concordia diagram showing all data, and (C) showing only youngest ages **100**
- Fig. 43.** U-Pb concordia and probability diagrams of zircon ages from the sample KRS-B01, the Kef Rzama section. (A) Histogram of probability density plots of zircon ages; (B) U-Pb concordia diagram showing all data; (C) data showing only youngest ages **102**

Fig. 44. Diagrams showing the Th/U ratio within the samples KMS-B29 from the Kef Maiz section, and KRS-B01 from the Kef Rzama section **103**

LIST OF TABLES

Table 1. Lithofacies of the Numidian Formation in the study area, with their corresponding sedimentary structures, trace fossils and interpretation of the depositional processes **41**

Table 2. Description and interpretation of the three facies associations of the Numidian Formation in the study area **53**

Table 3. Distribution of trace fossils and the corresponding facies in the investigated sections of the Numidian Formation in the Ouarsenis Mountains, NW Algeria. Abundance: very rare (VR; 1 ichnotaxon), rare (R; 2–6 ichnotaxa), common (C; 7–9 ichnotaxa), very common (VC; 10–22 ichnotaxa), abundant (A; 23–41 ichnotaxa), very abundant (VA; >42 ichnotaxa) **81**

Table 4. Distribution of trace fossils according to their ichnosubfacies **86**

Table 5. Detail data of palaeoflow measurement in the study area **97**

CHAPTER 1

INTRODUCTION

1.1. MOTIVATION AND OBJECTIVES

Many multidisciplinary studies on the Numidian Formation (NF) deposits were conducted in the Mediterranean region, but very few in Algeria, where they mainly refer to the regional geology and are commonly limited to the general geological data. [Hoyez \(1975, 1989\)](#) performed general sedimentological studies on all the NF of the Mediterranean, including some data results on the palaeoenvironment and the provenance of the detrital material. The first detailed sedimentological study on the NF in Algeria was carried out by [Moretti et al. \(1991\)](#) in the Constantine Mountains, including detailed results about the petrography and the depositional processes.

This PhD thesis deals with multidisciplinary studies that involve various aspects of sedimentology, stratigraphy, and ichnology as well as geochemical and isotopic analysis. The studies on ichnofossils are an important part of this project. This study aims to: (1) identify of the palaeoenvironments of the Numidian Formation in the study area, with a better understanding of the factors controlling the dynamics of deposition (foremost sedimentological and ichnological methods are applied); (2) determine of a more precise age and palaeoecological conditions of these deposits on the basis of microfossils (foraminifers and calcareous nannoplankton); (3) determine of the provenance of detrital material that feed the NF basin of this area using U/Pb zircon dating and the orientation of the depositional palaeoflow.

1.2. PRESENTATION OF THE NUMIDIAN FORMATION

The Numidian Formation (NF) is an extensive deep-sea series of clastic deposits, which outcrops run over the distance of 2500 km in a 100 km wide belt, from Gibraltar through Morocco, Algeria, and Tunisia to Calabria ([Fig. 1](#)). It is placed within the Maghrebic orogenic domain, which is called the Maghrébides ([Durand-Delga and Fonboté, 1980; Wildi, 1983](#)). The term "Numidien" was coined for the first time by [Ficheur \(1890\)](#) to define the Numidian stage (corresponding to the Upper Eocene), which was represented (as understood at that time) by a series of clays overlying by thick-bedded sandstones in the Algerian coastal chains NW of Greater Kabylia. This term was integrated in Tunisia by [Aubert \(1891\)](#), and in Morocco by [Fallot \(1937\)](#). Later, the Numidian stage was transferred to the rank of "facies" to distinguish the Numidian series made up of a series of mudstone and sandstone, in coincidence with the time when the new concept of allochthonous tectonics in the Algerian Tell was established ([Glangeaud, 1932; Flandrin, 1948](#)). In this thesis, the term Numidian Formation (NF) is used instead of the Numidian Flysch, because the term "flysch" is considered ambiguous in application to these deposits ([Patacca et al., 1992; Guerrera et al., 1993, 2012](#)).

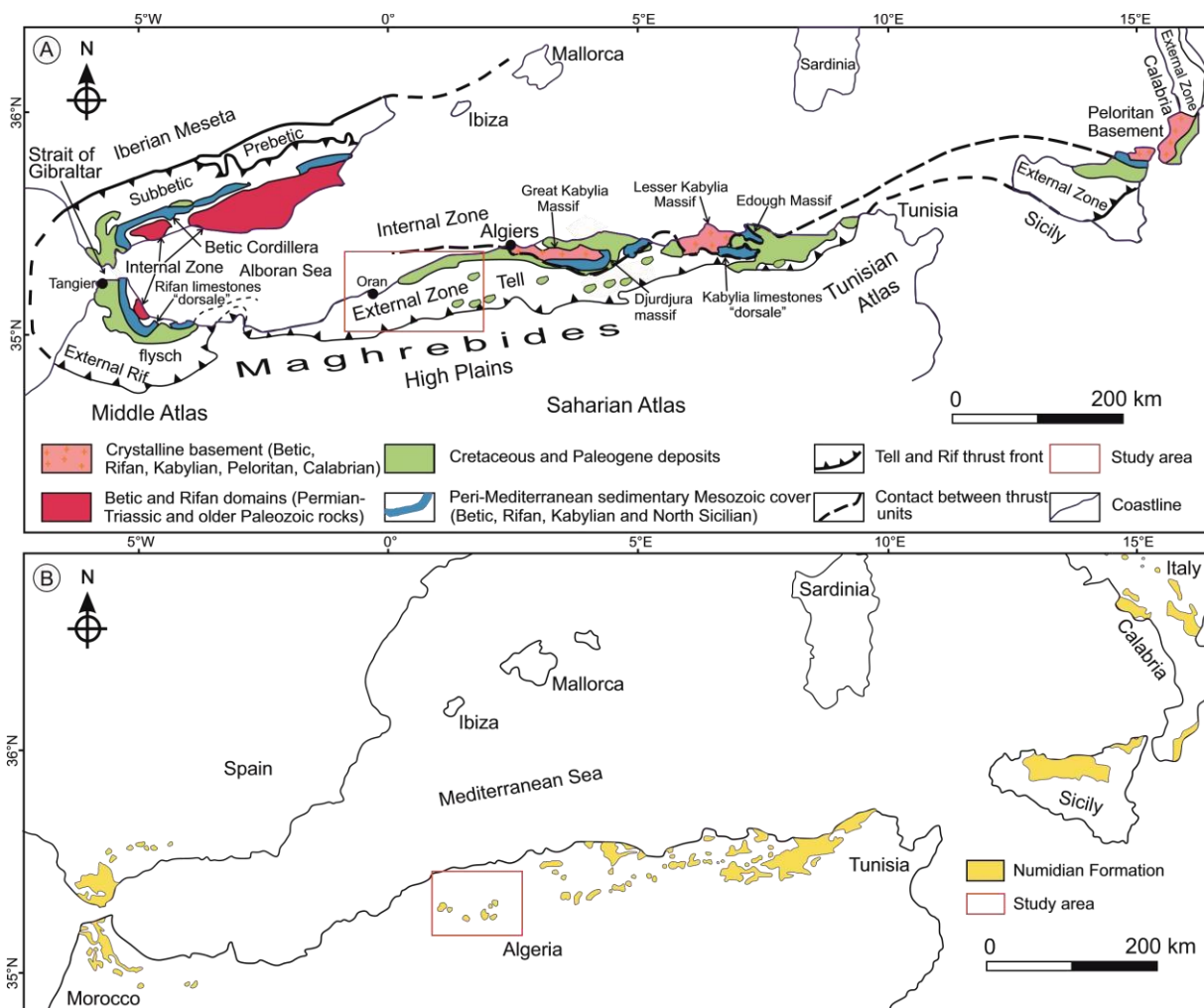


Fig. 1. (A) Location of the study area with indication of the principal Alpine domains in the western Mediterranean (after Durand-Delga, 1969, modified); (B) Location of the main outcrops of the Numidian Formation in the Mediterranean (Hoyer, 1989).

1.3. GEOLOGICAL SETTING

The Numidian Formation (NF) in Algeria is built mostly of deep sea turbiditic sandstone and mudstone deposits, which are Late Oligocene to early Burdigalian in age (Durand Delga and Magné, 1958; Mattauer, 1958; Magné and Raymond, 1972; Raoult, 1974; Raymond, 1976; Bizon and Hoyez, 1979; Lahondère et al., 1979; Feinberg et al., 1981; Hoyez, 1989; Moretti et al., 1991) and form a part of the Maghrebian domain. This domain is interpreted as an Alpine-type orogen which resulted from closure of the Maghrebian part of the Tethys Ocean (Wildi, 1983; Bouillin, 1992). Deposits of the NF accumulated in the Maghrebian Flysch Basin (MFB) (Fig. 2), which is considered as a foreland basin, remnant of the neo-Tethys Ocean in the western part of the current Mediterranean Basin (Thomas et al., 2010b). The MFB was located in the western palaeo-Tethys realm, bordered to the north by a southward verging accretionary prism, underlain by European crustal blocks which rode above northwards subducting oceanic crust

(Guerrera et al., 2005; Thomas et al., 2010b). It is bordered to the south by the African passive margin.

The MFB was opened after the Pangaea breakup during the Jurassic-Cretaceous transition (Wildi, 1983; Bouillin, 1986). In general, sedimentation of the NF deposits ceased 16–15 Ma at the end of the Burdigalian (see Vila et al., 1994; Esteras et al., 1995) except for the Apennines and Sicily, where it was extended into the Langhian (Guerrera et al., 2005; Thomas et al., 2010; Pinter et al., 2018; Butler et al., 2020). At the beginning of the Langhian (15 Ma), the Kabyrides began accretion to Africa (Frizon de Lamotte et al., 2000). The NF underwent north verging folding and thrusting. Part of the flysch succession was detached as thrust sheets and overthrust in the external zone of the Maghrebides (Bouillin, 1977; Vila, 1980). This conditioned distribution of the NF in several commonly isolated areas in the northern Algeria (Fig. 2).

The NF occurs in three different zones (Bouillin, 1986), i.e. in (1) an internal position, superimposed on the Kabyria massifs, where the NF deposits are referred to as the North Kabyride Flysch, in (2) a relatively external position at the southern margin of the Kabyria massifs, where the NF is called the South Kabyride Flysch, and in (3) a very external position, as isolated masses floating on the Tellian series (Paleozoic–Eocene), where they have been tectonically transported up to 100 km to the south, and are preserved in the hinge of synclinal folds. The study area in the Ouarsenis Mountains refers to this position. The most stratigraphically complete deposits of the NF are present in the outcrops of Greater Kabyria. It is subdivided for the first time by Raymond (1976) into three “termes” (Fig. 3): (1) the “terme inférieur” (Upper Oligocene) represented by varicoloured clays with the common trace fossil “*Tubotomaculum*” (assigned to *Ophiomorpha recta* in Riahi et al., 2014 and *Tubulichnium mediterraneum* in Uchman and Wetzel, 2017); (2) the “terme médian” (Aquitanian) represented by alternating sandstones, quartz pebble conglomerates and mudstones; it is known as the Numidian Sandstone; and (3) the “terme supérieur” (Aquitanian to lower Burdigalian) formed by mudstones, marlstones and cherts (“silexites”) and referred to as the supra-Numidian succession. This lithostratigraphic scheme is similar to those in other Mediterranean outcrops of the NF, i.e. in Tunisia (Glacon and Rouvier, 1967; Rouvier, 1977; Riahi et al., 2010, 2015), Sicily (Broquet, 1968; Guerrera et al., 1992; Patacca, 1992), the Apennines (La Manna et al., 1995), Spain (Didon et al., 1984; Martín Algarra, 1987; Esteras et al., 1995), and Morocco (Chalouan et al., 2008) (Fig. 3).

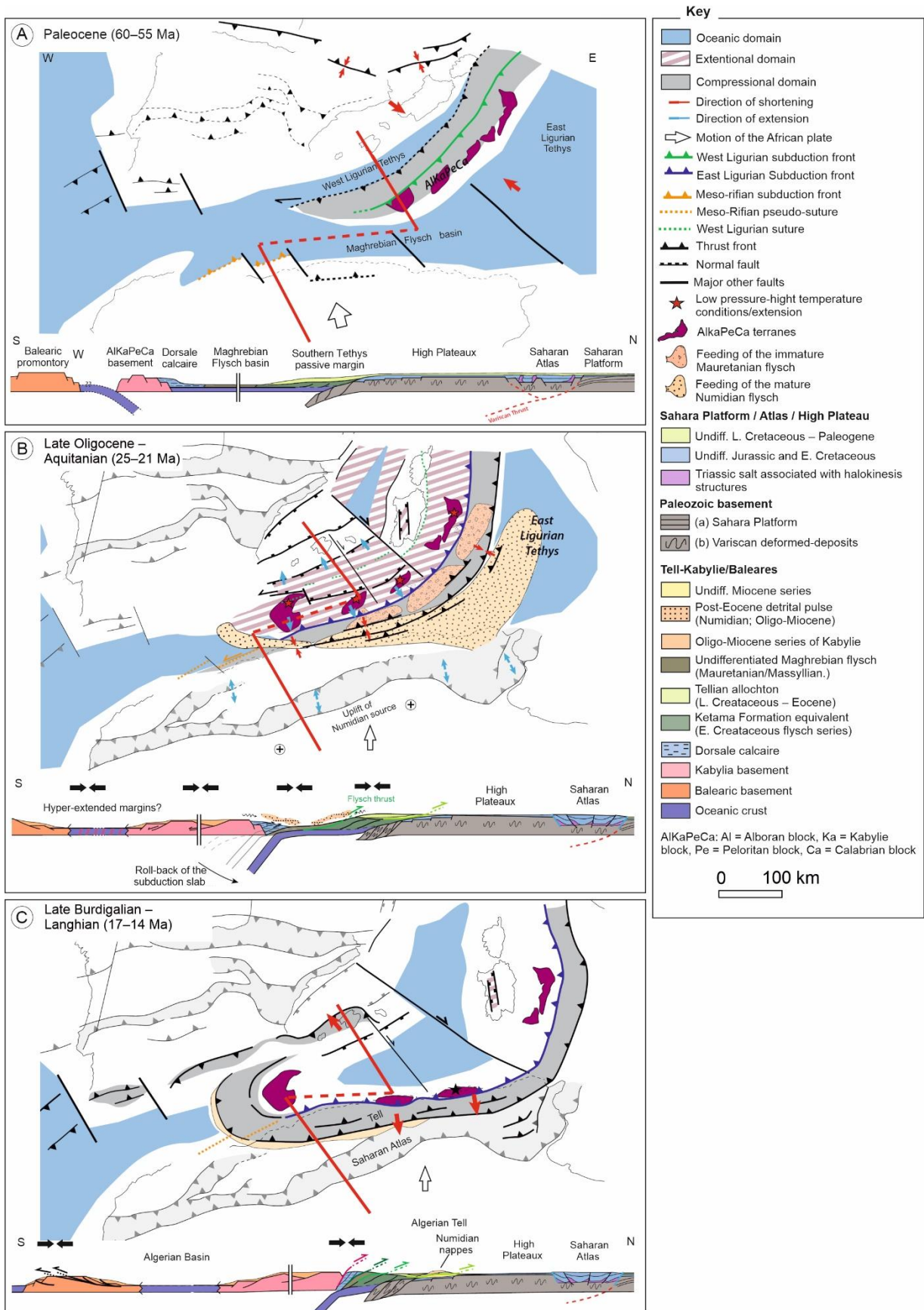


Fig. 2. Palaeogeographic reconstruction from the Paleocene to the late Burdigalian with simplified cross-section of the Maghrebian Basin. (A) Paleogene (60–55 Ma); (B) Late

Oligocene–Early Miocene (25–21 Ma); (C) Late Burdigalian–Langhian (17–14 Ma) (Leprêtre et al., 2018, modified).

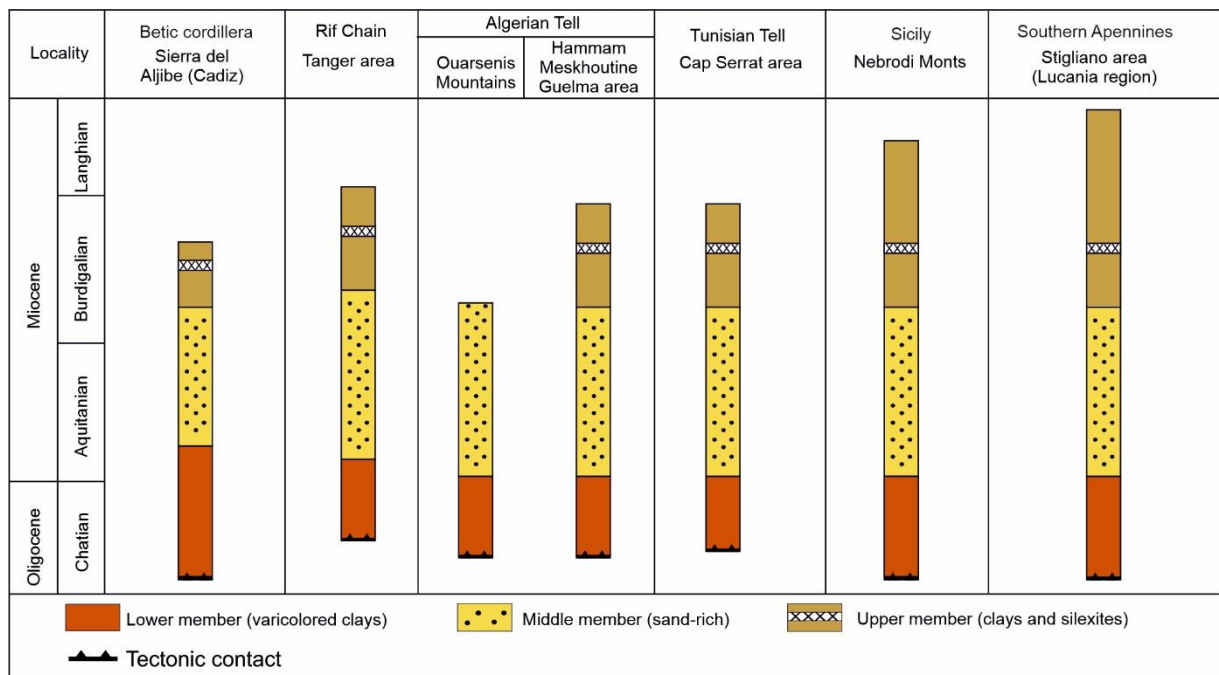


Fig. 3. Chronostratigraphy of the main Numidian successions in the Mediterranean (Guerrera, 2012, modified).

1.4. OVERVIEW ON THE STUDY AREA

This thesis focuses on the NF outcropping in the Ouarsenis Mountains, NW Algeria. The latest forms a part of the External Domain of the Algerian Northern Belt. The Ouarsenis Mountains are bordered to the north by the Chlef Plain (developed on a vast Neogene basin) and by Zaccar Mount (Djebel Zaccar), to the south by the Sersou Plateau, to the east by the Bibans Mountains (near Médéa city) and by the post-Miocene formations of the Miliana region. To the west, there is no distinct boundary, although Polvêche (1960) considered the Miocene deposits of Zemmoura as the western limit of the NF in the study area. The NF in the study region occurs in a complex of allochthonous units stacked above Triassic and Cretaceous deposits (Mattauer, 1958; Polvêche, 1960) (Figs. 4, 5). It comprises two main lithological units: (1) varicoloured (greenish to dark brown) marly mudstone of the Upper Oligocene at the base (the equivalent of the “terme inférieur” in Greater Kabylia); and (2) alternating sandstones, quartz pebble conglomerates and bluish grey mudstones at the top (Mattauer, 1958), which are an equivalent of the “terme médian” in Greater Kabylia. The contact between these two units is unclear (covered) in the study area; it is marked by a lithological change.

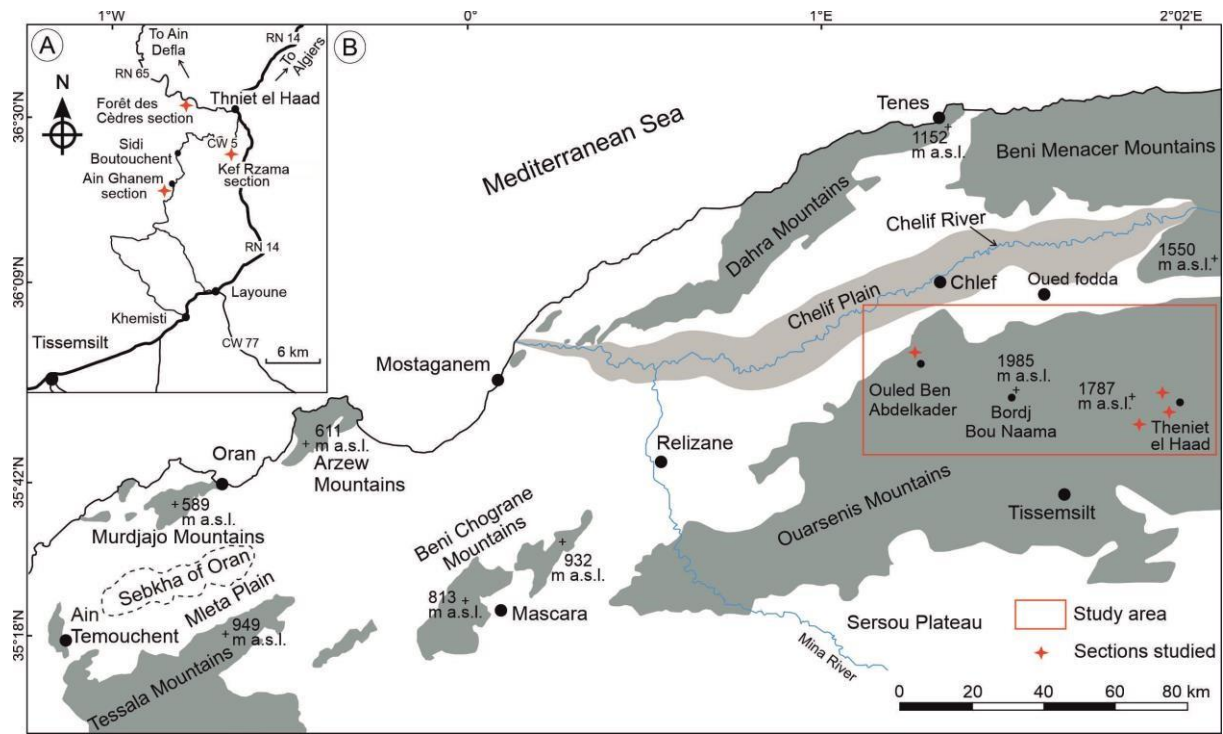


Fig. 4. (A) Location of the Ouarsenis Mountains; (B) Map showing the location of the Ouarsenis Mountains (modified from Benhamou, 1996 after Perrodon, 1957).

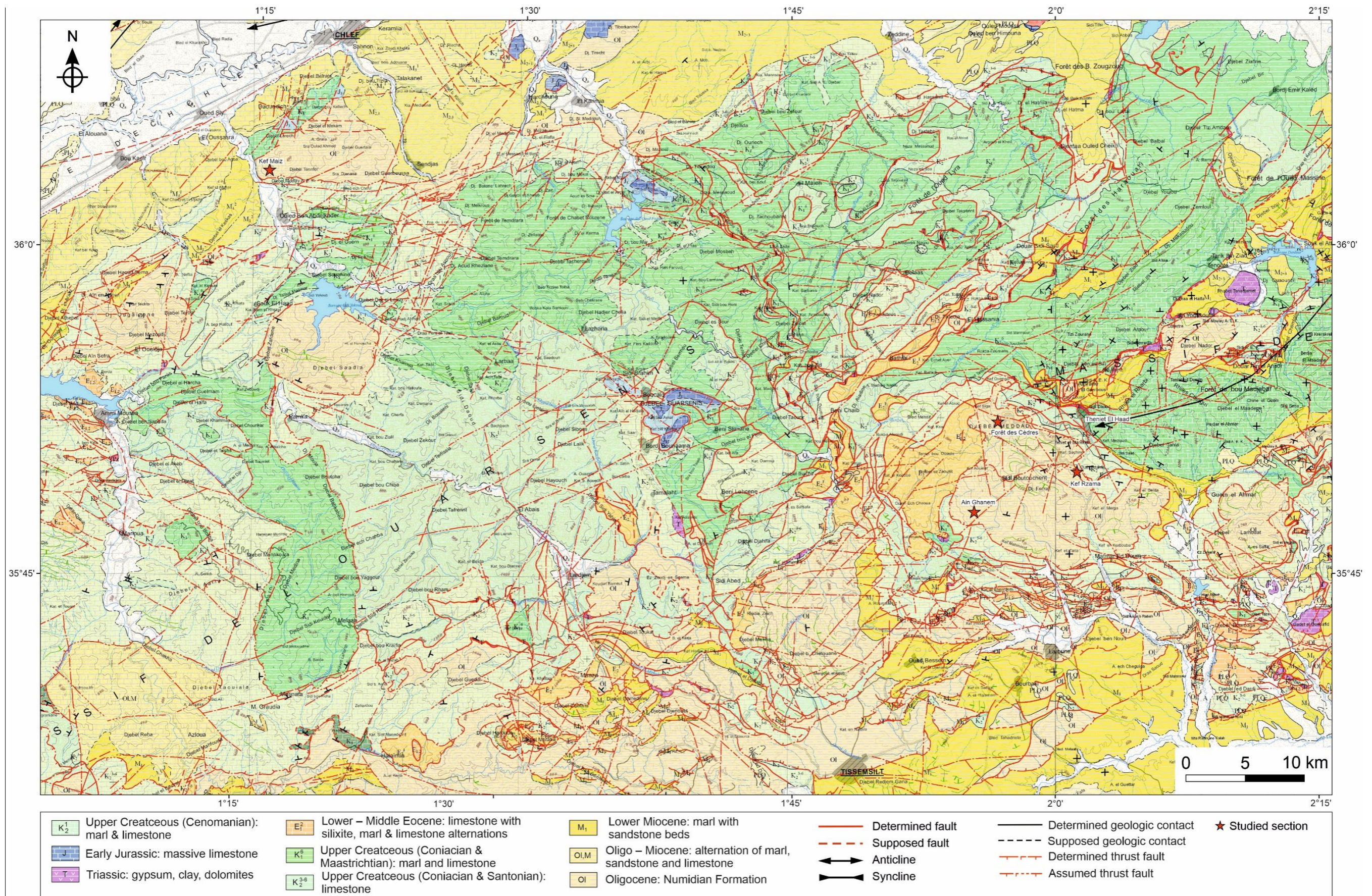


Fig. 5. Geological map showing the main studied sections (interpretative Geological Map of Algeria 1: 200 000, N°: NI-31-XX/NJ-31-XXI/NJ-31-II/NJ-31-III, ANRH, 2008).

1.5. PREVIOUS RESEARCH

The history of the Numidian Formation went through many periods, starting from the discovery of these deposits gradually all around the Mediterranean, followed by numerous studies attempting to understand its genesis.

1.5.1. The recognition and stratigraphy of the Numidian Formation

The term "Numidien" was coined for the first time by [Ficheur \(1890\)](#) to define the Numidian stage (corresponding to Upper Eocene), which was represented (as understood at that time) by a series of clays overlying by thick-bedded sandstones in the Algerian coastal chains NW of Greater Kabylia. It was recognized in the study area (Ouarsenis Mountains, NW Algeria), for the first time by [Repelin \(1895\)](#), in the outcrops of Kef Tachta, Djebel Saadia, and Djebel Maiz, considering its age as Upper Eocene, in accordance with the ideas of [Ficheur \(1890\)](#).

This term was integrated in Tunisia by [Aubert \(1891\)](#) to describe the sandstone outcrops from the north-western massifs of "La Caile" in Bizerte. In Morocco, this term was used for the first time by [Fallot \(1937\)](#), [Flandrin \(1948\)](#), and in the Betic Cordillera by [Gavala \(1924\)](#). However, this term was used later in the southern Apennines by [Flandrin \(1948\)](#).

[Ficheur \(1890\)](#) subdivided the Eocene into two stages, i.e. the upper stage E corresponding to the "Numidien", and the lower stage D, made up of mudstone and sandstone (stratotype in de Chellata), named later the "Médjanien" by the same author ([Ficheur, 1893](#)). This terminology was used in Algeria until the beginning of the 20th century.

[Dareste de la Chavanne \(1910\)](#) modified the proposition of [Ficheur \(1890\)](#) by inclusion of the Médjanien Flysch and the "Numidian" Flysch to the Oligocene, because this author considered that these two facies are coeval, but without any palaeontological proof. However, the subdivisions by [Ficheur \(1890\)](#) remained in use. [Erhmann \(1923\)](#) discovered the first fossil, i.e. the foraminifer *Lepidocyclina* which suggests an Oligocene age of the Numidian sandstone, However, the impact of this discovery remains weak, and some doubts arouse about the stratigraphic value of this foraminifer.

Later, the Numidian stage was transferred to the rank of facies which includes the Numidian series composed of mudstones and sandstones ([Glangeaud, 1932](#)). This was in coincidence with the time when the new concept of allochthonous tectonics in the Algerian Tell was established ([Glangeaud, 1932](#); [Flandrin, 1948](#)).

Important stratigraphic details were presented by [Flandrin \(1948\)](#) in his monograph on the Algerian Nummulitic Paleogene. The term Médjanien Flysch was abandoned because it

appeared that its stratotype section in Chellata belongs to the Cretaceous. The new finding of large foraminifera permits the attribution of the thick sandstone unit of the NF to the Oligocene and the underlying mudstone unit to the Priabonian. However, this stratigraphic attribution was not used later.

As this period was known by the introduction of the concepts of allochthonous tectonics, Caire (1951) defined the stacking of three nappes in the sub-Bibanic region, and named them nappes A, B, and C. The concept of allochthonous tectonics was also applied to the Ouarsenis Mountains (Mattaue, 1953; Polvêche, 1958, 1960), in the Setifian region (Glacon, 1955, 1961), and in the region of Oued Athménia (Van De Fliert *et al.*, 1958), but not in the Constantine region and in Tunisia at that time.

Significant fossils from the Numidian Formation in north-western Algeria were discovered by Mattauer (1953), who identified the foraminifers with *Miogypsina* in the lower part of the Numidian Formation in the Ouarsenis Mountains. This allowed dating of the sandstone unit to the end of the Oligocene. New findings of foraminifers and calcareous nannoplankton in the Numidian Formation of eastern Algeria (Martini, 1971; Raymond & Magné, 1972; Raoult, 1974; Gélard, 1979; Lahondère *et al.*, 1979) allowed dating of the lower mudstone unit to the upper Oligocene (Chattian), and the upper sandstone unit to the lower Burdigalian–Aquitainian.

1.5.2. Provenance of the Numidian Formation material

In the middle of the 20th century, an intensive debate began about the provenance of the sedimentary material that feeds the MFB. Two opposite views point to (1) a northern provenance, represented by the European AlKaPeCa domain. This suggestion was supported by: Mattauer (1958, 1973), Caire (1961), Caire and Duée (1971); Magné and Raymond, (1972); Ivaldi, (1977); Lahondère *et al.* (1979); Vila *et al.*, 1995; Van Houten (1980), Parize *et al.* (1986, 1999), Benomran *et al.* (1987), Yaïch *et al.* (2000), and recently Fildes *et al.* (2010) based on the interpretation of zircon dating carried out from the northern Tunisia and Sicily; or to (2) the southern provenance represented by the African craton (Durand Delga (1955, 1980), Ogniben (1960), Wezel (1970a), Gaudette *et al.* (1995); Hoyez (1975, 1989), Lancelot *et al.*, 1977; Moretti *et al.*, 1991; Johansson *et al.* (1998) ; Thomas *et al.* (2010a, 2010b); Guerrero *et al.* (1992, 2012); Fornelli *et al.* (2015); Azdimousa *et al.* (2019). The review of the problems by Thomas *et al.* (2010b) favours a southern provenance of the Numidian material.

1.6. MATERIAL AND METHODS

The methods used in the preparation of this thesis include two main parts: (1) field work, and (2) laboratory analysis.

1.6.1. Field work: Many field trips were carried out between 2015 and 2020 in the study area, located in the Ouarsenis Mountains, north-western Algeria. Four sections were studied in detail with a focus on sedimentological and ichnological data.

- **Logging:** A detailed lithological description bed by bed was performed for all the sections studied, associated with sketching and photography. The physical sedimentary structures were described and photographed in the field, with information about their occurrence, frequencies, and their associations. The orientation of directional sedimentary structures, including flute casts, groove casts, and frondescant marks, was measured with a compass to deduce the predominant orientation of the depositional palaeoflow.
- The terminology and the symbols used for the description are after [Tucker \(2003\)](#) and [Collinson et al. \(2006\)](#). The bed thickness classification is after [Ingram \(1954\)](#), with laminae (<1 cm), very thin beds (1–3 cm), thin beds (3–10 cm), medium beds (10–30 cm), thick beds (30–100 cm) and very thick beds (>100 cm).
- **Description of trace fossils:** The ichnofossils were photographed and partly described in the field with information on their occurrence, abundance. Their distribution is marked in the logs whenever possible. To determine their abundance, the terminology by [Knaust \(2017\)](#) is used, where very rare means 1 ichnotaxon, rare – 2–6 ichnotaxa, common – 7–9, very common – 10–22, abundant – 23–41, and very abundant – >42 ichnotaxa.
- **Sampling:** Samples were carried out from sandstones to prepare thin sections, and to perform the geochemical analysis. Some specimens of trace fossils were collected for further laboratory analysis. Samples from mudstones and marls are collected for the micropalaeontological studies.

1.6.2. Laboratory analysis: The samples carried out in the field are analysed in the laboratory as follows:

- Preparation and study of thin sections using a polarizing microscope. This method allows the determination of the petrographic composition of the samples. The sandstone rocks

were cut into small rectangular pieces ready to use in the preparation of thin sections, in the Laboratory 25, at the University of Tlemcen, Algeria. The study of the thin sections was done in the Institute of Geological Sciences of the Jagiellonian University, Poland.

- The identification of trace fossils was carried out from the field with the help of Prof. Alfred Uchman. The specimens taken from the field were analysed and photographed in the laboratory.
- The preparation of samples for micropalaeontological studies, including washing through a series of sieve (\emptyset : 63:80:125:250 μm). Pick-up and identification of foraminifers was done partly in the laboratory n° 25 of the University of Tlemcen, with the help of Dr. Adaci Mohamed, and in the Institute of Geological Sciences of the Jagiellonian University, with the help of Dr. Ewa Malata.
- Sample preparation for dinoflagellate cyst studies, including rock sample processing and taxonomical identification, was performed by Dr. Przemysław Gedl from the Institute of the Geological Sciences of the Polish Academy of Sciences, Research Centre in Kraków, Poland. A set of samples was selected and processed at the Institute of Geological Sciences, Polish Academy of Sciences, Research Centre in Kraków. The samples were subjected to the following processing procedure, which included treatment with 38% hydrochloric acid (HCl), 40% hydrofluoric acid (HF) treatment, heavy-liquid (ZnCl_2+HCl ; density $2.0 \text{ g}\cdot\text{cm}^{-3}$) separation, ultrasound for 10–15 s and sieving at 10 μm , on a nylon mesh. No nitric acid (HNO_3) treatment was applied. The quantity of each rock sample processed was 20 g. Two slides from each sample were made using glycerine jelly as a mounting medium.
- The preparation of slides for the study of calcareous nannofossils was performed in the Institute of Geological Sciences of the Jagiellonian University, with the help of Dr. Hab. Marta Oszczypko-Clowes, and MSc. Adam Wierzbicki from the Institute of Geological Sciences of the Jagiellonian University.
- **Calcimetry method:** samples from mudstone were tested for carbonate (CaCO_3) content in the University of Tlemcen with the help of Dr. Sid Ahmed Hamouda and in the Jagiellonian University with the help of MSc. Katarzyna Maj-Szeliga and MSc. Bartosz Kluska.
- **U-Pb detrital zircon geochronology PIG-PIB:** Two samples of sand-rich sandstone from Kef Maiz and Kef Rzama sections were analyzed for zircon geochronology in the Polish

Geological Institute – National Research Institute, Warsaw, Poland, and supported financially by the International Association of Sedimentologists (IAS).

1.7. ORGANIZATION OF THE THESIS

This manuscript includes five main chapters:

Chapter 1: An introduction, including a presentation of the problem and the objectives of this thesis, a geological overview, an overview of the study area, a literature review showing the results of the studies done so far on the subject, and the methods.

Chapter 2: Lithostratigraphy and remarks on biostratigraphy, focuses on the description of the studied sections with characterisation of the main lithostratigraphic units and some remarks on their biostratigraphy.

Chapter 3: Sedimentology, focuses on the study of lithofacies, their interpretations, and their association to give an overview on the depositional environment.

Chapter 4: Ichnology & Palaeoenvironment, focuses on the study of trace fossils occurring in the study area, including their detailed systematic description, palaeoenvironmental significance, and a comparison with their analogues from the NF in the Mediterranean.

Chapter 5: Sediment provenance analysis, including a study of provenance of the Numidian material using U/Pb zircon dating and palaeoflow orientation.

Chapter 6: General conclusions showing the main results of our study.

Chapter 7: References.

CHAPTER 2

LITHOSTRATIGRAPHY & REMARKS ON BIOSTRATIGRAPHY

2.1. INTRODUCTION

This chapter is dedicated to the lithostratigraphy of the Numidian Formation outcropping in the Ouarsenis Mountains, NW Algeria, with some remarks on biostratigraphy. This was made on the basis of detailed bed-by-bed logs of representative outcrops, which were documented by sketches and photographs. Sedimentary structures and trace fossils were described and photographed in the field, with information about their occurrence and abundance. Samples of mudstone were analysed for foraminifers, calcareous nannoplankton, and dinocysts in order to give a precise age to the studied deposits.

This study focuses on four main outcrops: (1) the outcrops of Theniet El Haad, which include three main sections (Forêt des Cèdres, Ain Ghanem, and Kef Rzama), situated at 7 km, 12 km and 2.5 km northwest of Theniet El Had city, respectively, and around 50 km northeast of the Wilaya of Tissemsilt, and (2) the Chlef region with one main outcrop in Kef Maiz mount, which is located 4 km north of Ouled Ben Abdelkader city and 20 km south-west of the Wilaya of Chlef (Fig. 6).

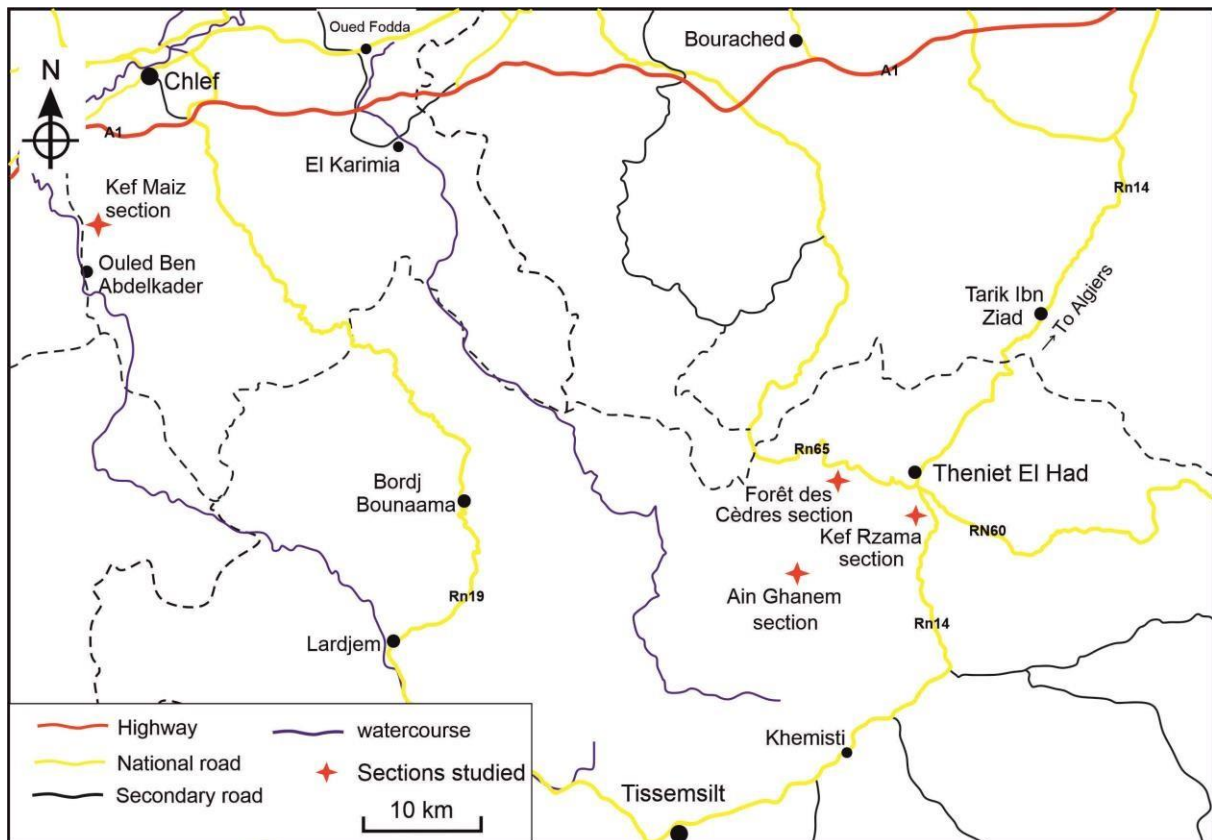


Fig. 6. Map showing the distribution of the main Numidian outcrops in the Ouarsenis Mountains.






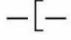



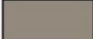



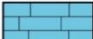














Key			
C	Clay		Cross bedding
VF	Very fine sand		Normal grading
F	Fine sand		Flute cast
M	Medium		Gutter cast
C	Coarse sand		Ridge and furrow
V	Very coarse sand		Groove cast
G	Gravel		Fluid escape structures
	Sandstone		Load cast
	Mudstone		Convolute lamination
	Mud clasts		Slump
	Limestone		Ichnofossil
	Ichnofossil		High degree of bioturbation
	High degree of bioturbation		Low degree of bioturbation
	Low degree of bioturbation		Ripple marks
	Ripple marks		Climbing ripple cross-lamination
	Climbing ripple cross-lamination		Parallel lamination
	Parallel lamination		Ripple cross-lamination
	Ripple cross-lamination		

Fig. 7. Key for Figures 9, 11, 13, 15.

2.2. DESCRIPTION OF THE STUDIED SECTIONS

2.2.1. KEF RZAMA SECTION

Figs. 8, 9

The Kef Rzama section (GPS-coordinates: N36°3.733', E1°15.786') is 127 m thick. The beds gently dip (10–15°) to the SSW, and strike at NNW–SSE. It includes two distinct units: the lower unit (mud-dominated) and the upper unit (sand-dominated).

The lower unit: It consists of varicoloured marly mudstones (greenish to dark brown), with rare discontinuous, fine grained, thin to very thin-bedded (2–15 cm) sandstone, beige, dark brown to greenish in colour, showing rare trace fossils. The mudstone shows full relief trace fossils, including *Tubulichnium mediterraneum* called “*Tubotomaculum*” in the former literature, and rare *Alcyonidiopsis* isp.

The upper unit: It is made up of yellowish to fair grey, fine to very coarse-grained, conglomeratic in some parts, thin to very thick-bedded sandstone (0.07–6 m thick) alternating with greenish mudstone and grey siltstone (0.05–3 m thick). All the sandstone beds are discontinuous, with normal, inverse grading or ungrading, and show commonly sharp base and sharp top. The normally graded sandstone shows commonly erosive bases with sole structures (flute casts, groove casts). It includes also plane-parallel, ripple cross-laminations, and rarely load casts. The inversely grading occurs at the base of very thick bedded-pebbly sandstone with erosive bases. Ungraded sandstone beds are commonly thick to very thick, either structureless or showing some bedding. Fluid escape structures and slump structures are present in them. Convolute lamination occurs in fine-grained sandstone beds in association with other Bouma divisions or separately within siltstone beds. The load casts occur commonly on the sole of fine-grained medium-bedded sandstone. The siltstone beds show plane-parallel lamination and convolute lamination in some parts. The mudstone dominated parts include thin bedded-siltstone/fine-grained thin-bedded sandstone showing ripple cross lamination and plane-parallel lamination.



Fig. 8. Panoramic view of the Kef Rzama section showing the lower and upper units.

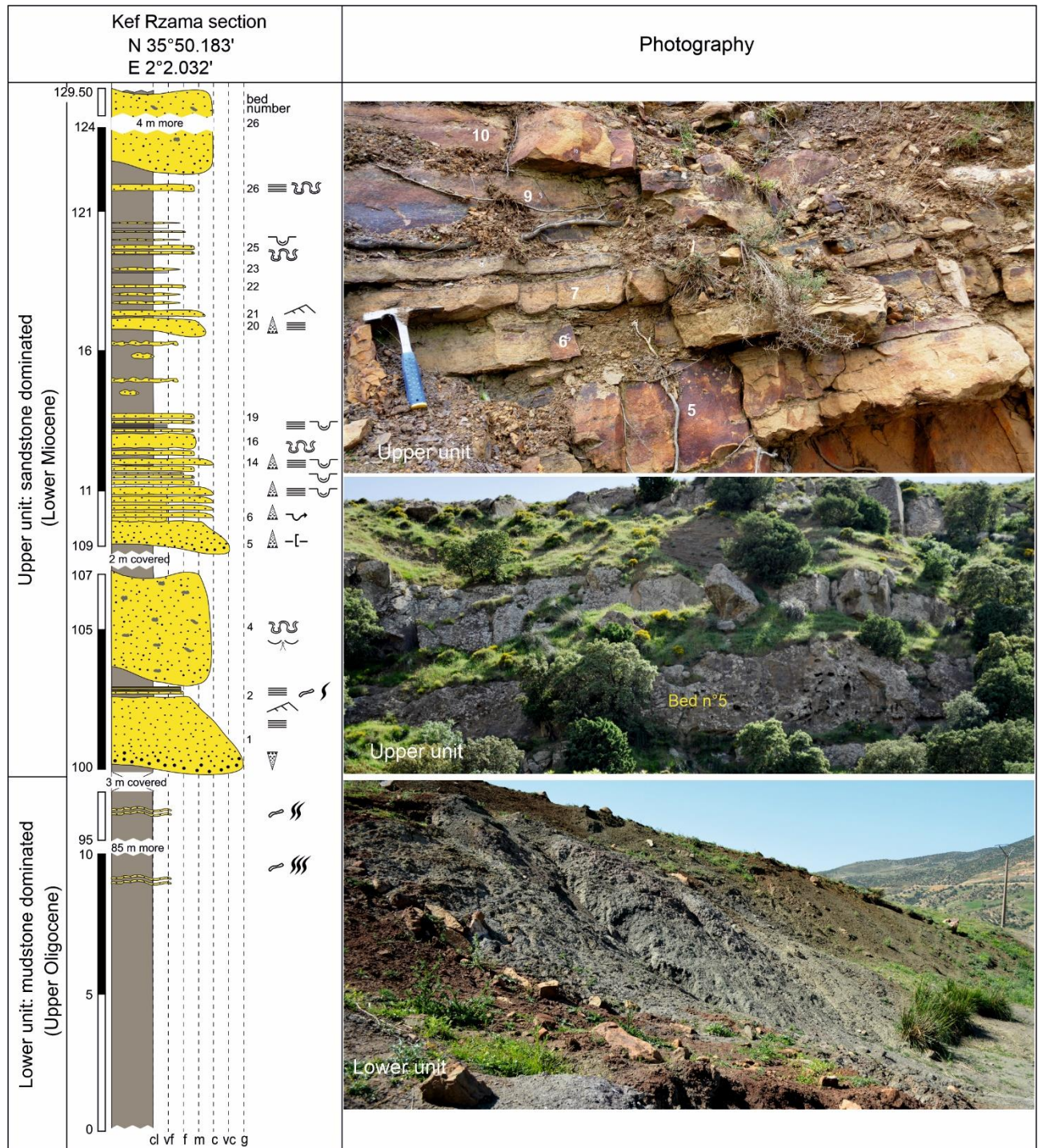


Fig. 9. Lithological column of the Kef Rzama section with indication of the numbering of beds and sedimentary structures.

2.2.2. AIN GHANEM SECTION

Figs. 10, 11

The Ain Ghanem section (GPS-coordinates: N35°47.841', E1°56.413') is 154 m thick. The beds weakly dip (10–15°) to the NNE and strike at ESE–NNW. Two main units have been distinguished: the lower unit (mud-dominated) and the upper unit (sand-dominated).

The lower unit: It consists of the varicoloured (greenish to dark brown) marly mudstones, which are very rich in full relief trace fossil *Tubulichnium mediterraneum* called “*Tubotomaculum*” in the former literature, including discontinuous intercalations of very thin to thin siltstone lenses and fine- to medium-grained thin, medium to rarely thick bedded sandstone (0.03–0.75 m), beige to yellowish, dark brown to greenish in colour, scattered randomly within the mudstone. Sandstone beds are generally deformed, showing different dip angles. They are rarely structureless. Most of them show depositional sedimentary structures (horizontal laminations, cross lamination, ripple marks, groove casts, flute casts) and soft sedimentary deformation structures (convolute laminations, fluid escape structures). The thinner beds are intensively bioturbated. A single thin limestone bed (0.07 m), greenish in colour, alternating with thin-bedded sandstones is present. The siltstone occurs as thin discontinuous lenses within the mudstone.



Fig. 10. Panoramic view of the Ain Ghanem section, showing the lower unit, varicoloured marly mudstone, and the upper unit (sand-dominated).

The upper unit: It consists of coarse- to fine-grained, very thick- to thin-bedded sandstone (0.05–6 m), yellowish to beige, dark brown to greenish in colour including some intercalation of mudstone/siltstone (0.05–3 m). The mudstone dominated parts include thin- to medium-bedded sandstone with ferruginous irregular levels rich in *Tubulichnium mediterraneum*; siltstone as thin layers or discontinuous lenses; some septarian nodules occur. The sandstone

beds are dominated by ungraded beds, showing convolute laminations and fluid escape structures. Normally graded beds show commonly flute casts, groove casts, longitudinal scours, horizontal lamination, and ripple marks. Mud clasts occur commonly in the upper part of the thick- to very thick-bedded sandstone.

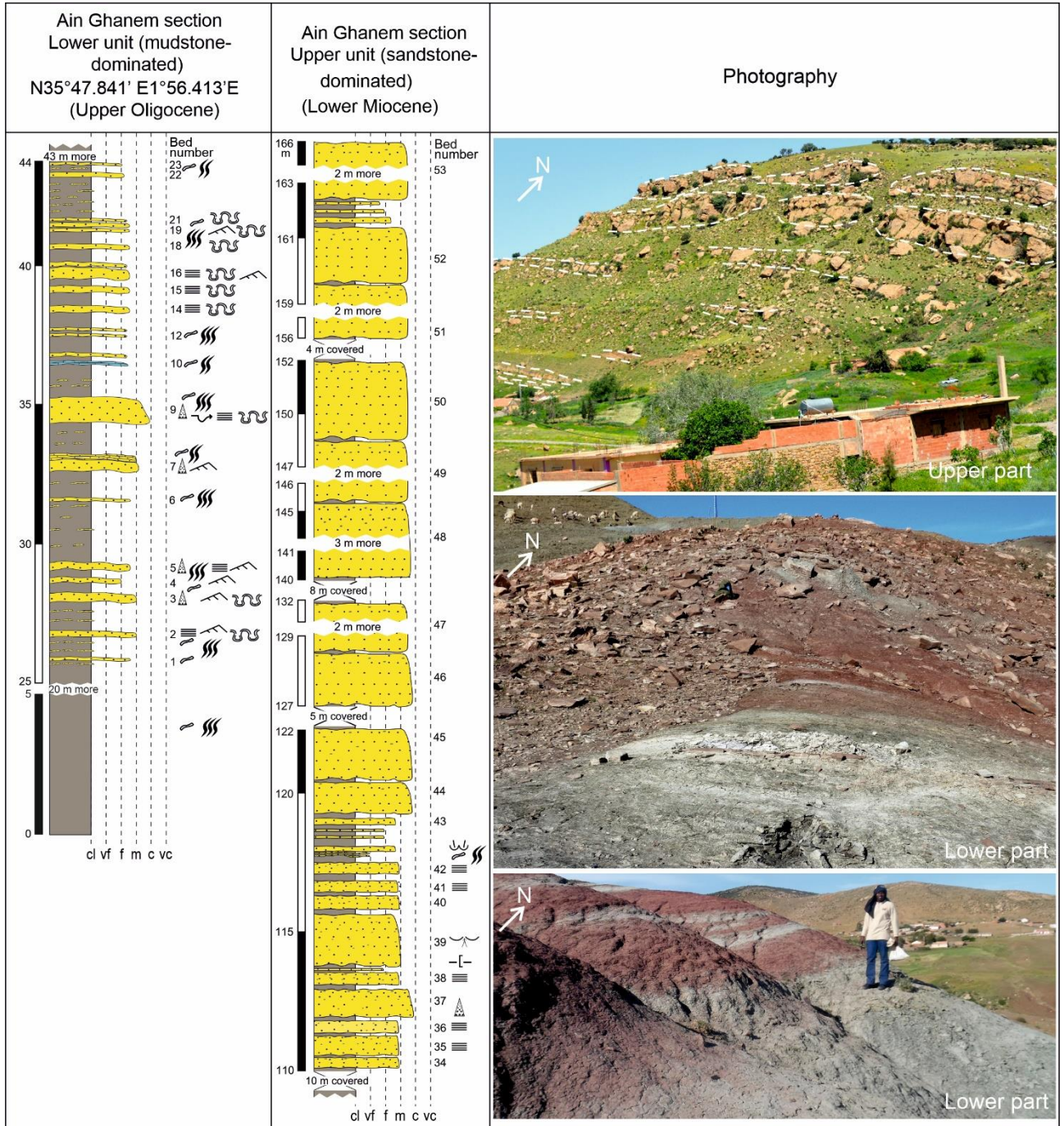


Fig. 11. Lithological column of the Ain Ghanem section with indication of the numbering of beds and sedimentary structures.

2.2.3. KEF MAIZ SECTION

Figs. 12, 13

The Kef Maiz section (GPS-coordinates: N36°3.733' / E1°15.786') is 233 m thick. Beds are tabular in general, striking at NNE–SSW. The section includes two distinct units: the lower unit (mud-dominated) and the upper unit (sand-dominated).

The lower unit: It consists of varicoloured marly mudstones (greenish to dark brown), including some lenticular intercalations of bioturbated fine-grained, medium to thin bedded sandstone (3–30 cm), yellowish to beige, dark brown to greenish in colour. These beds are highly deformed, showing in some cases convolute lamination, whereas the thinner beds show intense bioturbation. Moreover, some deformed thick-bedded sandstone (0.30–2 m), yellowish to beige in colour, was observed as a random isolated mass within marly-mudstone.

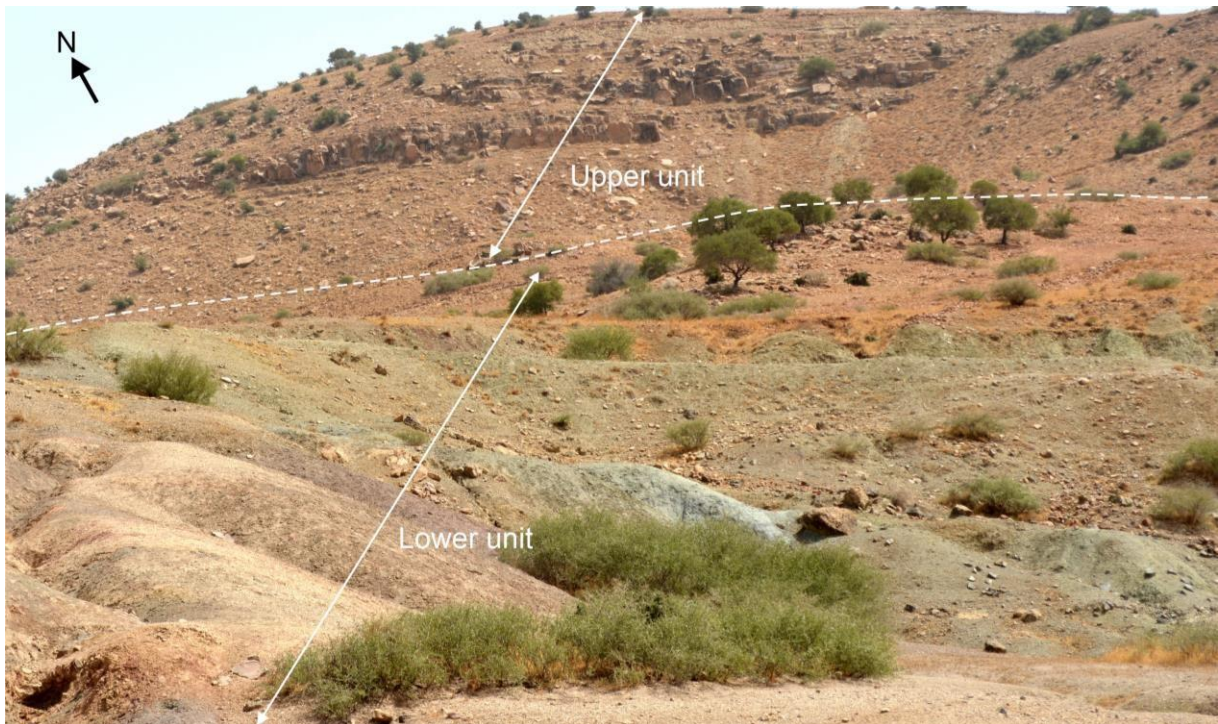


Fig. 12. Panoramic view showing the lower and upper units of the Kef Maiz section.

2.2.3.2. The upper unit: It is made up of greenish, yellowish to fair grey, fine to very coarse-grained, thin to very thick-bedded sandstone (0.05–7 m thick) alternating with greenish mudstone and siltstone (0.07–1.10 m thick) showing in some parts shale fissility. Conglomerate is very rare and occurs as thin gravelly horizons within normally graded sandstone beds. All the sandstone beds have an uneven thickness, with normally-grading or an ungrading and show commonly sharp base and sharp top. Normal graded sandstone shows a commonly irregular base with flute casts, groove casts, amalgamation, ripple marks, and incomplete Bouma

sequence (T_a , T_{bc} , T_{abc} , T_{abce}) with rare fluid escape structures. Convolute lamination occurs separately within siltstone and fine-grained sandstone beds or in association with other Bouma divisions. The ungraded sandstone beds are commonly thick to very thick and show commonly fluid escape structures (pipes, dishes and convolute lamination). The load casts occur commonly on the soles of fine-grained medium sandstone beds. Mud clasts (0.2–10 cm long) are common at the top of medium, thick- to very thick sandstone beds. The mudstone dominated parts include fine-grained thin to medium-bedded sandstone intensively bioturbated and siltstone yellowish to grey in colour as thin lenses within mudstone. Thin to thick silty sandstone, friable beds (0.07–0.80) were observed below the very thick-bedded sandstone.

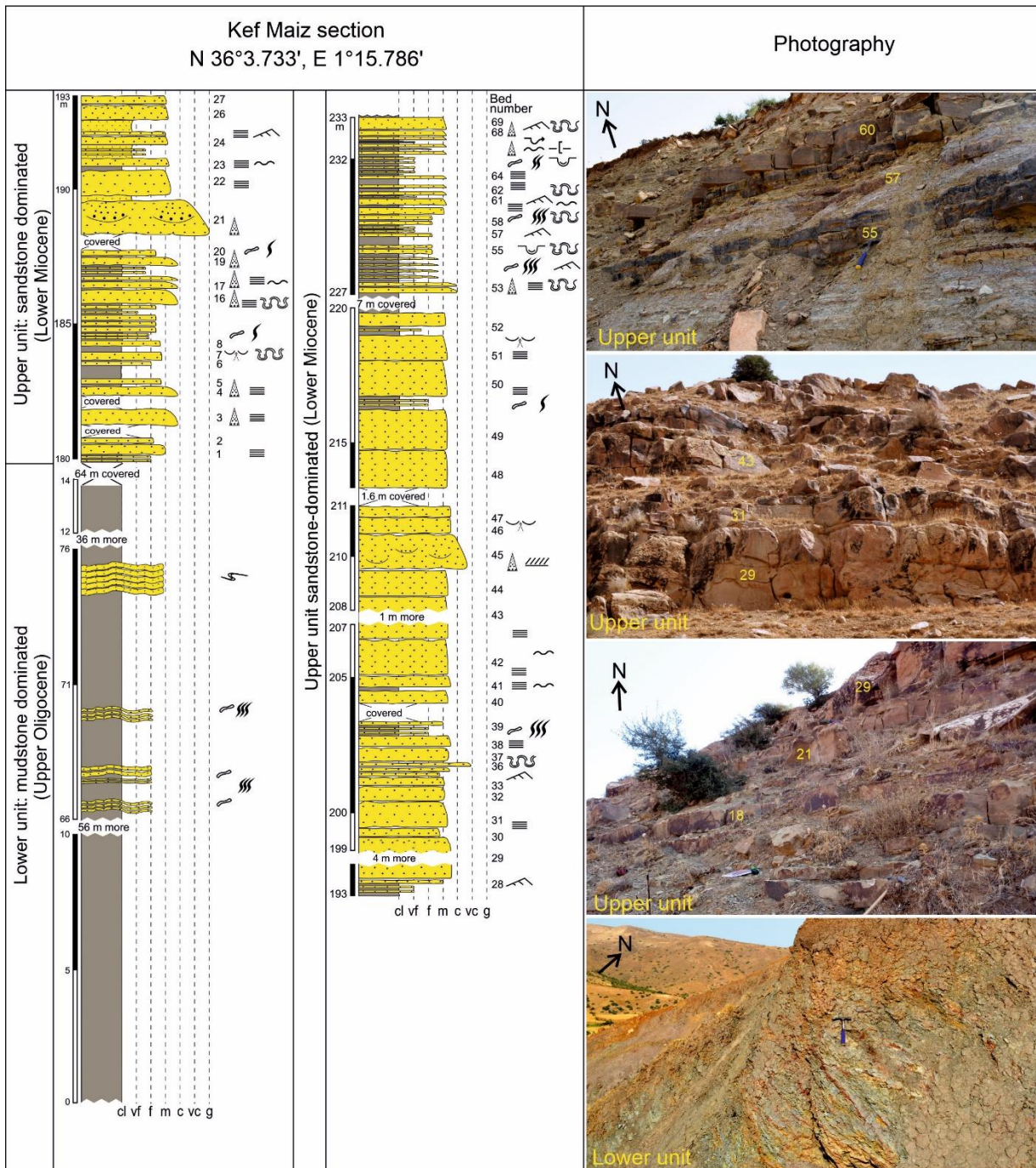


Fig. 13. Lithological column of the Kef Maiz section with indication of the numbering of beds and sedimentary structures.

2.2.4. FORÊT DES CÈDRES SECTION

Figs. 14, 15

This section (GPS-coordinates: N35°52.469', E1°57.020') is well exposed in a road cut; however, only the sand-dominated unit (upper unit) is observed. It is 56 m thick and dominated by sandstone beds (89% of the section) intercalated with mudstones. The beds are in the overturned position steeply dipping (60–70°) towards the SW and striking at approximately 150° (i.e. NNE–SSW). Some faulted/folded beds show gentler dipping. It consists of beige to pale grey/white, fine- to very coarse-grained, medium- to very thick-bedded sandstones (0.15–11 m thick), alternating with greenish to grey, thin silty mudstone units (0.10–0.30 m thick).



Fig. 14. Panoramic view of the Forêt des Cèdres section (A) The lower part, (B) Succession of medium-to thick-bedded sandstone in the middle part of the section.

The sandstone beds are either normally-graded or ungraded. Many of the thicker beds show irregular erosional bases covered by a variety of different sole structures (groove casts, flute marks). At the top, they contain greenish mud clasts, which are 0.2–20 cm long. Most of the thinner sandstone beds are generally fine- to medium-grained, rich in muscovite and trace fossils. They show horizontal, plane-parallel lamination, and more rarely, ripple lamination. Post-depositional deformation structures are common in some beds, especially in fine- to

medium-grained sandstones, including slide and slump structures, load casts, ball-and-pillow structures and fluid escape features. Most of these beds show a sharp and planar base, rather than erosive. Both thickening-up and thinning-up trends are present in some parts.

The top of this section shows thicker mudstone intervals (0.05–1.50 m thick). It includes fine- to medium-grained sandstone beds, 0.10–0.15 m thick, with load casts at their base and ripple marks at their top.

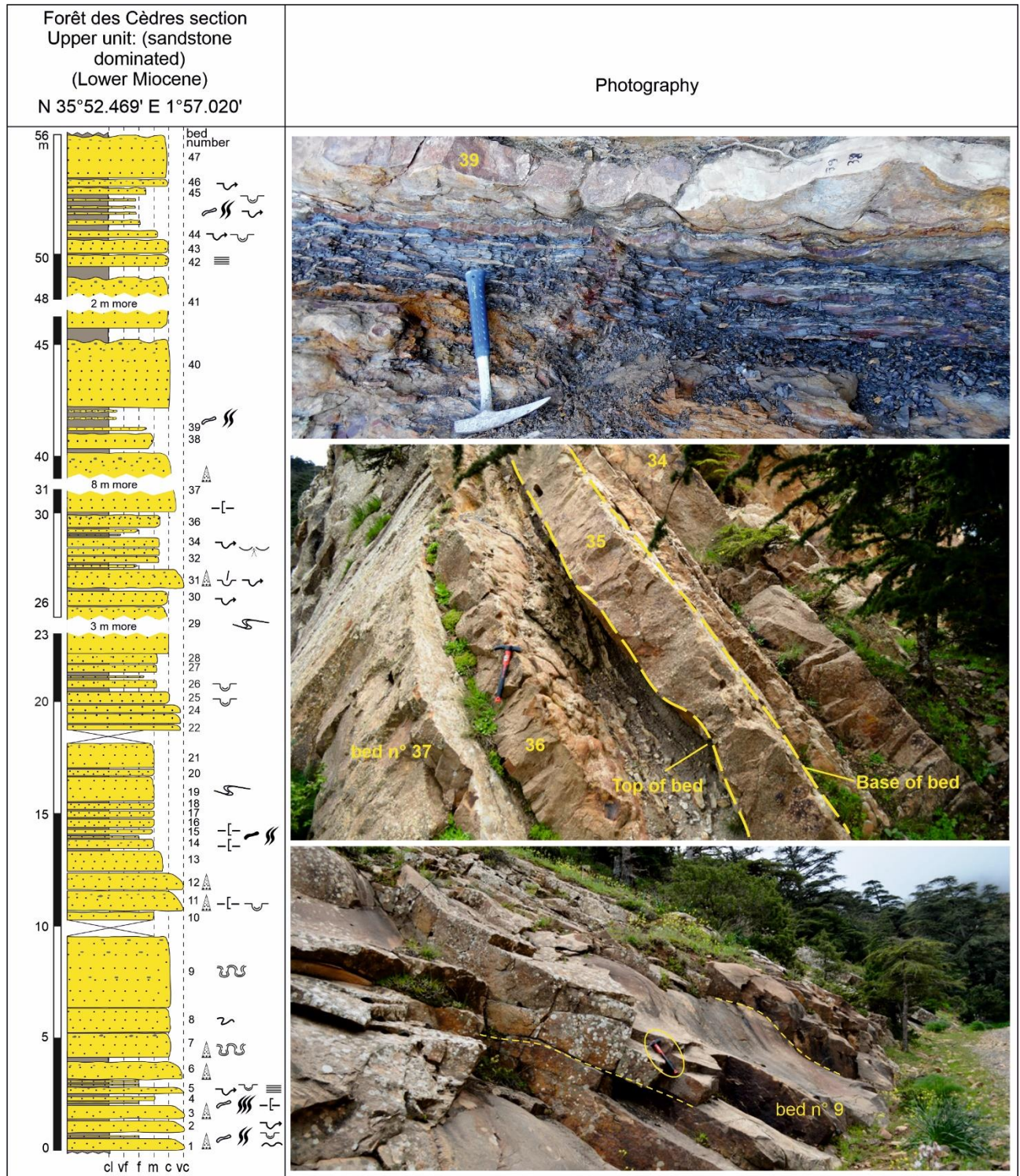


Fig. 15. Lithological column of the Forêt des Cèdres section with indication of the numbering of beds and sedimentary structures.

2.3. PARTIAL CONCLUSIONS

The Numidian Formation in the Ouarsenis Mountains is represented by the four sections described above of siliciclastic deposits with intercalated hemipelagic mudstones. These sections are subdivided into two main informal lithostratigraphic units: (1) the lower unit (mud-dominated) made up of varicoloured mudstones (greenish to dark brown) with abundant full relief trace fossil *Tubulichnium mediterraneum* and rare ?*Alcyonidiopsis* isp., including isolated bodies of sandstone and mudstone alternations or discontinuous thin-bedded, fine grained-sandstone; (2) the upper unit (sand-dominated) consists of beige to pale grey/white, fine- to very coarse-grained, conglomeratic in some parts, medium- to very thick-bedded sandstones, alternating with greenish to grey, thin silty mudstone. The contact between these two units is unclear (covered) in the study area; it is marked by a lithological change. The two upper and lower aforementioned units are present in three of the four sections; the Forêt des Cèdres section comprises only the sand-dominated upper unit.

Based on lithological similarities and biostratigraphic data, correlation between the lithostratigraphic subdivisions here and in the NF of Great Kabylia shows that the lower unit in the study area, dated to the Upper Oligocene by [Mattauer \(1958\)](#) is considered as an equivalent of the lower member in Great Kabylia, dated to the upper Oligocene, and the upper unit as an equivalent of the middle member, which is dated to the Lower Miocene in Great Kabylia ([Raymond, 1976](#)).

Investigations of the calcareous nannoplankton and foraminifers by the author of the thesis are based on several samples. Samples from the lower units contain rare agglutinated foraminifers, such as *Glomospira* sp., *Ammodiscus* sp., *Paratrochamminoides* sp., *Haplophragmoides* sp., *Trochamminoides* sp., and *Recurvoides* sp. Unfortunately, samples from the upper unit appeared to be barren, similarly to previous attempts to find microfossils there. Unlike calcareous nannoplankton and foraminifers, investigations of dinoflagellate cysts in the lower and upper units of the studied sections gave positive results. Both units yielded rich, although taxonomically impoverished, dinoflagellate cyst assemblages associated with other aquatic palynomorphs. Biostratigraphic interpretation of the assemblages from the interval studied is difficult and imprecise so far, but it suggests a time span from the late Paleogene to early Miocene.

CHAPTER 3

SEDIMENTOLOGY

3.1. INTRODUCTION

The NF deposits in the sections studied consist of siliciclastic turbidites associated with hemipelagic mudstones. They are organized into two lithostratigraphic units except for the Forêt des Cèdres section, which shows only the sandstone dominated upper unit. Ten thin sections were prepared and examined under polarizing microscope to confirm lithological determinations in the field and obtain a brief overview of the mineralogical content. The sandstone composition shows a quartz-dominated mineral assemblage, with a minor contribution of feldspar, muscovite, and polycrystalline quartz. Dispersed grains of heavy minerals include zircon, tourmaline, glauconite, and opaque minerals (Fig. 16).

This chapter focuses on the study of lithofacies, their interpretations, and their association to give an overview on the depositional environment. The distribution and occurrence of trace fossils is marked in the lithological columns and mentioned in the description of lithofacies according to their occurrence. The occurrences and abundance of trace fossils are summarized in Table 3.

3.2. LITHOFACIES

Based on bed thickness, sedimentary structures, grain size, texture, and petrographic content, eight distinct facies have been identified (Table 1).

3.2.1. Structureless sandstone (F1)

Fig. 17A, B

This facies consists of fine- to medium-grained, thick- and very thick-bedded sandstones, commonly occurring as a package of amalgamated layers, 0.40–11 m thick and <150 m wide. Individual layers do not show any grading but have sharp, erosional lower boundaries, sharp upper boundaries, and uneven thicknesses. They tend to be structureless, except for some soft-sediment deformation structures, which include fluid-escape structures and load casts. The fine-grained sandstones, which mostly constitute the upper parts of the layers, are rich in muscovite and floating mud clasts. Such layers are occasionally overlain by greenish mudstone with discontinuous siltstone laminae. Trace fossils are absent.

This facies is interpreted to represent deposition from rapidly decelerating concentrated density flows (cf. Arnott and Hand, 1989; Kneller and Branney, 1995) or rapid mass deposition due to intergranular friction in a concentrated dispersion (cf. Pickering and Hiscott,

2015). On a small scale, these beds are comparable to division S3 of Lowe's (1982) sequence and to facies F8 of Mutti (1992).

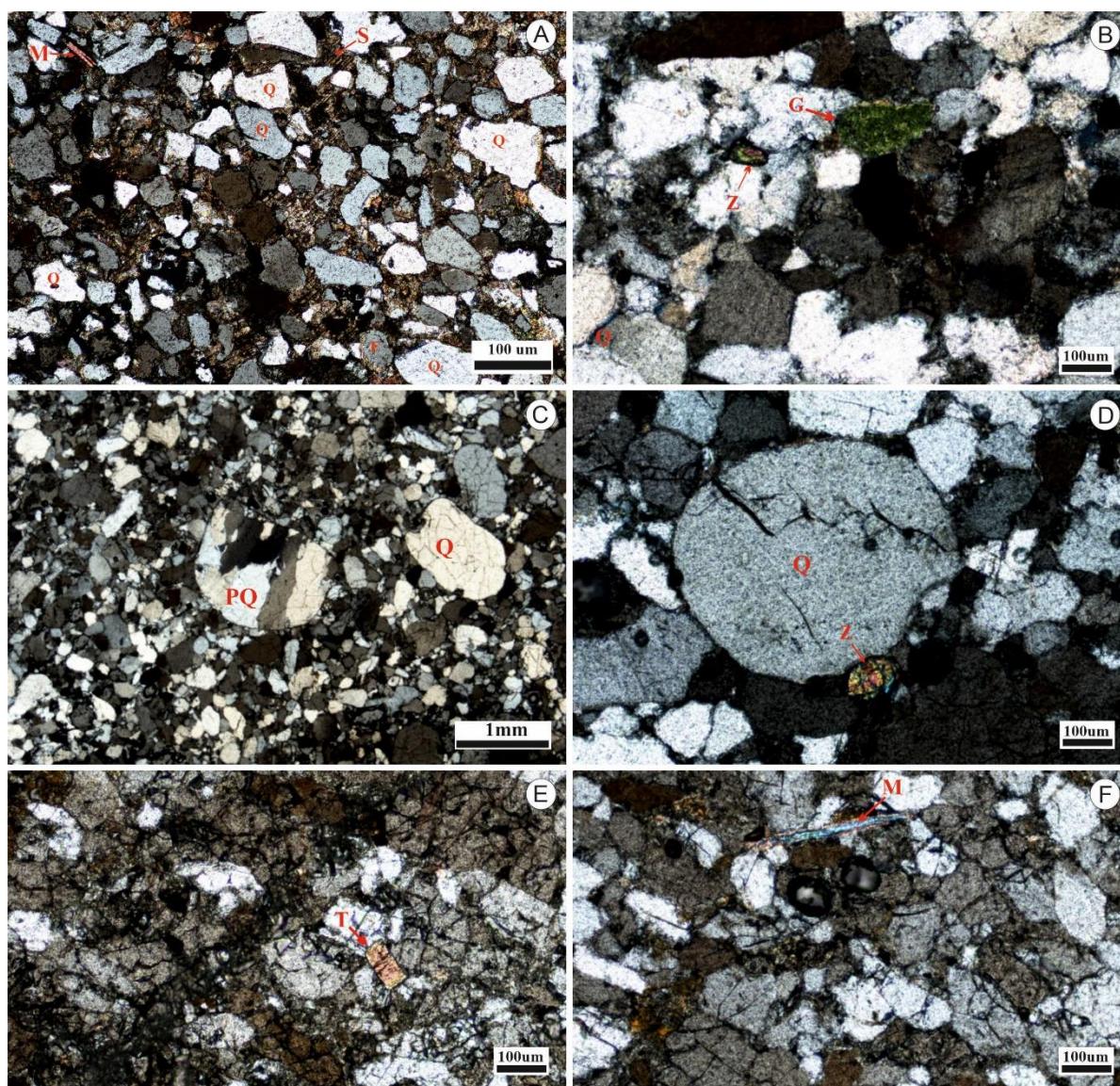


Fig. 16. Photomicrographs of thin section analysis in cross polarized. (A) Subangular to angular quartz grains associated with rare feldspars (F), Muscovite (M), sparite cement (S), Kef Maiz section; (B) Quartz rich thin section including glauconite (G), and zircon grains (z), Forêt des Cèdres section; (C) Polycrystalline quartz grains (PQ), Forêt des Cèdres section; (D) Coarse cracked quartz grain (Q) with zircon crystal (Z), Forêt des Cèdres section; (E) Tourmaline crystal (T), Forêt des Cèdres section; (F) Muscovite (M), Forêt des Cèdres section.

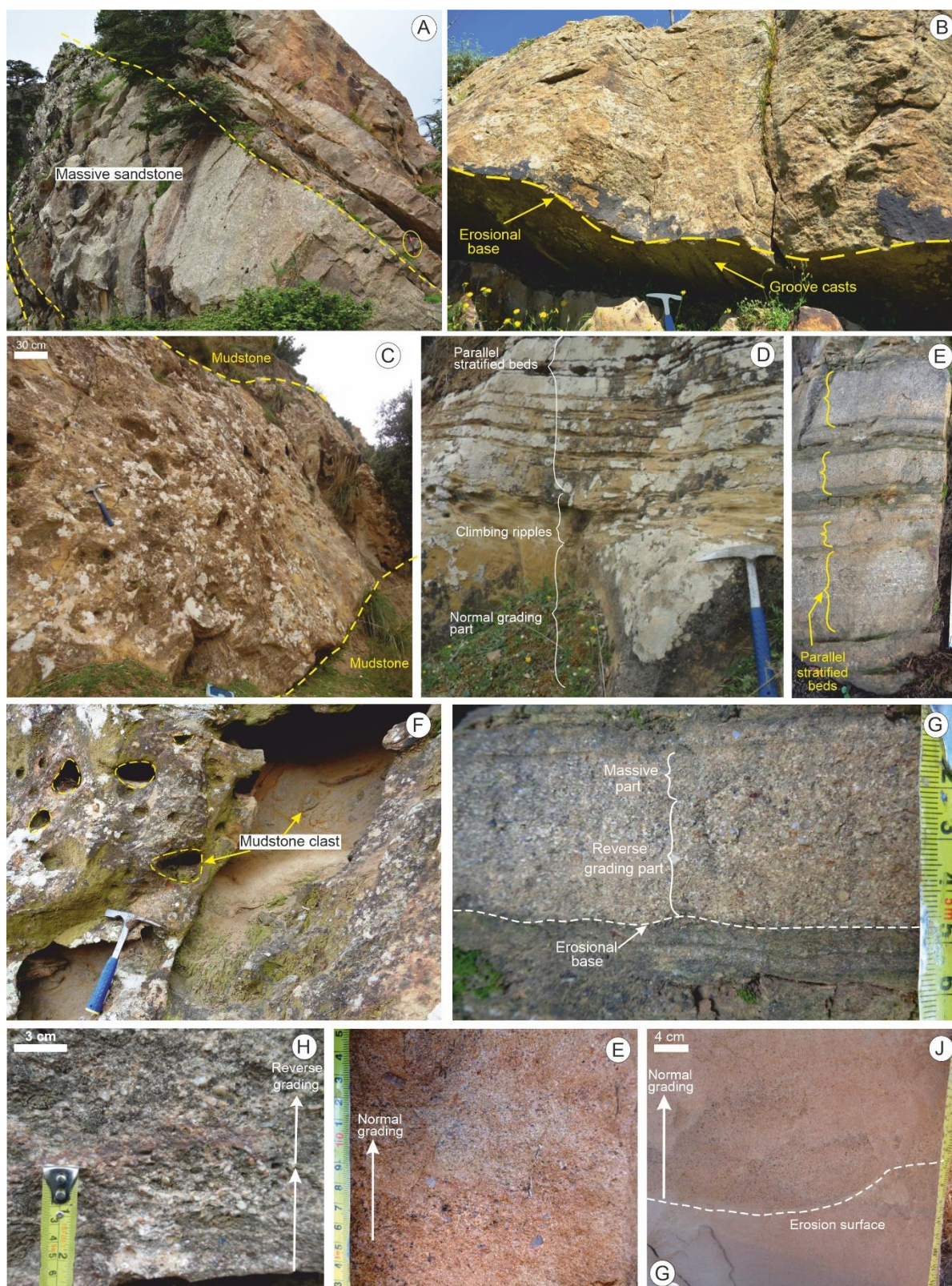


Fig. 17. Photographs of the main described lithofacies. (A) Massif sandstone bed (F1), Forêt des Cèdres section; (B) Massif sandstone bed (F1), Ain Ghanem section; (C), (F) Conglomerates rich in mudstone clasts (F5), upper unit of Kef Rzama section; (D), (E), (G) Inversely-graded pebbly sandstone to parallel stratified sandstone (F3), upper unit of the Kef

Rzama section; (H) Reverse grading in F3, upper unit of Kef Rzama section; (I), (J) Normal grading (F2) from the upper unit of the Ain Ghanem section.

3.2.2. Normally-graded, medium- to very coarse-grained sandstone (F2)

Figs. 17E, J, 18A–E, 19A–H

Facies F2 consists of one bed or a package of two to four beds of medium- to thick-bedded sandstones (10–80 cm thick), which show uneven thicknesses. The sandstones are medium-, coarse- to granule-grained and show normal grading. Their soles show abundant scour marks (gutter casts, flute casts, crescent marks, gutter casts, longitudinal ridge, furrow marks, frondescant marks), tool marks (groove casts), (Fig. 19A–H). Sedimentary structures are frequent, mostly parallel and convolute laminations. In some beds, the normally graded part is followed by plane parallel lamination and occasionally by convolute lamination and ripple cross-lamination. Fluid-escape structures are rare. Some beds show amalgamation. The beds are often overlain by laminated silt- and or mudstone. Greenish floating mud clasts of 0.2–5 cm in size are randomly distributed in the upper part of some beds. Trace fossils are rare; *Thalassinoides* isp. is present within normally graded intervals, and *Ophiomorpha rudis* occurs within intervals with parallel lamination.

This facies is interpreted to probably represent concentrated density flows. The normally graded intervals equivalent to the T_a intervals of Bouma (1962) were deposited grain-by-grain from suspension, with rapid burial and no significant traction transport on the bed (Pickering and Hiscott, 2015). The successive Bouma intervals T_b , T_c , and T_d in the upper part of the layers probably resulted from the continuous deposition by a low-density turbidity current characterized by occasional phases of sediment reworking or bypassing (Talling et al., 2012).

Sole marks are very common within this facies, mostly in the Forêt des Cèdres section, where they are clearly seen on the bases of the overturned beds. A new type of flute-mark structure (Fig. 19) has been documented for the first time on the base of medium-grained sandstone beds (F2) in this section (Menzoul et al., 2019). These features are designated as curved flute marks. It is suggested that they are the result of the flow interaction with an obstacle or an irregular relief on the sea floor in the path of a strong turbidity current. Similar features were generated in laboratory simulations by Dżułyński (1965) and have never been documented from the field.

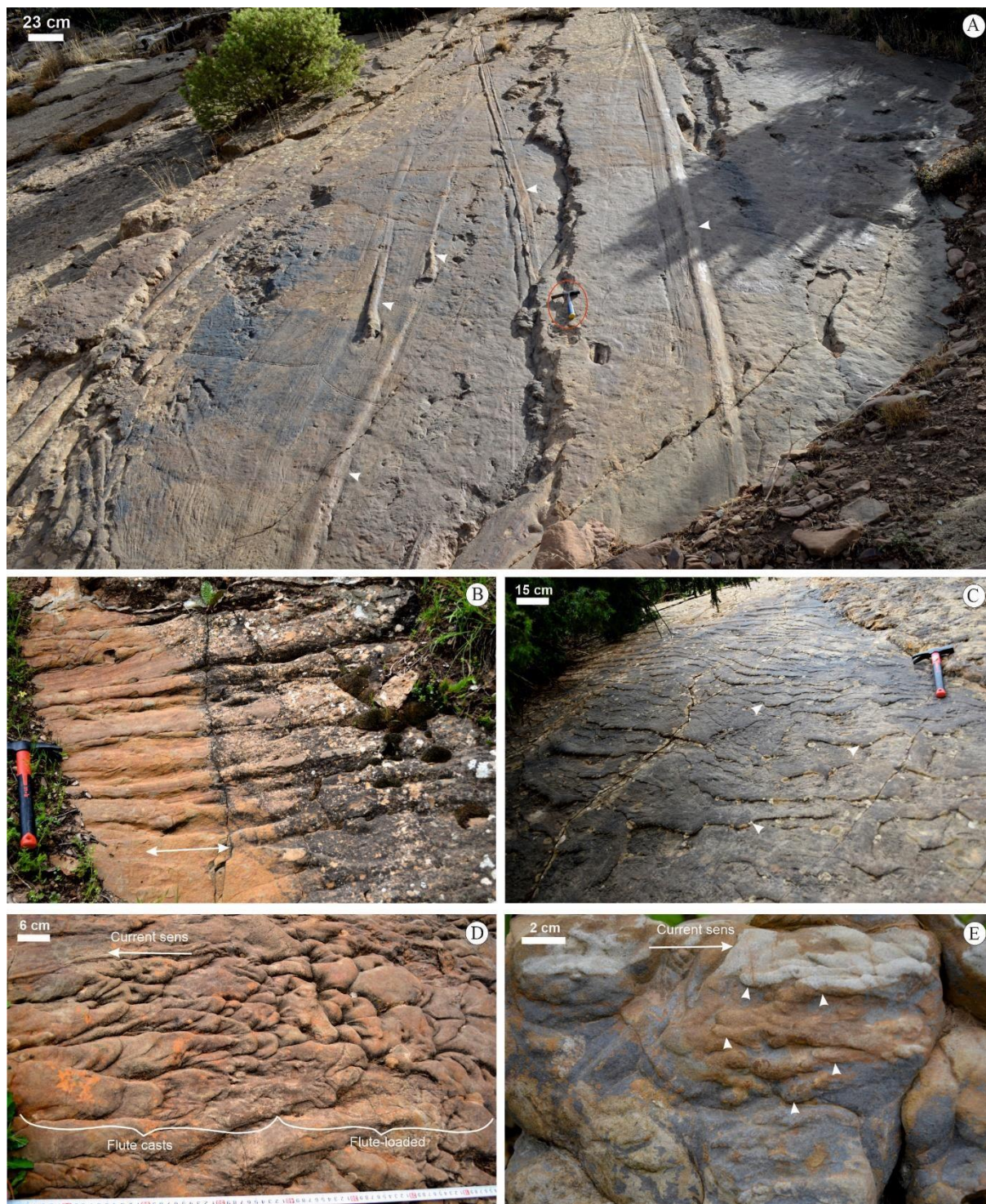


Fig. 18. Photographs of some sole marks from the sections studied. (A), (B) Groove casts within F2, Forêt des Cèdres section; (C) Casts of mud ripples within F2, Forêt des Cèdres section; (D) Flute casts associated with flute-loaded within F2, Forêt des Cèdres section; (E) Small-size flute casts within F4, Forêt des Cèdres section.

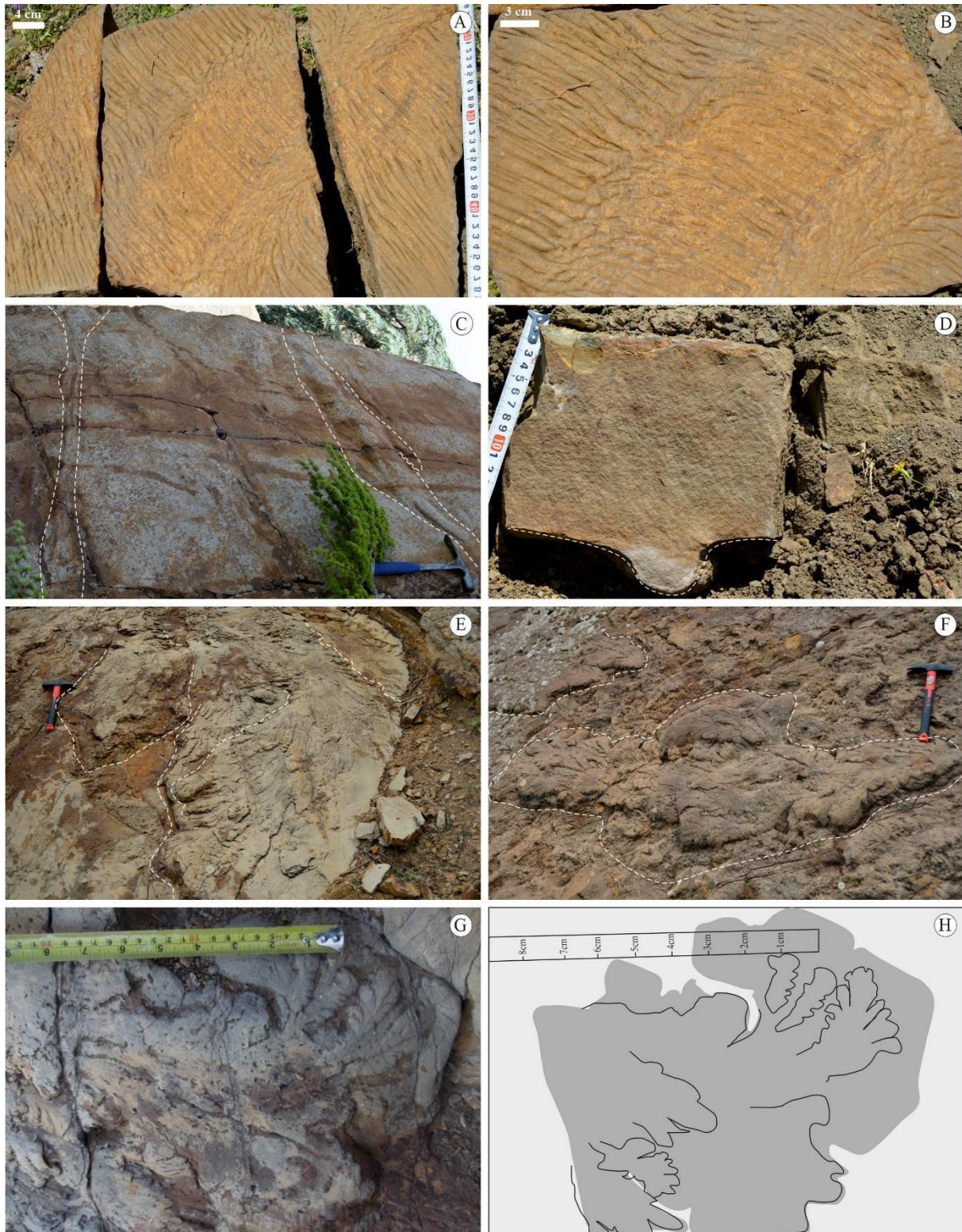


Fig. 19. Photographs of other sole marks from the sections studied. (A), (B) Casts of longitudinal scours (ridge and furrow structures) within F2, upper part of the Ain Ghanem section; (C), (D) Gutter casts within F2, Forêt des Cèdres section; (E), (F), (G), (H) Frondose mark casts, F2 sandstone, Forêt des Cèdres section.



Fig. 20. Photographs of the Curved flute structure; (A), (B) panoramic photographs of the curved flute structure, Forêt des Cèdres section; (C) structure obtained experimentally by [Dżułyński \(1965\)](#) described as asymmetrical flute.

3.2.3. Inversely-graded pebbly sandstone to parallel stratified sandstone (F3)

[Figs. 17D, E, G, H](#)

Facies F3 occurs only once in the Kef Rzama section as a thin package (2–2.60 m thick) of amalgamated sandstone beds. This package begins with an erosional surface. The lower part of the package shows repetitive intervals of inversely graded pebbly sandstones followed by normally graded sandstones and is overlain by sandstone with climbing ripples (ripple drift

cross-lamination). The upper part of the package is composed of repetitive amalgamated layers of medium- to coarse-grained sandstone (10–15 cm thick). Each of these layers has an erosional base; they show inverse grading in the lower part, and massive sandstone in the upper part. Groove casts are common on the sandstone soles. The whole package is overlain by mudstones alternating with siltstones.

The reverse grading is interpreted to result probably from the “kinetic sieve” process, whereby coarser grains rise to the top because of sheared dispersion (Middleton, 1970), or from coarser sub-populations of grains lagging behind finer sub-populations along the transport path (Hand and Ellison, 1985). The sediments were deposited by concentrated density flows (cf.

Pickering and Hiscott, 2015) generating climbing ripples due to simultaneous settling from suspension, with some episodes of bypass (Lowe, 1982). The lower part of the inversely graded beds reflects a traction carpet, similar to the facies F5 of Mutti (1992) and the division S2 of Lowe (1982). The overlying parallel stratified sandstone layers are identical to those that were first described by Hiscott and Middleton (1979) and later referred to as “spaced stratification” by Hiscott (1994b); they are interpreted as a result of concentrated density flows, in which the lower erosional surface and the inversely graded intervals are formed by repeated burst/sweep cycles of large turbulent eddies, and of which the overlying massive part is formed by rapid fallout from suspension. No trace fossils have been found in this facies.

3.2.4. Medium- to fine-grained sandstone (F4)

This facies consists of medium- to thin-bedded sandstones (3–30 cm thick) with uneven thicknesses. Individual layers extend over less than 100 m in the outcrops. Some layers are structureless, whereas others show parallel and/or convolute lamination; rare load casts are present on their soles. Most layers are overlain by mudstone and siltstone. Occasionally, this facies occurs as a unit composed of 2–4 sandstone layers separated by very thin layers of mudstone. Trace fossils are common in the thinner beds; almost all the ichnotaxa mentioned in the present study are present. They include (1) pre-depositional taxa (*Spirophycus bicornis*, *Spirophycus* sp., *Oravaichnium* sp., *Phycodes* sp., *Thorichnus* sp., *Squamodictyon tectiforme*, *Megagraption irregulare*, ?*Arthropycus tenuis*, *Cosmorhapha lobata*, *C. sinuosa*, *Gordia arcuata*, *Helminthoidichnites* sp., *Helminthopsis* sp., *Paleomeandron rude*, *Rutichnus* sp., *Paleodictyon strozzii*) and (2) post-depositional taxa (*Planolites montanus*, *P. beverleyensis*, ?*Planolites* sp., *Siphonichnus* sp., *Nereites* sp., *Chondrites* sp., *Phycosiphon*

incertum, *Taenidium* isp., *Lophoctenium* isp., ?*Scolicia vertebralis*, *S. strozzii*, *Gyrochorte* isp., *Zoophycos* isp., *Oravaichnium* isp., *Halimedes* isp., *Ophiomorpha annulata*, *O. rudis*, *Palaeophycus tubularis*, *Palaeophycus striatus*, *Palaeophycus* isp., ?*Parataenidium* isp., *Thalassinoides* isp., *Tubulichnium rectum*, *Lockeia* isp., and *Diplocraterion* isp.). In contrast to the thin layers with abundant trace fossils, the thicker layers are poorly bioturbated. They may contain *Thalassinoides* isp., *Diplocraterion* isp., and *Zoophycos* isp.

The sediments of this facies are interpreted to have probably been deposited by low-density turbidity currents. Their internal structures correspond to the Bouma (1962) intervals T_a, T_c, T_d, and T_e.



Fig. 21. Photographs of soft-sediment deformation structures from the sections studied. (A), (B) Fluid-escape structures (dish structures) within F1, upper unit of the Kef Maiz section; (C), (D) Fluid-escape structures, F2, lower unit of the Ain Ghanem section; (E), (F) Load casts, F1, Forêt des Cèdres section.

3.2.5. Conglomerates rich in mudstone clasts (F5)

Fig. 17C, F

This facies occurs only in the Kef Rzama section. It is built of very fine- to- medium-grained, very thick-bedded, massive, muddy pebbly sandstones, organized in bodies of variable thickness (1–4 m). The sandstones contain dispersed quartz pebbles, but also contorted huge siltstone and mudstone clasts of up to one metre in size (Fig. 17F). However, most clasts are smaller in size, thus forming intraformational mudstone clasts. These clasts are built of gently to highly folded siltstones, mudstones, or sandstones (similar to facies F4), which show deformed lamination, and ball-and-pillow structures. The lower and upper boundaries of these layers are highly uneven, commonly resulting in a lens shape of the whole body

This facies is interpreted to have been deposited by cohesive debris flows and mudflows (cf. Talling et al., 2012; Pickering and Hiscott, 2015 and references therein).

3.2.6. Strongly deformed sand/siltstones (F6)

Figs. 22A, B, 23B

This facies is characterized by abundant soft-sediment deformation structures (SSDS), commonly within fine- to medium-grained sandstones and siltstones. Deformations range from centimetre-scale (Figs. 22A, B) contorted lamination to slump folds in metre-scale thick-bedded sandstones (Fig. 23B). Contorted lamination commonly occurs within fine-grained, thin- and medium-bedded sandstone/siltstone layers. Fluid-escape structures are common within massive sandstones. Load casts are common on the soles of massive, medium- to fine-grained sandstone layers. Most large folds occur within fine- to medium-grained, medium- to very thick-bedded (dm to m) sandstones, commonly in the sand-dominated part between undisturbed layers or as isolated units in the mud-dominated part of some sections. Ball and pillow structures are common.

The SSDS are interpreted to represent gravitational instabilities (cf. [Allen, 1982](#); [Owen, 1996](#)), reflecting slumping ([Allen, 1982](#)). No trigger mechanism can be deduced with any certainty from the field data, but earthquakes, sediment overloading and wave action seem the most likely ([Owen, 2008](#)).

3.2.7. Mudstones with intercalated sand/silt/mudstones (F7)

[Figs. 22C, B](#)

Facies F7 consists of light green, light grey to dark grey laminated mudstones, 5 cm to 3 m thick. Some parts of the mudstones contain intercalations that start with thin- to very thin-bedded, parallel-laminated sandstone grading into siltstone and mudstone ([Fig. 22C](#)), representing Bouma's (1962) T_d and T_e intervals. These intercalations may form lenses. This facies occurs within all previously described facies.

The Bouma divisions can be compared with [Stow's \(1980\)](#) divisions T6 and T7. This facies results from suspension fall-out during a final gravity flow event associated with hemipelagic sedimentation ([Stow and Piper, 1984](#)).

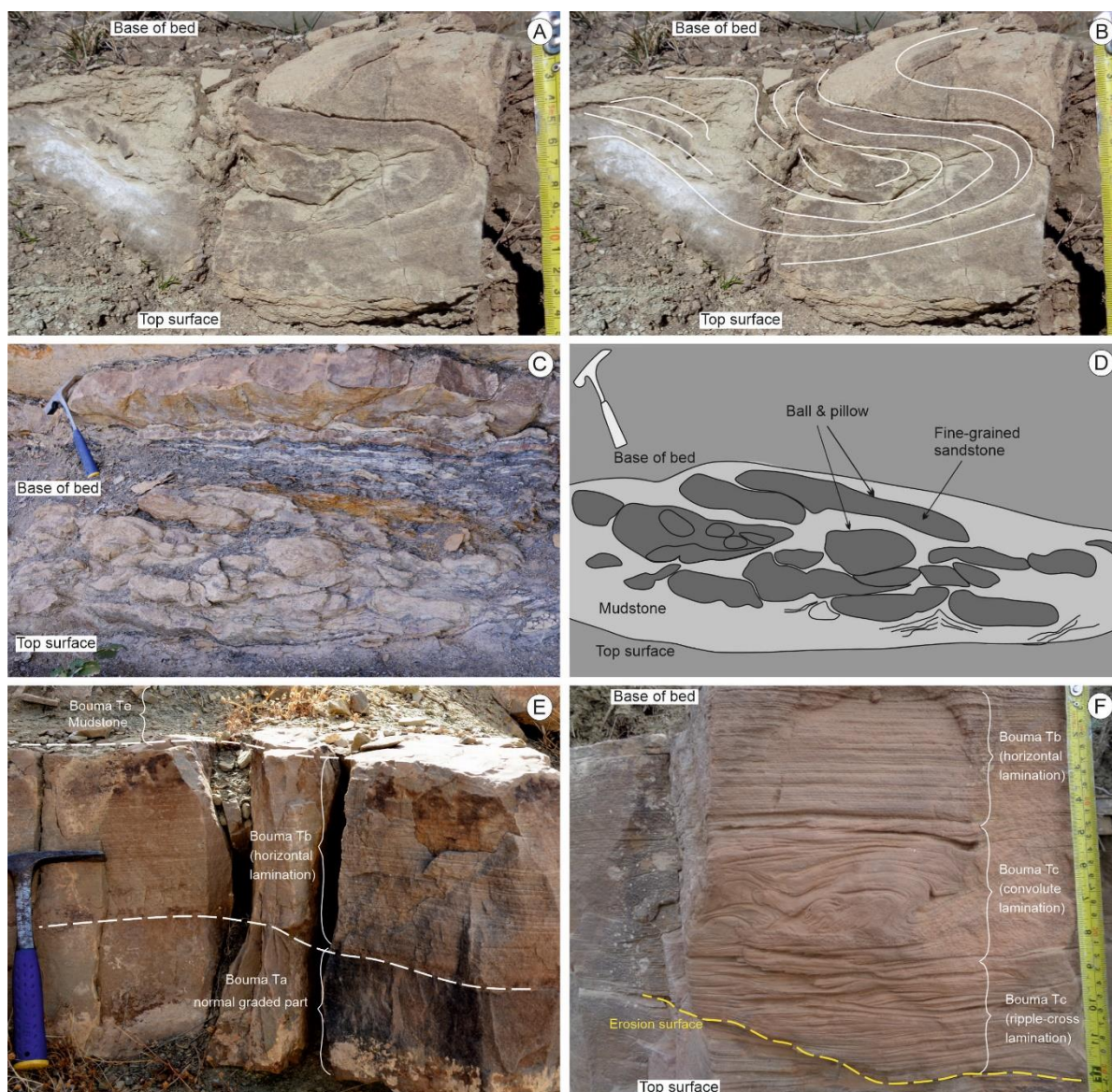


Fig. 22. Photographs showing some soft-sediment deformation structures with incomplete intervals of Bouma sequences within the studied sections. (A), (B) Deformed bed (F6), the lower unit of the Ain Ghanem section; (C), (D) Ball-and-pillow structures within F6, the Forêt des Cèdres section; (E) Incomplete Bouma sequence (F2), the upper unit of the Kef Maiz section; (F) Incomplete Bouma sequence (F2), the lower unit of the Ain Ghanem section.

3.2.8. Marly mudstones (F8)

Fig. 23A, B

Facies F8 constitutes the main component of the lower unit in almost all four sections. It consists of greenish, reddish to dark brown, grey to dark grey massive marly mudstones (Fig. 23A), with 1.11–23% CaCO_3 . The trace fossils ?*Alcyonidiopsis* isp. and *Tubulichnium*

mediterraneum are abundant. There are some discontinuous intercalations of siltstones and thin-bedded fine-grained sandstones, with a ferruginous rusty to brownish colour, with locally parallel lamination. Septarian concretions are common. Isolated slump/slide-deformed, medium to fine-grained sandstones of facies F6 occur as rare intercalations (Fig. 23B). A preliminary biostratigraphic investigation showed the occurrence of rare agglutinated foraminifers such as *Glomospira* sp., *Ammodiscus* sp., *Paratrochamminoides* sp., *Haplophragmoides* sp., *Trochamminoides* sp., and *Recurvoides* sp.

The mudstones are interpreted to have been deposited by suspension settling from a mud cloud after flow cessation and from hemipelagic processes and suspension fall-out during the final phase of gravity flow events. The rare silt/sandstone intercalations result from low-density turbidity currents (Stow and Piper, 1984; Pickering et al., 1986; Stow et al., 1996; Stow and Tabrez, 1998).

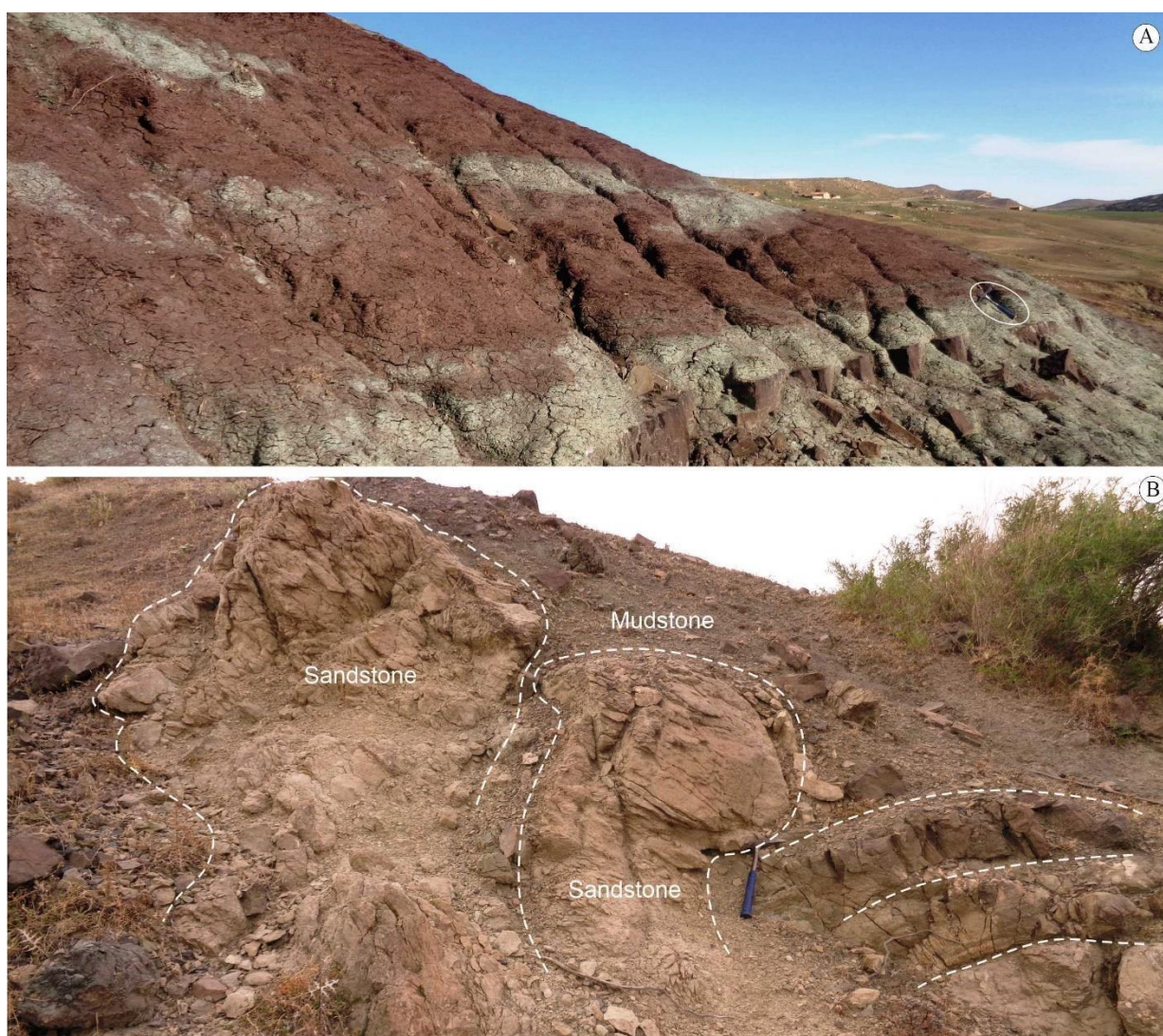


Fig. 23. Photographs of the lower unit of the studied sections; (A) Varicoloured marly mudstone, F8, lower unit of the Ain Ghanem section; (B) Soft-sediment deformed sandstone, F6, lower unit of the Kef Maiz section.

Table 1. Lithofacies of the Numidian Formation in the study area, with their corresponding sedimentary structures, trace fossils and interpretation of the depositional processes.

litho-facies	primary sedimentary structures	Trace fossils	interpretation of the depositional process (es)
F1: Structureless massive sandstones	hydroplastic deformations, fluid-escape structures (pillars and dish structures), load casts		concentrated density flows, deposited from rapidly decelerating flows (Arnett and Hand, 1989; Kneller and Branney, 1995)
F2: normally-graded, medium- to very coarse-grained sandstones	parallel lamination, ripple cross-lamination, scour marks (gutter casts, flute casts, scours around obstacles, gutter casts, longitudinal ridge and furrow marks, and frondescant marks), tool marks (groove casts), rare convolute lamination and fluid-escape structures	<i>Thalassinoides</i> isp., <i>Ophiomorpha rudis</i>	concentrated density flows; the normally graded intervals (Ta intervals of Bouma, 1962) were deposited grain-by-grain from suspension, with rapid burial and no significant traction transport on the bed (Pickering and Hiscott, 2015)

<p>F3: inversely-graded pebbly sandstones to parallel-stratified sandstones</p>	<p>climbing ripple lamination, groove casts</p>	<p>concentrated density flows (Pickering and Hiscott, 2015)</p>
<p>F4: medium- to fine-grained sandstones</p>	<p>abundant convolute lamination, parallel lamination, rare load casts</p>	<p>low-density turbidity currents (Stow & Shanmugam, 1980)</p>

Spirophycus bicornis, *Spirophycus* isp.,
Oravaichnium isp., *Phycodes* isp., *Thorichnus* isp., *Squamodictyon tectiforme*, *Megagraption irregulare*, *?Arthropycustenuis*, *Cosmorhappe lobata*, *C. sinuosa*, *Gordia arcuata*,
Helminthoidichnites isp., *Helminthopsis* isp.,
Paleomeanderonrude, *Rutichnus* isp.,
Paleodictyon strozzii) and (2) post-depositional taxa (*Planolites montanus*, *P. beverleyensis*,
?Planolites isp., *Siphonichnus* isp., *Nereites* isp.,
Chondrites isp., *Phycosiphon incertum*,
Taenidium isp., *Lophoctenium* isp., *?Scolicia vertebralis*, *S. strozzii*, *Gyrochorte* isp.,
Zoophycos isp., *Oravaichnium* isp., *Halimedides* isp., *Ophiomorpha annulata*, *O. rudis*,
Palaeophycus tubularis, *Palaeophycus striatus*,

		<i>Palaeophycus</i> isp., ? <i>Parataenidium</i> isp., <i>Thalassinoides</i> isp., <i>Tubulichnium rectum</i> , <i>Lockeia</i> isp., and <i>Diplocraterion</i> isp.	
F5: conglomerates with mudstone clasts	folded sandstone beds, convolute lamination, ball and pillow structures		cohesive debris flows and mudflows (Talling et al., 2012; Pickering and Hiscott, 2015 and references therein)
F6: sandstone/siltstone deformed while still unlithified	convolute lamination within the siltstones, ball and pillow structures slump folds within the sandstones		convolutions are related to fluidization processes, which create gravitational instabilities (Allen, 1982; Owen, 1996); the slump folds resulted from slope-down shear stress (Allen, 1982)
F7: mudstones with siltstone and sandstone intercalations	parallel lamination		suspension fall-out during a final gravity flow event associated with hemipelagic sedimentation (Stow and Piper, 1984)
F8: varicoloured marly mudstones	parallel lamination	<i>Alcyonidiopsis</i> isp., <i>Tubulichnium mediterraneum</i>	suspension settling of hemipelagic processes and suspension fall-out during last phase of a gravity flow

3.3. DESCRIPTION OF THE STUDIED SECTIONS

Facies and facies association are mentioned here in the description of the sections. The distribution of trace fossils is marked in the lithological columns (Figs. 24–28).

3.3.1. Forêt des Cèdres section

Fig. 24

This section contains only the sand-dominated upper unit of the NF. It belongs to FA1, and consists of beds of facies F1, F2, and F4 (0.15–11 m thick), alternating with facies F7 (0.10–0.30 m thick). The sandstone beds (F4) are generally rich in muscovite and contain trace fossils. Post-depositional deformation structures are common in a few beds, especially in fine- to medium-grained, non-graded sandstone beds (F1), including slump folds, load casts, and fluid escape features. The uppermost part of this section shows thicker mudstone intervals (F7) (0.05–1.50 m thick), including beds of facies F4, which are 0.10–0.15 m thick.

3.3.2. Kef Maiz section

Figs. 25, 26

The section includes two distinct units: (1) a lower unit which is mud-dominated (FA3) and consists of facies F8, contains isolated bodies of FA2 and alternations of mudstones and beds of F4 (3–30 cm); facies F4 is commonly deformed and very rich in trace fossils. Isolated very thin- to thin-bedded sandstones of facies F4 occur separately within the mudstones.

Deformed thick-bedded sandstones (F6) (0.30–2 m) occur randomly as isolated masses within marly mudstone (F8); (2) the upper unit dominated by sand- (FA1), composed of beds of facies F1, F2, and F4 (0.05–7 m thick) alternating with facies F7 (0.07–1.10 m thick). Conglomerates are very rare and occur in thin layers within the sandstone beds (F2). The mudstone dominated intervals (F7) contain beds of facies F4 which are rich in trace fossils. Thin to thick beds of friable (non-cemented) silty sandstones (0.07–0.80 m thick) occur between beds nos. 25 and 26.

3.3.3. Kef Rzama section

Fig. 27

This section comprises (1) a lower unit dominated by varicoloured mudstones (facies association FA3), very rich in full relief trace fossils *Tubulichnium mediterraneum* and rare

?*Alcyonidiopsis* isp., and (2) an upper unit, which is sand-dominated (FA1) and consists of facies F1, F2, F3, F5, and F4 (0.07–6 m thick) alternating with facies F7 (0.05–3 m thick).

3.3.4. Ain Ghanem section

Fig. 28

This section includes (1) the unit, mud-dominated (FA3), with the abundant full relief trace fossil *Tubulichnium mediterraneum*, including isolated bodies of FA2, composed of an alternation of mudstone and beds of facies F4, F2 (0.03–0.75 m), commonly deformed, and in an overturned position, showing different dip angles. The thinner beds of facies F4 are intensively bioturbated. A single thin limestone bed (0.07 m), greenish in colour, occurs within a series of thin beds of facies F4; (2) the upper unit is sand-dominated (FA1), composed of beds of facies F1 and F2 (0.05–6 m), including a few intercalations of facies F7 (0.05–3 m). The mudstone dominated intervals (F7) include thin ferruginized beds (F4) rich in *Tubulichnium mediterraneum* and septarian concretions.

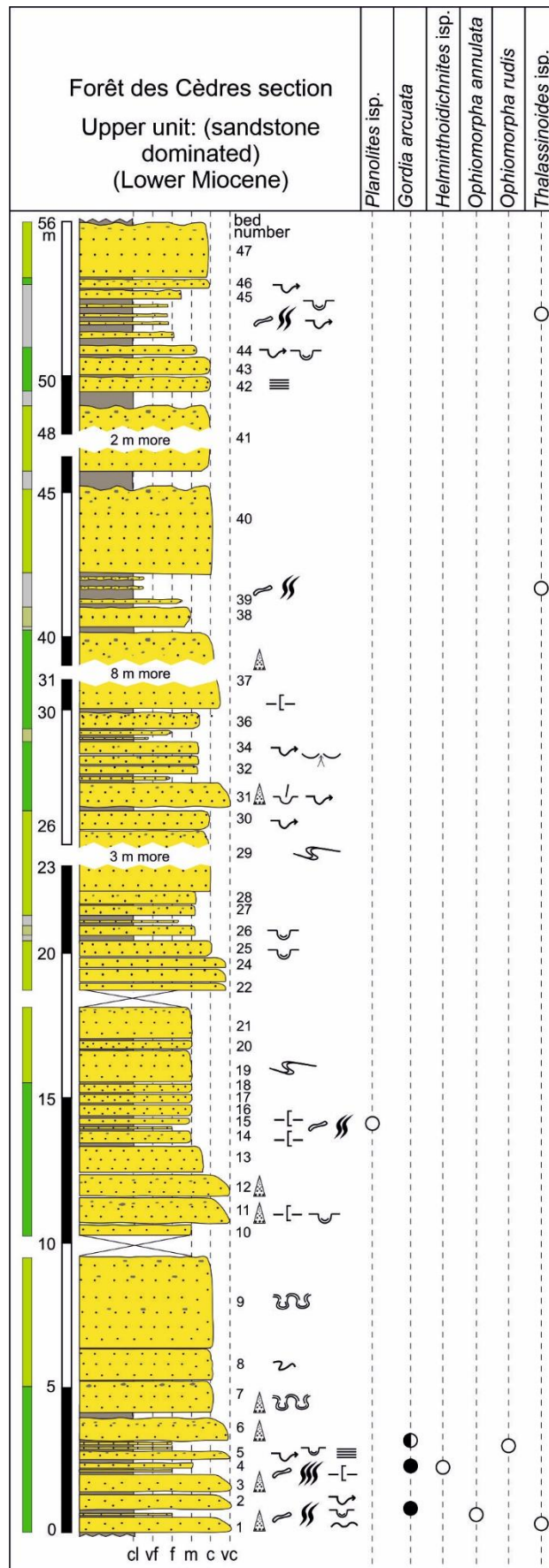


Fig. 24. Lithological column of the Forêt des Cèdres section with indication of the numbering of beds, trace fossils and sedimentary structures.

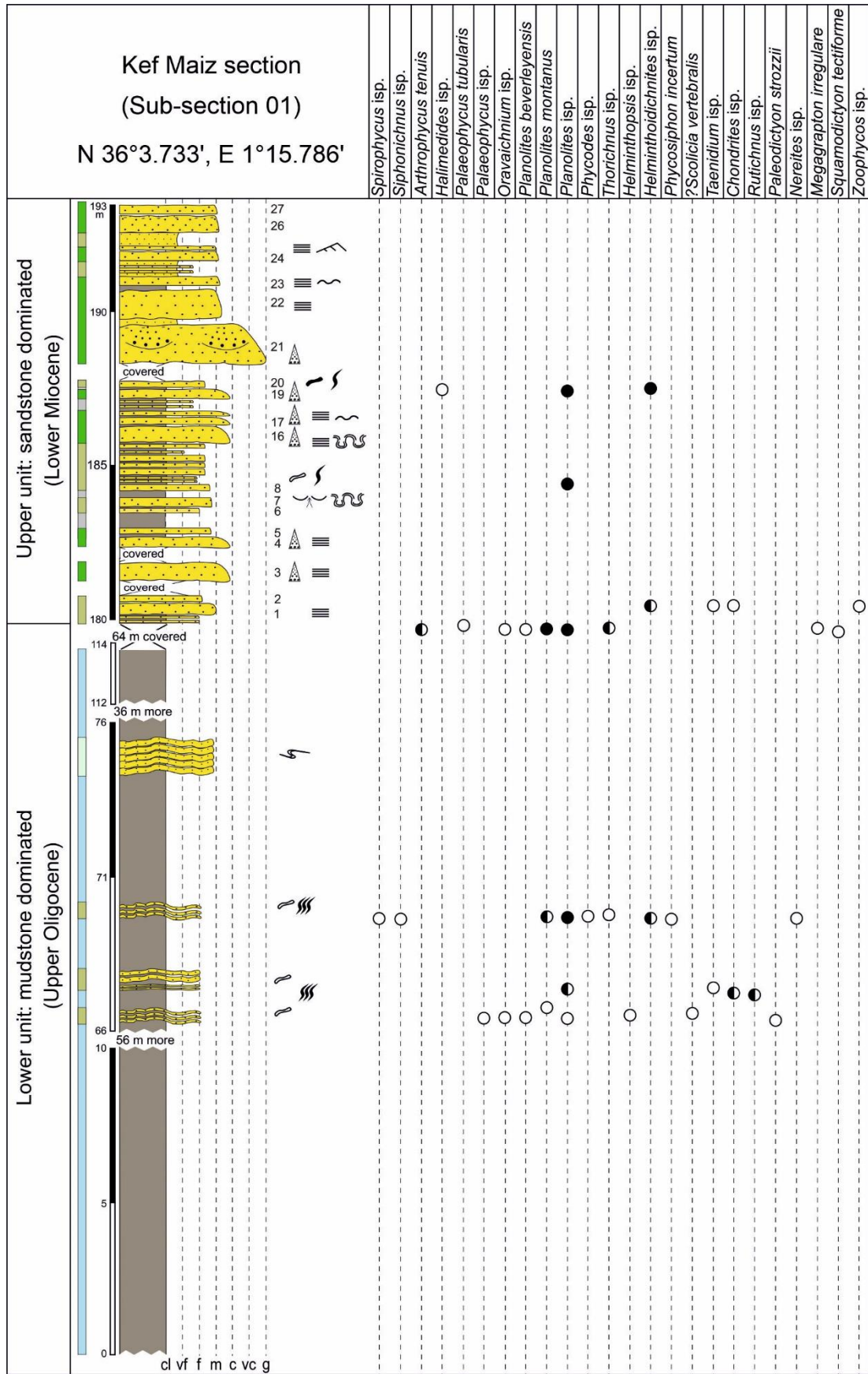


Fig. 25. Lithological column (part 01) of the Kef Maiz section with indication of the numbering of beds, trace fossils and sedimentary structures.

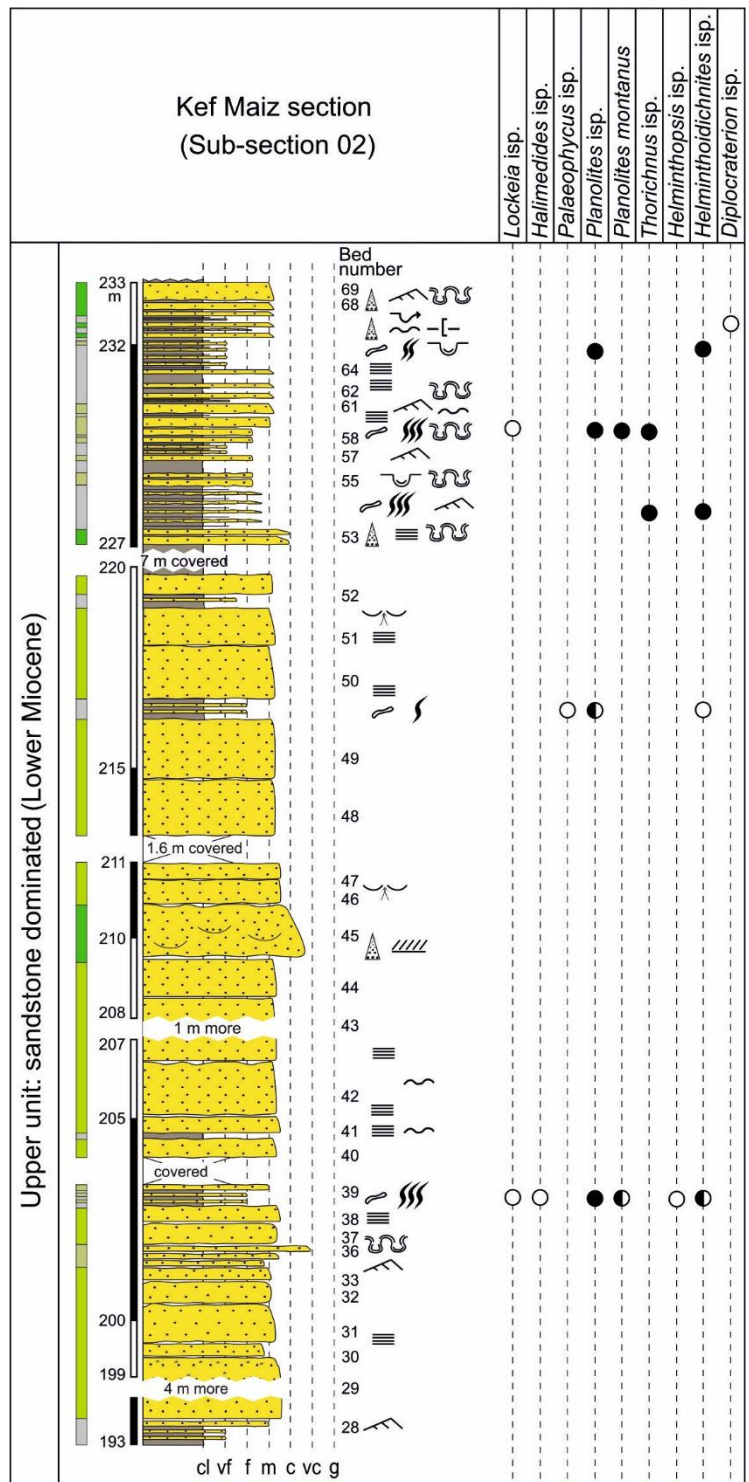


Fig. 26. Lithological column (part 02) of the Kef Maiz section with indication of the numbering of beds, trace fossils and sedimentary structures.

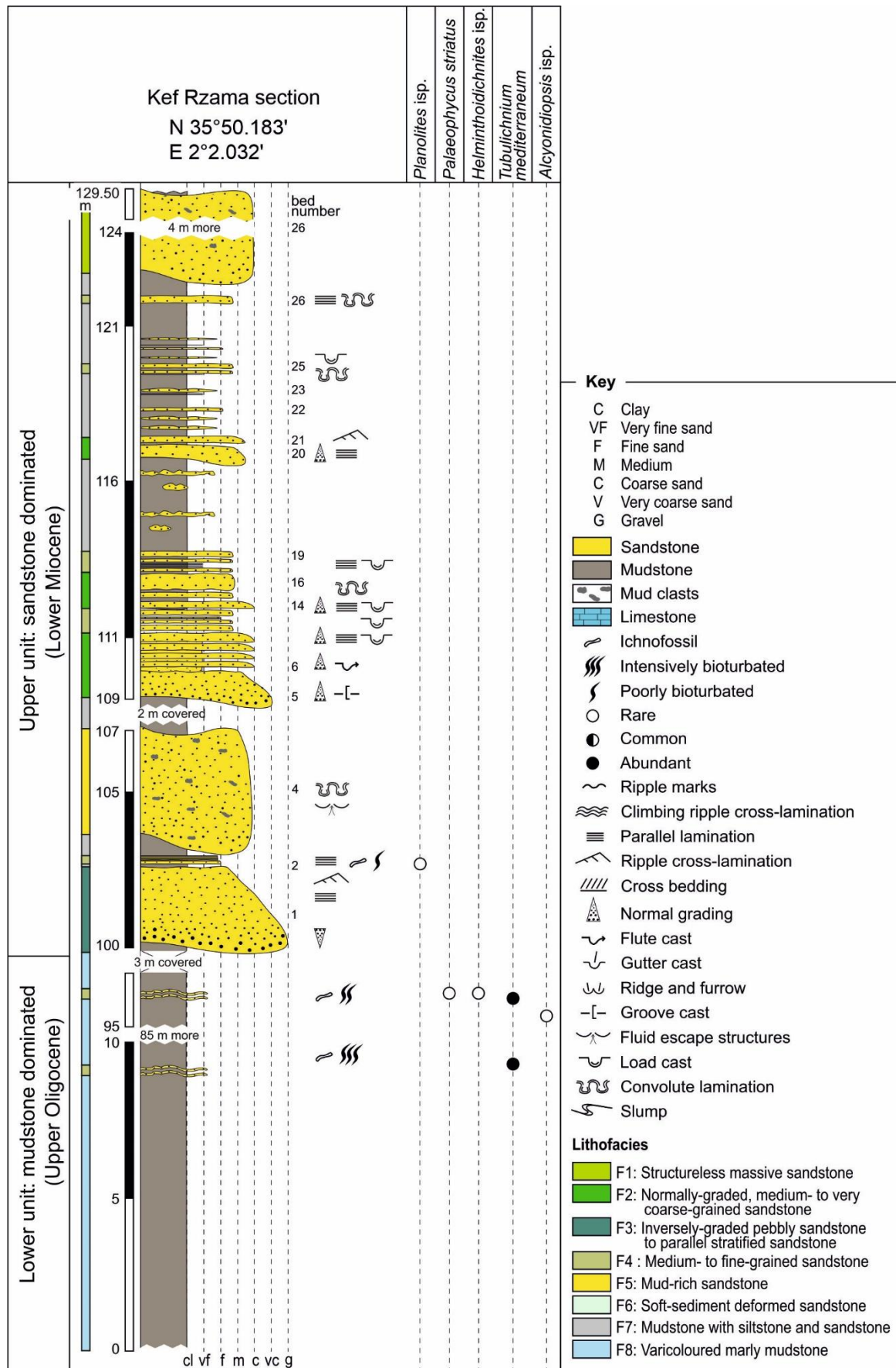


Fig. 27. Lithological column of the Kef Rzama section with indication of the numbering of beds, trace fossils and sedimentary structures.

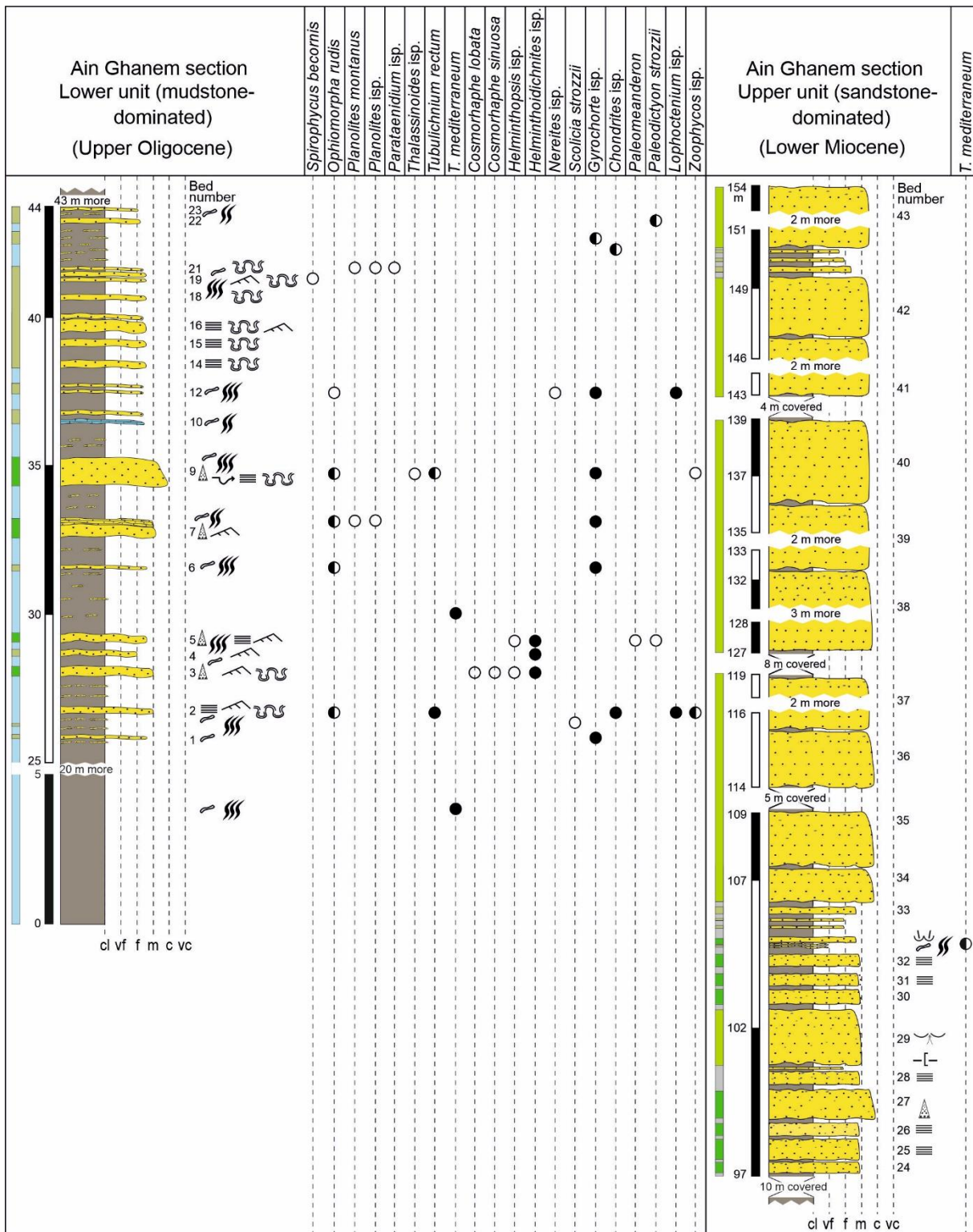


Fig. 28. Lithological column of the Ain Ghanem section with indication of the numbering of beds, trace fossils and sedimentary structures.

3.4. FACIES ASSOCIATIONS

The eight lithofacies can be grouped into three facies associations (FA1 through FA3). Each facies association corresponds to a specific depositional sub-environment.

3.4.1. Sand-rich channel fills (FA1)

The facies association FA1 forms the upper part of the four sections studied. It consists mostly of massive sandstones from facies F1, which form packages of amalgamated sandstone layers, with or without mudstone intercalations of facies F7. Facies F2, F4 and F6 are less common, and facies F5 is rare. FA1 is 30–60 m thick and occurs in bodies up to 150 m wide which commonly show a thinning- and fining-upward trend. These bodies are interbedded with, or pass laterally into, FA2. Facies F3 and F5 occur only in the upper unit of the Kef Rzama section as isolated thick beds overlain by facies F7 and subsequently facies F1. Trace fossils (*Thalassinoides* isp. and *Ophiomorpha rudis*) occur within the thinner sandstone layers.

FA1 is comparable to the massive sandstone facies, including deep-water massive sands (DWMS) described by [Stow and Johansson \(2000\)](#) and interpreted as the product of high-density turbidity currents and sandy debris flows. This facies association has also been reported from the Numidian Formation of Sicily ([Johansson et al., 1998](#)) and Tunisia ([Riahi et al., 2009](#); [Riahi et al., 2021](#)).

The main features of FA1, such as the high sand content, the frequent erosional features, amalgamation, lateral discontinuity of beds, and fining- and thinning-upward trends are characteristic of a channel-fill environment ([Mutti and Ricci Lucchi, 1975](#); [Walker, 1978](#); [Hendry, 1978](#); [Normark, 1978](#); [Stow and Johansson, 2000](#); [Huneke and Mulder, 2010](#)).

3.4.2. Mudstone and sandstone alternations from channel margins, channel/levee/overbank systems, crevasse-splays and lobes (FA2)

This facies association is built mainly by facies F4 and F7, and occasionally facies F2. It is represented by fine-, medium- to coarse-grained, thin- to medium-bedded sandstones (a few to 50 cm thick), alternating with thin- to very thick-bedded mudstones and siltstones (F7). The sediments of this association form lenticular bodies (<50 m wide) in the transverse section. The layers of facies F2 consist of incomplete Bouma intervals (T_{ae} , T_{ade} , T_{ae} , T_{bde} , T_{bcde} , T_{cde}), and show thinning, thickening- and fining-upward trends.

This facies association is interpreted as the product of medium- to low-density turbidity currents that interrupt hemipelagic sedimentation. It occurs in three main stratigraphic positions: (1) in the lower part (Upper Oligocene) of the Ain Ghanem and Kef Maiz sections as isolated lithological units within the marly mudstone of facies F8, (2) in the lower part of the upper unit of the Kef Maiz section, and (3) as intercalations with association FA1 in the upper unit of all the sections under study here. These features jointly suggest deposition within narrow submarine channels and/or in a crevasse-splay setting (Mutti and Ricci Lucchi, 1975; Walker, 1978; Hendry, 1978; Normark, 1978; Stow and Johansson, 2000; Huneke and Mulder, 2010; Pickering and Hiscott, 2015 and references therein). The alternations of mudstones and siltstones of facies F7 and the sandstones of facies F4, the folds, the incomplete Bouma intervals, and the thinning- and fining-upward trends suggest deposition within a channel/levee/overbank setting or a crevasse-splay setting (cf. Pickering et al., 1995; Hubbard et al., 2008; Huneke and Mulder, 2010; Pickering and Hiscott, 2015). The upward thickening of the beds, characterized by tabular morphology and a well-developed cyclicity suggest deposition within lobes setting (Mutti and Ricci Lucchi, 1975).

3.4.3. Basin floor mudstones (FA3)

This facies association is composed mainly of facies F8 and is present in the lower unit of three of the sections under study; it is not present in the Forêt des Cèdres section. It forms isolated bodies of mudstone/sandstone alternations of facies association FA2 (F7 alternating with F2 and F4, <50 m wide), slumped units of medium- to fine-grained sandstones (F6), and rare thin- to very thin-bedded sandstones isolated within mudstones. Trace fossils are common (?*Alcyonidiopsis* sp. and *Tubulichnium mediterraneum*). The latter trace fossil has also been reported from the deep-sea Cretaceous-Palaeogene mudstones of the lower part of the Numidian Formation in the Mediterranean region (Pautot et al., 1975).

The joint characteristics simply show that these sediments were deposited on a basin floor or on a sloping apron cut by sparse, narrow channels. The channels were occasionally fed by turbidites, which penetrated the channel levees and formed crevasse-splay deposits and small lobes at their distal end. The abundance of facies F6, mostly in the Kef Maiz section, also suggests deposition in a slope setting (cf. Stow and Johansson, 2000).

Table 2. Description and interpretation of the three facies associations of the Numidian Formation in the study area.

facies association	lithology	included lithofacies	description	interpretation of the depositional sub-environment
FA1	mostly sandstones	F1, F2, F7, F5, F4	packages of amalgamated massive sandstones, with or without mudstone intercalations; characterised by erosional features, lateral discontinuity of beds, and fining- and thinning-upward trends	channel-filling on submarine fans
FA2	alternating mudstones and sandstones	F4, F7, F6, F2	Fine-, medium- to coarse-grained, thin- to medium-bedded sandstone (a few centimetres to 50 cm thick) alternating with thin- to very thick-bedded mudstones and siltstones	channel margins with, levees, crevasse and overbank deposits, probably on lobes
FA3	mostly mudstones	F8, F7, F5, F6	marly mudstones, occasionally isolated bodies of alternating mudstones and sandstones; occasional slumps of medium- to fine-grained sandstones	basin floor or slope aprons cut by sparse, narrow channels

3.5. PARTIAL CONCLUSION

The sedimentological study of the NF in the Ouarsenis Mountains, NW Algeria, permit to characterize eight main lithofacies including structureless sandstone (F1), normally-graded, medium- to very coarse-grained sandstone (F2), inversely-graded pebbly sandstone to parallel stratified sandstone (F3), medium- to fine-grained sandstone (F4), and mudclast conglomerates (F5), soft-sediment deformed sandstone/siltstone (F6), mudstone with siltstone and sandstone (F7), and varicoloured marly mudstone (F8). The association of these lithofacies yielded three main facies associations, corresponding to the depositional subenvironment setting, including (1) FA1 sand-rich facies association deposited in the channel-fill setting. It occurs in the upper part of all the studied sections; (2) FA2 mudstone and sandstone alternations facies association, corresponding to channel margin, channel-levee-overbank, crevasse-splays and lobes. This facies association occurs occasionally in the lower and the upper unit of the studied sections; (3) FA3 mud-rich facies association deposited on the basin-floor or slope-apron settings, which were cut by sparse, narrow channels, occurring in the lower unit of all the studied sections except for the Forêt des Cèdres section.

CHAPTER 4

ICHOLOGY & PALAEOENVIRONMENT

4.1. INTRODUCTION

Ichnology is the study of biogenic sedimentary structures formed by organisms (plants, animals, and microbes) as a result of their life activity by modifying the original structure of the substrate. It involves both disciplines, paleontology, and sedimentology. According to (Schafer, 1956), two main categories of biogenic sedimentary structures are distinguished; (1) trace fossils, which have a distinct shape with clear outlines, permitting their classification; (2) biodeformational structures, do not show a definite shape nor a clear outline, and which destroy the pre-existing structures (e.g., Wetzel, 1983).

Ichnology is considered a powerful tool for the recognition of the sedimentary environment, especially when it is coupled with sedimentological and palaeontological data (e.g., Buatois and Mángano, 2011). This chapter is dedicated to the study of trace fossils occurring in the Numidian Formation of the Ouarsenis Mountains, including their detailed systematic description, palaeoenvironmental significance, and a comparison with their analogue deposits in the Mediterranean. The distribution and occurrence of trace fossils is marked in the lithological columns and mentioned in the description of lithofacies according to their occurrence in the third chapter. The occurrences and abundance of trace fossils are summarized in Table 3. The data presented in this chapter have already been published in a paper intituled "Deep-sea trace fossils from the Numidian Formation (Upper Oligocene – Lower Miocene) in the Ouarsenis Mountains, north-western Algeria" (Menzoul et al., 2022).

4.2. SYSTEMATIC DESCRIPTION OF TRACE FOSSILS

4.2.1. Circular and elliptical structures

Lockeia James, 1879 *Lockeia* isp.

Fig. 29B, C

Description. A hypichnial, isolated, elongate, slightly curved, smooth, almond-shaped mound, preserved in full relief. The two illustrated specimens are 13 mm long and 8 mm wide, and 9 mm long and 4 mm wide.

Remarks. *Lockeia* is commonly interpreted as a bivalve resting trace produced by its wedgeshape foot (Seilacher and Seilacher-Drexler, 1994). However, small crustaceans may also

produce such traces (Bromley and Asgaard, 1979). *Lockeia* in general occurs in marine and non-marine environments since the ?late Cambrian (Fillion and Pickerill, 1990).

4.2.2. Spiral structures

Spirophycus Häntzschel, 1962

Spirophycus bicornis (Heer, 1877)

Fig. 29G, I, J

Description. Hypichnial, horizontal, semi-circular ridge ending with one spiral whorl. The analysed specimens are 10–30 mm wide, at least 40–115 mm long, filled with the same material as the host sediment, smooth or occasionally covered with rare tubercles and preserved in semirelief. The spiral whorl is 48–75 mm wide.

Remarks. *Spirophycus* has been considered as a preservational variant of *Nereites* MacLeay (Wetzel vide Uchman, 1998). It is commonly reported in deep-sea turbiditic deposits (e.g., Seilacher, 2007).

Spirophycus isp.

Fig. 29F

Description. Incompletely preserved hypichnial smooth ridge with an incomplete circular whorl at the end. The ridge is 6–9 mm wide, preserved in semi-relief and filled with the same material as the host sediment. The whorl is 55 mm in diameter.

Remarks. Radius of the whorl with respect to the width of the ridge is larger than in *Spirophycus bicornis*.

4.2.3. Simple and branched structures

Siphonichnus Stanistreet, le Blanc Smith and Cadle, 1980

Siphonichnus isp.

Fig. 29E

Description. Hypichnial, circular, flat-top mound with steep flanks. It shows a circular depression in the centre. The mound is 4.5–5.5 mm in diameter and the central depression is 2 mm in diameter.

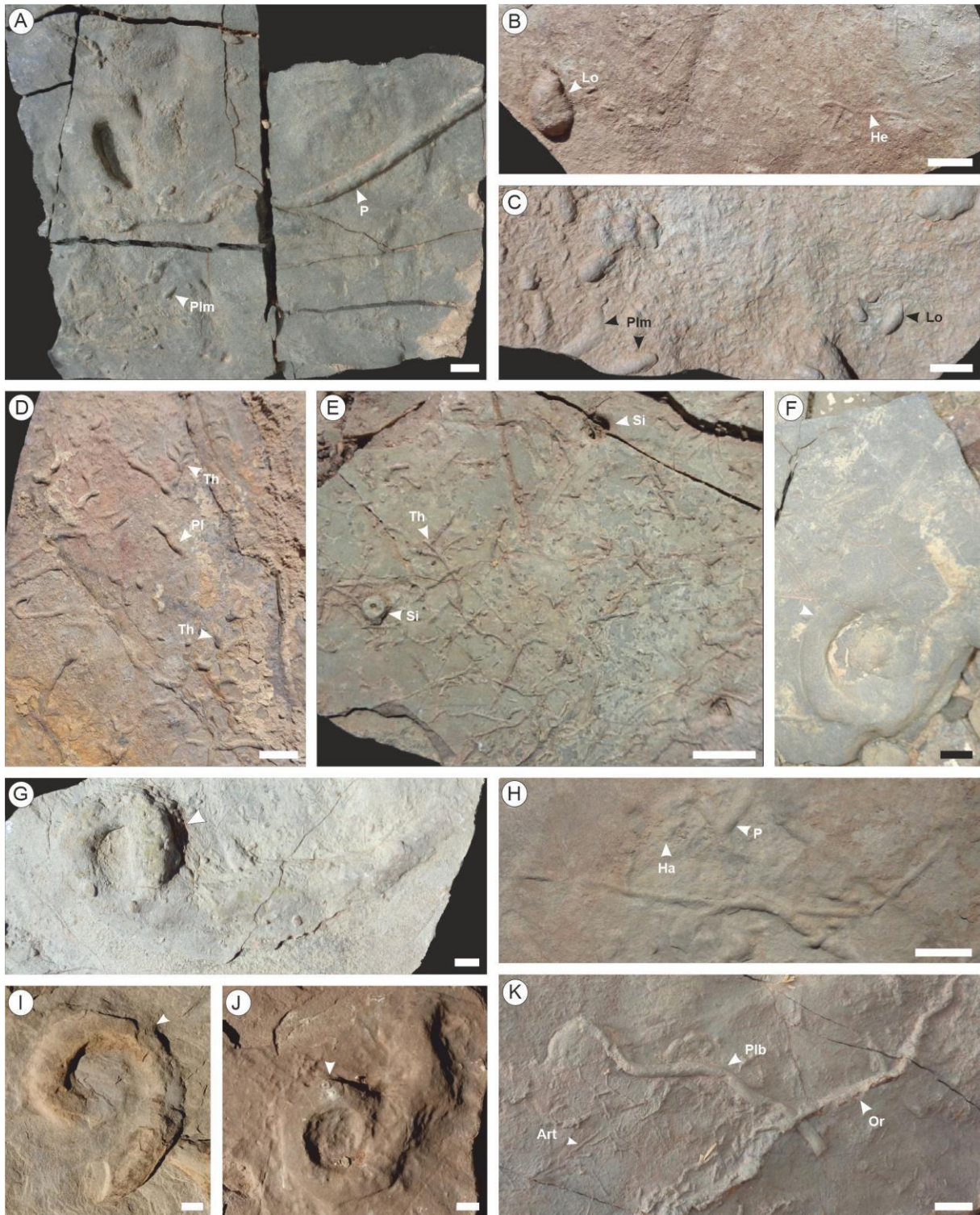


Fig. 29. Elliptical, simple and branched structures from the Numidian Formation in the Ouarsenis Mountains, NW Algeria. (A) *Planolites montanus* (*Plm*) and ?*Palaeophycus* isp. (*P*),

hypichnial full reliefs; (B) *Lockeia* isp. (*Lo*) and *Helminthoidichnites* isp. (*He*), hypichnial full and semi-reliefs, respectively; (C) *Lockeia* isp. (*Lo*) and *Planolites montanus* (*Plm*), hypichnial full reliefs; (D) ?*Planolites* isp. (*Pl*) and *Thorichnus* isp. (*Th*), hypichnial full and semi-reliefs, respectively; (E) *Siphonichnus* isp. (*Si*), full relief manifested on the lower bedding surfaces and *Thorichnus* isp. (*Th*), preserved in hypichnial semi-relief; (F) *Spirophycus* isp. (arrowed), hypichnial semi-relief; (G), (I), (J) *Spirophycus bicornis* (arrowed), hypichnial semi-reliefs; (H) *Halimedides* isp. (*Ha*) and *Palaeophycus* isp. (*P*), hypichnial semi-reliefs; (K) *Oravaichnium* isp. (*Or*), ?*Arthropycus tenuis* (*Art*), and *Planolites beverleyensis* (*Plb*), hypichnial full reliefs; scale = 1 cm.

Remarks. The described structure represents the bedding-plane preservation of a vertical or oblique, cylindrical burrow with a median core, which can be assigned to *Siphonichnus* (for similar preservational variants see [Knaust, 2015](#)). *Siphonichnus* is interpreted as a dwelling trace of a suspension feeder ([Stanistreet et al., 1980](#); [Gingras and Bann, 2006](#); [Gingras et al., 2008](#); [Dashtgard, 2011](#)) or a pascichnion of bivalves such as tellinids ([Knaust, 2015](#)). It is commonly reported from shallow-marine and marginal-marine deposits ([Calver, 1968a, b](#); [Melvin, 1986](#); [Pollard, 1988](#); [Rippon and Apears, 1989](#)), often related to salinity fluctuations and freshwater influx ([Knaust, 2015](#)). Rarely, it is reported from deep-sea deposits ([Krobicki et al., 2006](#)), which is also a case presented in this paper.

Arthropycus [Hall, 1852](#)

?*Arthropycus tenuis* ([Książkiewicz, 1977](#))

[Fig. 29K](#)

Description. Horizontal, subcylindrical, straight, simple ridges, covered with striations, preserved as hypichnial semi-reliefs, 0.2–1 mm in diameter and traced for the length of 10 mm.

Remarks. ?*Arthropycus tenuis* occurs in flysch deposits from the Valanginian ([Książkiewicz, 1977](#)) to the (?) Lower Miocene ([Alexandrescu and Brustur, 1981](#)). Its assignment to *Arthropycus* has been questioned ([Mángano et al., 2005](#)), but a possible solution of this problem requires separate studies.

Halimedides [Lorenz von Liburnau, 1902](#)

Halimedides isp.

[Fig. 29H](#)

Description. Poorly preserved, hypichnial, horizontal, smooth, straight ridge, 1.5–3 mm wide with irregularly oval or crescent chambers, each 3–8 mm wide and located symmetrically along the ridge, 8–11 mm apart. The trace fossil is preserved in semi-relief.

Remarks. The taxonomy of *Halimedes* was discussed by Uchman (1999). Lukeneder et al. (2012) distinguished the *Halimedes* Horizon within the Upper Barremian pelagic to hemipelagic succession (Southern Alps in Italy), which is characterized by stiffgrounds and firmgrounds developed below a discontinuity surface. *Halimedes* has been interpreted by Gaillard and Olivero (2009) as an agrichnion deep-sea trace fossil, probably produced by small crustaceans in stiff to firm substrates, where the chambers were used as traps and storage for food. The densely chambered specimens were considered to indicate lower oxygenation, while the sparse chambered point to higher oxygenation (Gaillard and Olivero 2009). Rodríguez-Tovar et al. (2019) underlined the agrichnial/sequestrichnial behaviour of *Halimedes* after the Toarcian Anoxic Event in the Lusitanian Basin, Portugal, and considered it as an indicator of palaeoenvironmental changes.

Ophiomorpha Lundgren, 1891

Ophiomorpha annulata (Książkiewicz, 1977)

Description. Cylindrical, straight or slightly curved, unbranched or rarely branched, horizontal hypichnion. It is preserved in full relief, 3–7 mm in diameter and at least 100 mm long. Its surface is smooth or rough locally.

Remarks. *Ophiomorpha annulata* is common in turbiditic facies (Uchman, 2001). It was produced by small crustaceans (Uchman et al., 2004).

Ophiomorpha rudis (Książkiewicz, 1977)

Figs. 30A, B, 31H,

Description. A hypichnial, tubular structure preserved in full relief, 2–9 mm in diameter, traced for 30–110 mm. It shows Y- and T-shaped branches. It is smooth or displays a wall covered with discoidal or ovoid pellets, which are 1–3 mm wide. The wall is smooth from the interior.

Remarks. *Ophiomorpha rudis* is the eponymous trace of the *Ophiomorpha rudis* ichnofacies, which characterizes sand-dominated flysch deposits since the Tithonian (Tchoumatchenco and Uchman, 2001; Uchman, 2009).

Oravaichnium Plička and Uhrová, 1990

Oravaichnium isp.

Figs. 29K, 30D

Description. Hypichnial, horizontal, simple, curved to irregularly meandering, smooth ridges, v-shaped in cross section, 1–8.5 mm wide, preserved in semi-relief.

Remarks. This trace fossil differs from *Oravaichnium hrabei* Plička and Uhrová, 1990 by its V-shaped cross section. *O. hrabei* occurs in Eocene turbiditic deposits and is interpreted as a locomotion trace of wedge footed bivalves (Uchman et al., 2011)

Palaeophycus Hall, 1847

Palaeophycus tubularis Hall, 1847

Figs. 30F

Description. Hypichnial, horizontal to subhorizontal, simple, straight to curved, unlined smooth semicircular ridge. It is filled with the same sediment as the host rock, preserved in full relief, 5–7.5 mm wide and at least 75 mm long.

Remarks. *Palaeophycus* is commonly interpreted as a domichnion/pascichnion produced by carnivorous or omnivorous invertebrates, mostly polychaetes (Pemberton and Frey, 1982; Jensen, 1997). It occurs in a wide range of continental to marine palaeoenvironments (Knaust, 2017).

Palaeophycus striatus Hall, 1852

Fig. 30E

Description. Hypichnial, simple, horizontal to subhorizontal, straight to slightly curved, semicircular ridge covered partially with longitudinal wrinkles and small mounds having the same burrow orientation. This trace fossil is preserved as a hypichnial full relief filled with the same sediment as the host rock, 5–6 mm in wide and 25 mm long.

?*Palaeophycus* isp.

Figs. 29A, H,

Description. Hypichnial, horizontal to subhorizontal, semicircular curved to winding simple ridge, 1.5–5.5 mm wide. The ridge diminishes its width along the course and terminates with an irregular elongated swelling. It is preserved in full relief.

Remarks. Assignment of this trace to *Palaeophycus* is unsure due to the atypical change in width and a swelling at the termination.

Planolites [Nicholson, 1873](#)

Planolites [beverleyensis](#) ([Billings, 1862](#))

[Figs. 29K, 30D, G](#)

Description. Hypichnial, horizontal to slightly inclined, simple or branched, straight to winding, smooth, cylindrical ridge, 3–7.5 mm in diameter, preserved in full relief.

Remarks. The trace fossil is ascribed to *Planolites* because there is no evidence of lining. *Planolites* is interpreted as a pascichnion produced by infaunal deposit-feeding vermiform organisms ([Pemberton and Frey, 1982](#)), occurring in a wide range of palaeoenvironments, from continental and fresh water to deep-sea deposits ([Keighley and Pickerill, 1995](#); [Pemberton et al., 2001](#)). It can be abundant in deposits of well-oxygenated as well as dysaerobic environments ([Wignall, 1991, p. 268](#); [Bromley, 1996](#)).

Planolites [montanus](#) [Richter, 1937](#)

[Figs. 29A, C](#)

Description. Hypichnial, horizontal to inclined, simple, rectilinear to slightly curved, subcylindrical smooth ridge, 1–3.5 mm in diameter, preserved in full relief.

Remarks. This trace fossil is distinguished by its short appearance on the bedding surfaces and its irregular, commonly contorted course ([Pemberton and Frey, 1982](#)).

?*Planolites* *isp.*

[Figs. 29D, 30C](#)

Description. A hypichnial, horizontal, unbranched, straight, curved or winding semicylindrical ridge, preserved in full relief or semi-relief, 5–8 mm in diameter and at least 10–30 mm long. The diameter may change along the burrow.

Remarks. The preservation in semi-relief does not permit to recognize if the burrows are lined or not. Without that it is impossible to distinguish between *Planolites* and *Palaeophycus*. Therefore, the trace fossil is reservedly described under *Planolites*.

Parataenidium [Buckman, 2001](#)

?*Parataenidium* isp.

[Fig. 30H, I](#)

Description. Epichnial, horizontal structure composed of a basal, slightly sinuous semicylindrical burrow with menisci-like structures at the top. The structures are 6–22 mm apart. The trace fossil is 9–24 mm wide and at least 140 mm long.

Remarks. The menisci-like structures are interpreted as the basal part of oblique, running up protrusions. *Parataenidium* was made by an unknown organism which processed the sediment and produced the structure mainly by the backfill action ([Seilacher, 1990](#)). The lower unit is attributed to locomotion and the upper part to feeding ([Buckman, 2001](#)). The taxonomy has been discussed by [Uchman and Gaździcki \(2006\)](#).

Phycodes [Richter, 1850](#)

Phycodes isp.

[Fig. 31A](#)

Description. Hypichnial, horizontal to subhorizontal, poorly outlined, low, flat ridges that diverge from a common stem. The ridges are straight to slightly curved, with a granulated surface. Their termination is poorly marked and welded with the bedding surface. The ridges are 2.2–4 mm wide and up to 45 mm long, preserved as semi-reliefs.

Remarks. *Phycodes* has been considered as a deposit-feeding trace made by annelids ([Fillion and Pickerill, 1990](#)). It was commonly reported from shallow marine environments but has also been found in brackish and deep-sea deposits ([Hakes, 1985](#); [Fillion and Pickerill, 1990](#); [Han and Pickerill, 1994a](#); [Hanken et al., 2016](#); [Jackson et al., 2016](#)). *Phycodes* ranges from the early Cambrian to the Miocene ([Crimes, 1987, 1992](#); [Han and Pickerill, 1994a](#)).

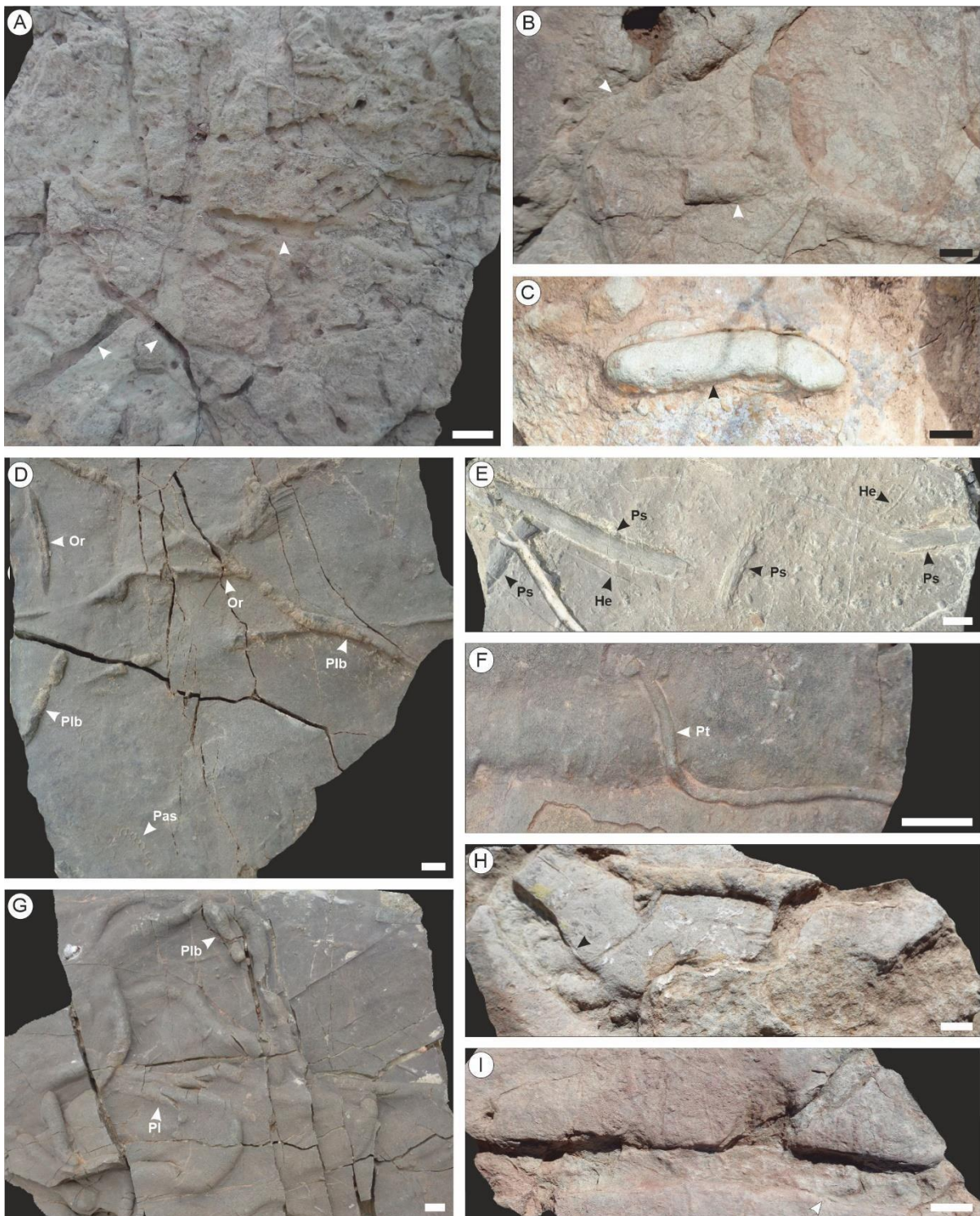


Fig. 30. Simple and branched structures, including a single ichnotaxon of network structures, from the Numidian Formation in the Ouarsenis Mountains, NW Algeria. (A), (B) *Ophiomorpha rudis* (arrowed), hypichnial full relief; (C) *?Planolites* isp., hypichnial full relief; (D) *Planolites beverleyensis* (*Plb*), hypichnial full relief; *Oravaichnium* isp. (*Or*), hypichnial semi-relief; *Paleodictyon strozzii* (*Pas*) hypichnial semi-relief; (E) *Palaeophycus striatus* (*Ps*), hypichnial full relief; *Helminthoidichnites* isp. (*He*), hypichnial semi-relief; (F) *Palaeophycus tubularis*

(Pt), hypichnial full relief; (G) *Planolites beverleyensis* (Plb), hypichnial full relief; wash-out ?*Planolites* isp. (Pl), hypichnial semi-relief; (H), (I) ?*Parataenidium* isp. (arrowed), epichnial semi-relief; scale = 1 cm.

Thalassinoides Ehrenberg, 1944

Thalassinoides isp.

Fig. 31B–E

Description. A hypichnial, horizontal or inclined tubular, branched ridge, 15–30 mm wide, without lining. The filling is massive. The ridges are preserved in full relief, occasionally in semi-relief. Three morphotypes are distinguished: (1) larger, showing Y-shaped branches, 30 mm wide and at least 250 mm long, occurring within medium to coarse-grained sandstone beds (Fig. 31B, C), (2) smaller, with Y-shaped branches, 5 mm wide and at least 50 mm long, found in thin, fine-grained sandstone beds (Fig. 31D), and (3) forms with an unspecified branching, 5–8 mm wide and 30–60 mm long, found in thin, fine-grained sandstone beds (Fig. 31E).

Remarks. *Thalassinoides* occurs in variable marine environments, commonly in shallow marine settings (Palmer, 1978; Archer and Maples, 1984; Frey et al., 1984; Mángano and Buatois, 1991; Pemberton et al., 2001), but also at greater depths (Uchman, 1995, 1998; Uchman and Tchoumatchenco, 2003; Wetzel et al., 2007). It is produced mostly by crustaceans and interpreted as a domichnion and fodinichnion (Frey et al, 1978; Schlirf, 2000).

Thalassinoides has been recorded since the Ordovician till the present (Swinbanks and Luternauer, 1987).

Thorichnus Pokorný, 2017

Thorichnus isp.

Fig. 29D, E

Description. Horizontal, smooth to granulated, curved or winding, semi-circular to flattened branched ridges, 2–0.5 mm in diameter. The branches are mostly short and run obliquely or perpendicularly from the main ridge at irregular distances. Second-order branching is rare. The trace fossil is preserved as a hypichnial semi-relief, traced for 25 mm.

Remarks. The general morphological features fit to *Thorichnus*, which was described from the Upper Miocene deep-lake turbiditic claystones and siltstones in SE Iceland and considered as a fodinichnion produced by annelids or arthropod larvae (Pokorný, 2017).

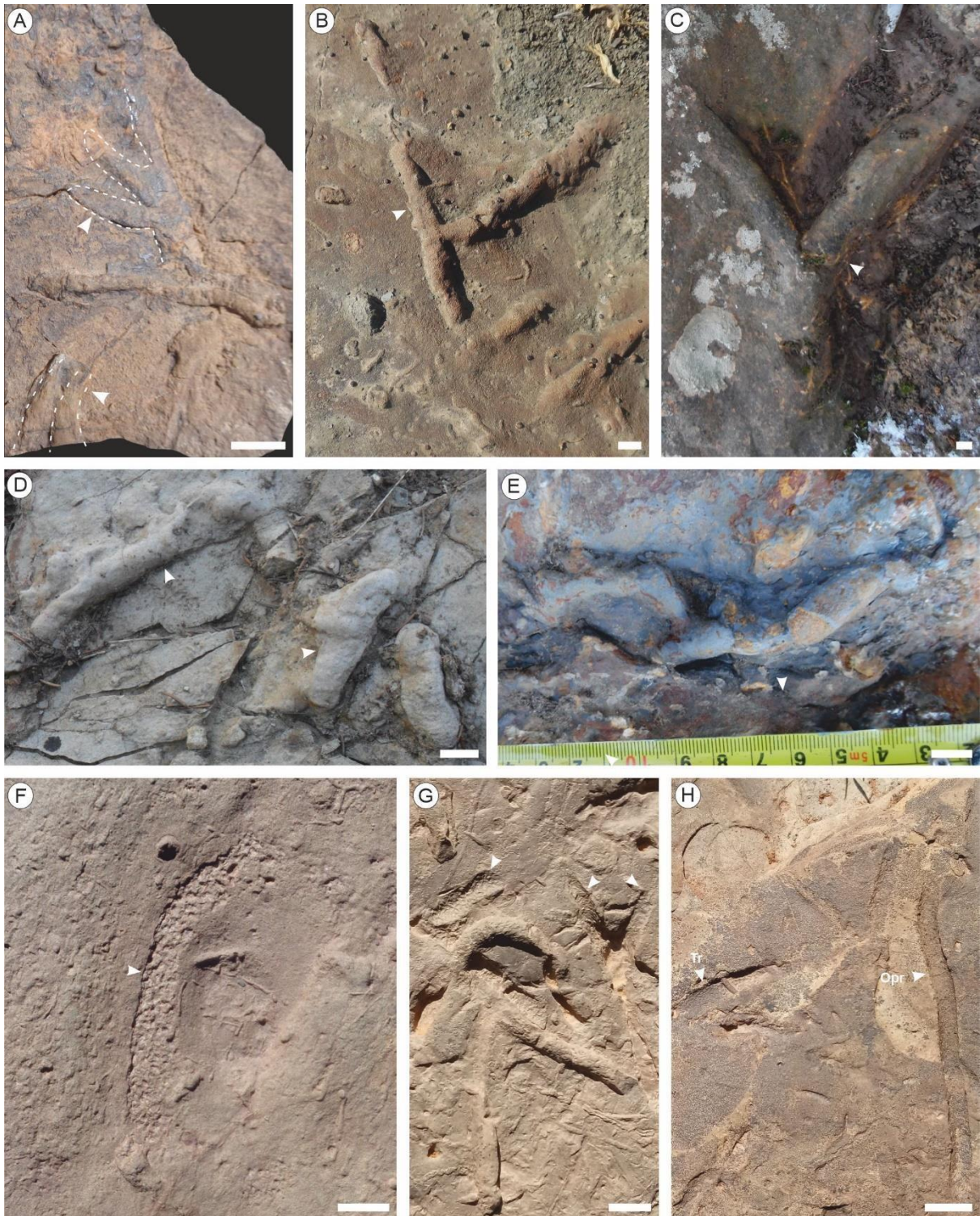


Fig. 31. Simple and branched structures from the Numidian Formation in the Ouarsenis

Mountains, NW Algeria. (A) *Phycodes* isp. (arrowed), hypichnial semi-relief; (B), (C) *Thalassinoides* isp. (arrowed), larger form, hypichnial semi-relief; (D), (E), *Thalassinoides* isp. (arrowed), smaller form, hypichnial full relief; (F), (G), (H) *Tubulichnium rectum* (*Tr*) (arrowed), hypichnial semi-relief; (H) with *Ophiomorpha rudis* (*Opr*), hypichnial full relief; scale = 1 cm.

Alcyonidiopsis [Massalongo, 1856](#)

?*Alcyonidiopsis* isp.

Description. Simple, straight cylindrical endichnial burrow, 9–11 mm in diameter showing randomly distributed, elongate pellets (1–3 mm in diameter) on the surface. The burrow is filled with oxidized siltstone. It is preserved in full relief.

Remarks. Probably, originally the pellets filled the whole burrow, but diagenesis obliterated their outline in the axial part of the burrow. *Alcyonidiopsis* is regarded as a polychaete feeding burrow ([Chamberlain, 1977](#); [Uchman, 1999](#)), although there is no convincing proof of that ([Rodríguez-Tovar and Uchman, 2004a, b](#)). *Alcyonidiopsis* occurs in a wide range of environments from the Ordovician to the Miocene ([Uchman, 1999](#)).

Tubulichnium [Książkiewicz, 1977](#)

Tubulichnium mediterraneum ([García-Ramos, Mángano, Piñuela, Buatois and Rodríguez-Tovar, 2014](#))

[Fig. 32A–C](#)

Description. An endichnial tubular structure preserved in full relief, 5–20 mm diameter and 10–70 mm long, covered with elongated pellets, which are 1–2 mm long, and 0.7–1 mm wide. In some specimens, the longer axis of these pellets follows the burrow course.

Remarks. This trace fossil was re-described under the ichnogenus *Tubotomaculum* ([García-Ramos Mángano, Piñuela, Buatois and Rodríguez-Tovar., 2014](#)) but it is considered an ichnospecies of *Tubulichnium* [Książkiewicz, 1977](#) ([Uchman and Wetzel, 2017](#)). So far, it has been found in the deep-sea Cretaceous-Paleogene deposits in the Mediterranean region, especially in mudstones of the lower part of the NF ([Pautot et al., 1975](#)), where it is abundant in the varicoloured clays ([Durand Delga, 1955](#); [Broquet, 1968](#); [Wezel, 1968](#); [Moretti et al., 1988](#)).

Tubulichnium rectum (Fischer-Ooster, 1858)

Fig. 31F, G, H

Description. Oblique to horizontal, unbranched, blindly ending tube with margins densely lined with ellipsoidal muddy pellets. The trace fossil is 4–7 mm wide and 27–60 mm long. The long axis of the pellets measures 1–2 mm.

Remarks. *Tubulichnium rectum* is considered a post-depositional structure, probably produced by vermiform organisms which fed on organic-rich sediment deposited seasonally or episodically on the sea floor (Uchman and Wetzel, 2017). It occurs commonly in muddy to fine sandy siliciclastic and marly deep-sea deposits from the Turonian to the Eocene, and possibly in the Oligocene-Miocene (Uchman and Wetzel, 2017). Here, the Oligocene-Miocene age is confirmed.

4.2.4. Winding and meandering structures

Cosmorhapse Fuchs, 1895

Cosmorhapse lobata Seilacher, 1977

Fig. 33C

Description. Horizontal, winding, hypichnial semi-circular string, 1. 5–2 mm wide, showing two-order dense meanders, higher than wider. The first and second order meanders display a wavelength of ~29 mm and ~100 mm, respectively, and their amplitude is ~24 mm and 150 mm, respectively. Single meanders have a smaller amplitude and amplitude/wavelength ratio. The string is preserved in semi-relief.

Remarks. *Cosmorhapse* is a pre-depositional trace fossil ascribed to agrichnia. It is common, but never abundant on the soles of sandy turbidites (Książkiewicz, 1977; Uchman and Wetzel, 2012) and reported from recent deep-sea pelagic sediments (e.g., Rona and Merrill, 1978; Ekdale and Berger, 1978; Ekdale, 1980; Gaillard, 1991).

Cosmorhapse sinuosa (Azpeitia Moros, 1933)

Fig. 33D

Description. Hypichnial, horizontal, semi-circular string showing two-order meanders, which are mostly wider than higher. The string is 1.5–2.5 mm wide and preserved in semi-relief. The first and second order meanders have a wavelength of ~26 mm and ~100 mm, respectively, and their amplitude is ~18 mm and ~150 mm, respectively.



Fig. 32. Simple structures from the Numidian Formation in the Ouarsenis Mountains, NW Algeria. (A) *Tubulichnium mediterraneum*, endichnial full relief; (B) *T. mediterraneum* within

marly mudstone in the lower unit of the Ain Ghanem section. (C) micrograph showing the cross section of the trace fossil in thin section, showing two main zones: (1) the internal zone filled with micrite, including quartz grains, some microfossils and shell fragments; (2) the external zone (envelope) made up of stacking pellets, without any internal structure, dominated by iron oxides, brown to dark brown in colour; scale = 1 cm.

Gordia [Emmons, 1844](#)

Gordia arcuata [Książkiewicz, 1977](#)

[Fig. 33E–G](#)

Description. A hypichnial, horizontal, smooth, sinuous, commonly semi-circular, unbranched ridge, 0.5–1 mm in diameter, commonly forming loops, preserved in semi-relief.

Remarks. *Gordia* is a grazing trace (pascichnion). It occurs in a variety of marine and nonmarine soft, low energy deposits, e.g., in marine (e.g., [Książkiewicz, 1977](#); [Gibert et al., 2000](#); [Trewin et al., 2002](#)), lacustrine turbiditic ([Buatois and Mángano, 1993](#)) and varve deposits ([Uchman et al., 2009](#)).

Helminthoidichnites [Fitch, 1850](#)

Helminthoidichnites isp.

[Figs. 29B, 30E, 33A, B, E, 34A](#)

Description. Hypichnial, horizontal, semi-cylindrical, winding, smooth ridges, occasionally overcrossing, rarely forming loops, 0.4–2 mm in diameter and traced for at least 220 mm, preserved as hypichnial semi-reliefs. The filling of the burrow is the same as the host sediment.

Remarks. This is a non-marine and marine eurybathic trace, common also in deep-sea facies, including flysch ([Chamberlain, 1971](#); [McCann and Pickerill, 1988](#); [Fillion and Pickerill, 1990](#); [Uchman, 1995, 1998](#); [Wetzel et al., 2007](#)). *Helminthoidichnites* is common from the Precambrian ([Narbonne and Aitken, 1990](#)) to the Pleistocene ([Uchman et al., 2009](#)).

Helminthopsis [Wetzel and Bromley, 1996](#)

Helminthopsis isp.

[Fig. 33A, B](#)

Description. Hypichnial, horizontal, simple, smooth, semi-circular, irregularly meandering ridge, which is 5–2.2 mm wide and traced for 700 mm. It is preserved in semi-relief. The meanders are 40–70 mm wide. Their amplitude ranges from 20 to 45 mm.

Remarks. The trace fossil resembles *Cosmorhaphe*, but the meanders are less regular than in representatives of that ichnogenus. Moreover, regular second-order meanders are not obvious; rather irregular turns of the general course are present. *Helminthopsis* is a repichnion produced probably by polychaetes or priapulids, and is common in flysch deposits (Książkiewicz, 1977; Fillion and Pickerill, 1990; Wetzel and Bromley, 1996). It occurs from the Cambrian (Crimes, 1987) to the recent (Swinbanks and Murray, 1981; Wetzel, 1983a, b).

Nereites MacLeay in Murchison, 1839

Nereites isp.

Fig. 33H, I

Description. Hypichnial, horizontal, unbranched, winding to meandering low ridges or bands, 0.5–1.2 mm wide and traced for ~100 mm. They are bounded by thin levees and preserved in semi-relief. The limbs of the meanders are 2–10 mm apart and their amplitudes are 8–26 mm.

Remarks. The levees are interpreted as reworked zones bounding faecal strings (cf. Uchman, 1995). *Nereites* is a pascichnion (Mángano et al., 2000), but it is also considered a fodinichnion (Knaust, 2017). *Nereites* is a typical element of deep-sea environments, with a tendency to occur within sediments deposited under moderate energy (Wetzel, 2002). It also occurs in slope (Callow et al., 2013; Demircan and Uchman, 2016), shelf (Knaust, 2017) and exceptionally in sandy estuarine deposits and tidal flats (Martin and Rindsberg, 2007; Neto de Carvalho and Baucon, 2010). *Nereites* ranges from the Cambrian (e.g., Aceñolaza and Alonso, 2001) to the Holocene (Wetzel, 2002).

Scolicia de Quatrefages, 1849

?*Scolicia vertebralis* Książkiewicz, 1977

Description. Epichnial, curved, V-shaped furrow, 3–10 mm wide, with elevated margins. The furrow bottom shows a rope-like elevation, which is 2–4 mm wide.

Remarks. *Scolicia* is interpreted as a deposit-feeding trace (e.g., Uchman, 1995; Fu and Werner, 2000), which is produced by irregular echinoids (e.g., Plaziat and Mahmoudi, 1988;

Uchman, 1995, 1998). *Scolicia* occurs commonly in shallow-marine (Fu and Werner, 2000) and deep-sea deposits, including turbiditic successions (Uchman, 1995). *Scolicia* ranges from the Tithonian (Tchoumatchenco and Uchman, 2001).

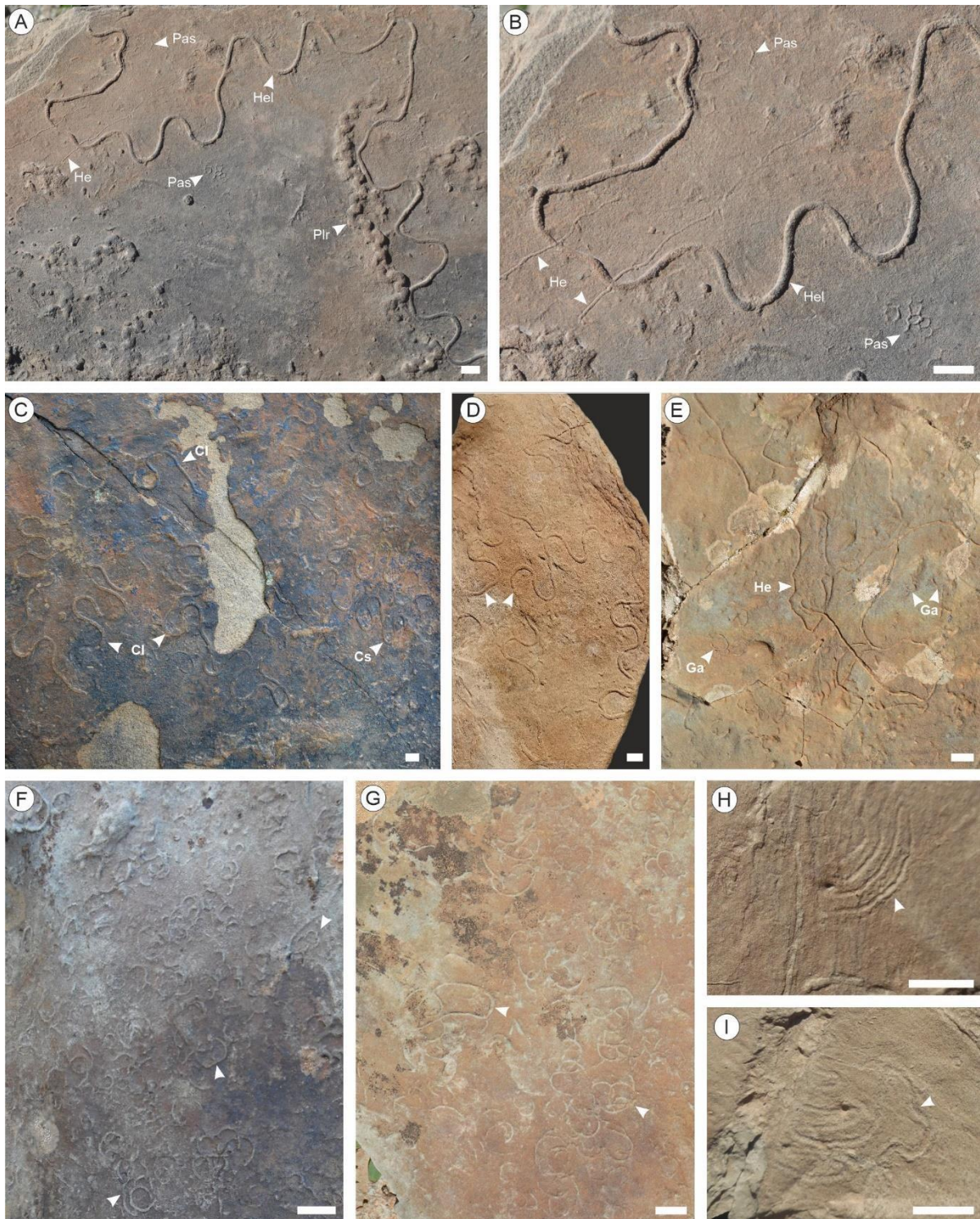


Fig. 33. Winding and meandering structures with one single network structure, from the Numidian Formation in the Ouarsenis Mountains, NW Algeria. (A), (B) *Helminthopsis* isp. (*Hel*), hypichnial semi-relief; *Paleomeanderson rude* (*Plr*), hypichnial semi-relief; *Paleodictyon*

strozzii (Pas), hypichnial semi-relief; *Helminthoidichnites* isp. (He), hypichnial semi-relief; (C), (D) *Cosmorhapse sinuosa* (Cs), hypichnial semi-relief; (C) *C. lobata* (Cl), hypichnial semi-relief; (E) *Helminthoidichnites* isp. (He), hypichnial semi-relief; *Gordia arcuata* (Ga), hypichnial semi-relief; (F), (G) *Gordia arcuata* (arrowed), hypichnial semi-relief; (H), (I) *Nereites* isp. (arrowed), epichnial semi-relief; scale = 1 cm.

Scolicia strozzii (Savi and Meneghini, 1850)

Fig. 34B

Description. Simple, winding, smooth, bilobate ridge, 15–30 mm wide, ~5 mm high, and at least 90–330 mm long, preserved as a hypichnial semi-relief.

Gyrochorte Heer, 1865

Gyrochorte isp.

Figs. 34D–F, 35J

Description. Epichnial, straight to curved or winding, bilobate ridge with median furrow, 0.7–1.2 mm wide and 5–130 mm long. The trace fossil shows overcrossings.

Remarks. *Gyrochorte* is interpreted as a feeding trace (e.g., Weiss, 1941; Fu and Werner, 2000; Gibert and Benner, 2002), produced by vermiform organisms, probably polychaetes (Seilacher, 2007; Fürsich et al., 2017). It was commonly reported from nearshore and shallow-marine deposits with moderate energy (Gibert and Benner, 2002), and rarely from deep-sea settings (Uchman and Tchoumatchenco, 2003 and references therein).

Taenidium Heer, 1877

Taenidium isp.

Fig. 34C

Description. Epichnial, horizontal, simple, curved ribbon or low ridge, 3–9 mm wide and 3–220 mm long, showing dense meniscate structure. The menisci are 3–5 mm apart.

Remarks. *Taenidium* is interpreted as a deposit-feeding trace produced by marine vermiform organisms (Gevers et al., 1971; Keighley and Pickerill, 1994; Smith et al., 2008b). It was reported from shallow-to deep-sea deposits (Keighley and Pickerill, 1994; Smith and Hasiotis,

2008; Jackson et al., 2016). *Taenidium* ranges from the Ediacaran to the recent (e.g., Crimes, 1992; Jenkins, 1995; Uchman, 1998; Jackson et al., 2016).

4.2.5. Branched winding and meandering structures

Chondrites von Sternberg, 1833

Chondrites isp.

Fig. 34C

Description. Patches of epichnial, circular to oval depressions filled with mudstone. The patches are 0.5–4 mm wide and the depressions are 0.3–1 mm wide.

Remarks. The depressions in patches are cross sections of downward spreading branched tunnels which are typical of *Chondrites* (cf. fig. 3c in Uchman, 2007). This ichnogenus is interpreted as a feeding trace (deep-tier chemichnion) of unknown vermiform organisms, which may burrow below the redox boundary (for discussion, see Uchman, 1999; Wetzel, 2008). It occurs mostly offshore and deeper, rarely in nearshore restricted environments (e.g., Knaust, 2017). *Chondrites* occurs from the Cambrian (Webby, 1984) to the Holocene (Wetzel, 1981, 2008).

Paleomeandron Peruzzi, 1880

Paleomeandron rude Peruzzi, 1880

Fig. 33A

Description. Hypichnial, winding tract built of a string bent in small, densely packed, relatively shallow, irregular, second-order rectangular meanders. The trace fossil is 3–5 mm wide and can be traced for about 150 mm.

Remarks. This trace fossil is ascribed to graphoglyptids (Seilacher, 1977) and occurs in turbiditic deposits (Uchman, 1998).

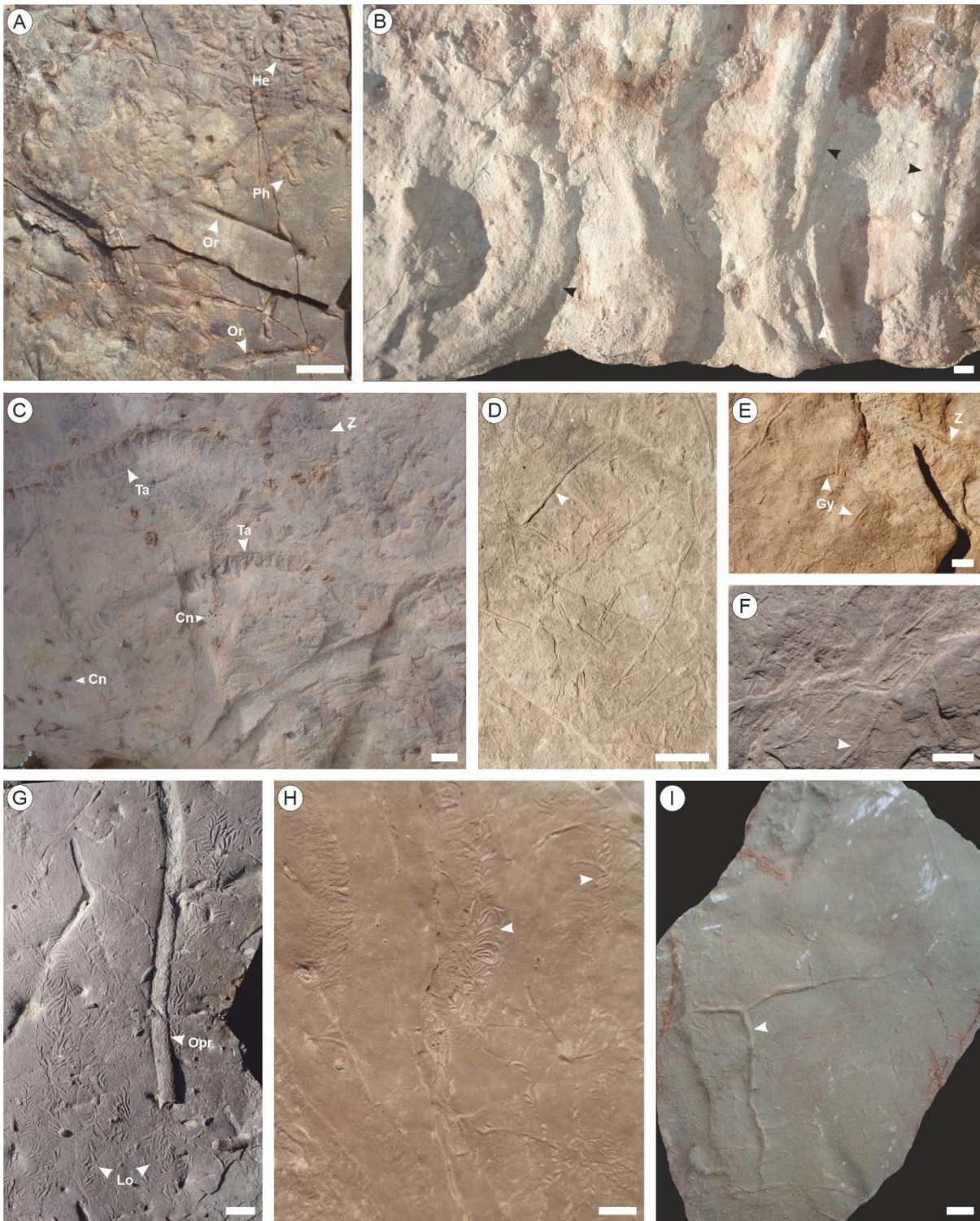


Fig. 34. Spreite, meandering, branched, and network structures from the Numidian Formation in the Ouarsenis Mountains, NW Algeria. (A) *Phycosiphon incertum* (*Ph*), epichnial semi-relief; *Helminthoidichnites* isp. (*He*), hypichnial semi-relief; *Oravaichnium* isp. (*Or*), hypichnial semi-relief; (B) *Scolicia strozzii*, hypichnial semi-relief; (C) *Taenidium* isp. (*Ta*), epichnial semi-relief; *Chondrites* isp. (*Cn*), epichnial full relief; *Zoophycos* isp. (*Z*), epichnial semi-relief; (D) (E), (F), *Gyrochorte* isp. (*Gy*), epichnial semi-relief; (E) *Zoophycos* isp. (*Z*), epichnial semi-

relief; (G), (H), *Lophoctenium* isp. (*Lo*), epichnial semi-relief; (G) *Ophiomorpha rudis* (*Opr*), hypichnial full relief; (I) *Megagraption irregulare* (arrowed), hypichnial semi-relief; scale = 1 cm.

Rutichnus D'Alessandro, Bromley and Stemmerik, 1987

Rutichnus isp.

Fig. 35A

Description. Hypichnial, horizontal to subhorizontal, winding, semi-circular, tubular ridges, 1–4 mm wide and 15–40 mm long, preserved in full relief. Their surface looks as a series of slightly distorted segments separated by narrow constrictions. The segments are 1–4 mm wide and 2–5 mm long. False branching is developed with tunnel overcrossings.

Remarks. *Rutichnus* is interpreted as a deposit-feeding trace produced by vermiform organisms or arthropods. It occurs in shallow-marine and deep-sea flysch deposits (D'Alessandro et al., 1987; Monaco, 2011).

4.2.6. Spirals and networks

Megagraption Książkiewicz, 1968

Megagraption irregulare Książkiewicz, 1968

Fig. 34I

Description. Hypichnial, horizontal, incomplete, irregular network, composed of winding strings (1–2.5 mm wide), branching at ~90°. The meshes are at least 80 mm across.

Remarks. *Megagraption irregulare* is interpreted as an agrichnion (Seilacher, 1977; Uchman, 1998) ranging from the Silurian (Crimes and Crossley, 1991) to the Miocene (D'Alessandro, 1982), and occurring mainly in deep-sea flysch deposits.

Paleodictyon Meneghini in Savi and Meneghini, 1850

Paleodictyon strozzii Meneghini in Savi and Meneghini, 1850

Figs. 30D, 33A, B

Description. Horizontal networks composed of regular, hexagonal meshes (2.5–2.5 mm wide; the strings are 0.2–1 mm wide) preserved as hypichnial semi-reliefs.

Remarks. *Paleodictyon* is interpreted as a farming trace (agricrion) produced by unknown organisms commonly in deep-sea turbiditic deposits (Seilacher, 1977) and less frequently in shelf sediments (Fürsich et al., 2007). It ranges from the Cambrian (Crimes and Anderson, 1985) to the recent (Ekdale, 1980; Miller, 1991).

Squamodictyon Vialov and Golev, 1960

Squamodictyon tectifforme (Sacco, 1886)

Fig. 35B

Description. Hypichnial, horizontal networks composed of irregular scale-like meshes (7.5–11 mm wide; the strings are 0.5–1 mm in diameter) preserved in semi-relief.

Remarks. *Squamodictyon tectifforme* is interpreted as a pascichnion produced by unknown organisms (Uchman, 2003). It was reported from Cretaceous and Cenozoic flysch deposits (Seilacher, 1977).

4.2.7. Spreite structures

Phycosiphon Fischer-Ooster, 1858

Phycosiphon incertum Fischer-Ooster, 1858

Fig. 34A

Description. Epichnial, horizontal, straight to curved lobes bifurcating into two curved to winding lobes, showing marginal tubes and internal spreite. The marginal tube is 0.3–0.5 mm wide, and the lobes are up to 1–2 mm wide and 5–7 mm long.

Remarks. *Phycosiphon* is interpreted as the deposit-feeding trace of small, unknown vermiform organisms that exploit the sediment for organic-rich matter (Wetzel, 2010; Izumi, 2014). It is reported from a wide range of palaeoenvironments, but mostly from fine-grained lower shoreface and deeper, mainly siliciclastic deposits (Goldring et al., 1991; Savrda et al., 2001; Pemberton et al., 2012; Callow et al., 2013). The tracemaker colonized freshly deposited

turbidites in the sequential colonization model, when the sediment contained abundant food resources and well-oxygenated pore waters (Wetzel and Uchman, 2001).

Diplocraterion Torell, 1870

Diplocraterion isp.

Fig. 35C, D

Description. Endichnial, vertical U-shaped burrows with a marginal tunnel, concave-upward spreite and a semi-circular bottom, preserved in full relief. Two morphotypes have been distinguished: (1) with parallel limbs, 2–3 mm in diameter, 15 mm apart and 30 mm deep; (2) with divergent downward limbs, 4–6 mm in diameter, 25–30 mm apart and 80 mm deep.

Remarks. *Diplocraterion* is interpreted as a suspension-feeding dwelling trace (Goldring, 1962; Ekdale and Lewis, 1991; Bromley, 1996), although deposit-feeding has been proposed as well (Leaman and McIlroy, 2016). It was produced probably by polychaetes (Arkell, 1939), although crustaceans have also been considered (Bromley, 1996).

Diplocraterion occurs mostly in shallow marine (Knaust, 2017), rarely in deep-sea (Crimes et al., 1981; Leszczyński et al., 1996) and continental deposits (Kim and Paik, 1997) from the Cambrian (Cornish, 1986; Bromley and Hanken, 1991; Mángano and Buatois, 2016) to the Holocene (Corner and Fjalstad, 1993), including recent, small incipient forms produced by amphipods (Dashtgard and Gingras, 2012).

Lophoctenium Richter 1850

Lophoctenium isp.

Fig. 34G, H

Description. Comb- and star-like traces composed of curved probes running from a main axis or centre. The probes (mm long, mm wide) are developed on both sides of the axis.

Remarks. *Lophoctenium* is interpreted as a deposit feeder trace, encountered mostly in deep water sediments (e.g., Książkiewicz, 1977). It ranges from the Ordovician (Häntzschel, 1975) to the Miocene (Uchman, 1995). It is interpreted as a product of repetitive lateral probing for feeding (Seilacher, 2007). Similar traces are produced by bivalves (Ekdale and Bromley, 2001) but they are usually only a part of a burrow system, such as *Hillichnus* (Bromley et al., 2003).

Zoophycos Massalongo, 1855

Zoophycos isp.

Fig. 35E–J

Description. Spreite-filled planar structures manifested on the bedding surface as small (Fig. 35E, F) or large whorls or lobes (Fig. 35G–J). They are part of a helical structure having similar elements at different levels of the same bed (Fig. 35I). The spreite laminae, which are mostly straight to curved, run radially from a central point. The structure is encircled by a marginal tunnel, which is 0.3–5 mm wide. The whole structure is from 30–50 mm (smaller forms) to 140 mm wide (larger forms). The margin is lobate. In some specimens, spreite-filled tongues are present. The tongues are 9–50 mm wide and 30–80 mm long. They are encircled by a marginal tunnel as in the other parts of this trace fossil.

Remarks. *Zoophycos* is interpreted as a deposit-feeding trace of a vermiform organism (Wetzel and Werner, 1981), possibly polychaetes (Bischoff, 1968; Knaust, 2009), echiurans (Kotake, 1991) or sipunculids (Wetzel and Werner, 1981; Olivero and Gaillard, 2007). *Zoophycos* ranges from the Cambrian (Alpert, 1977; Jensen, 1997) to the recent (Seilacher, 2007; Wetzel, 2008).

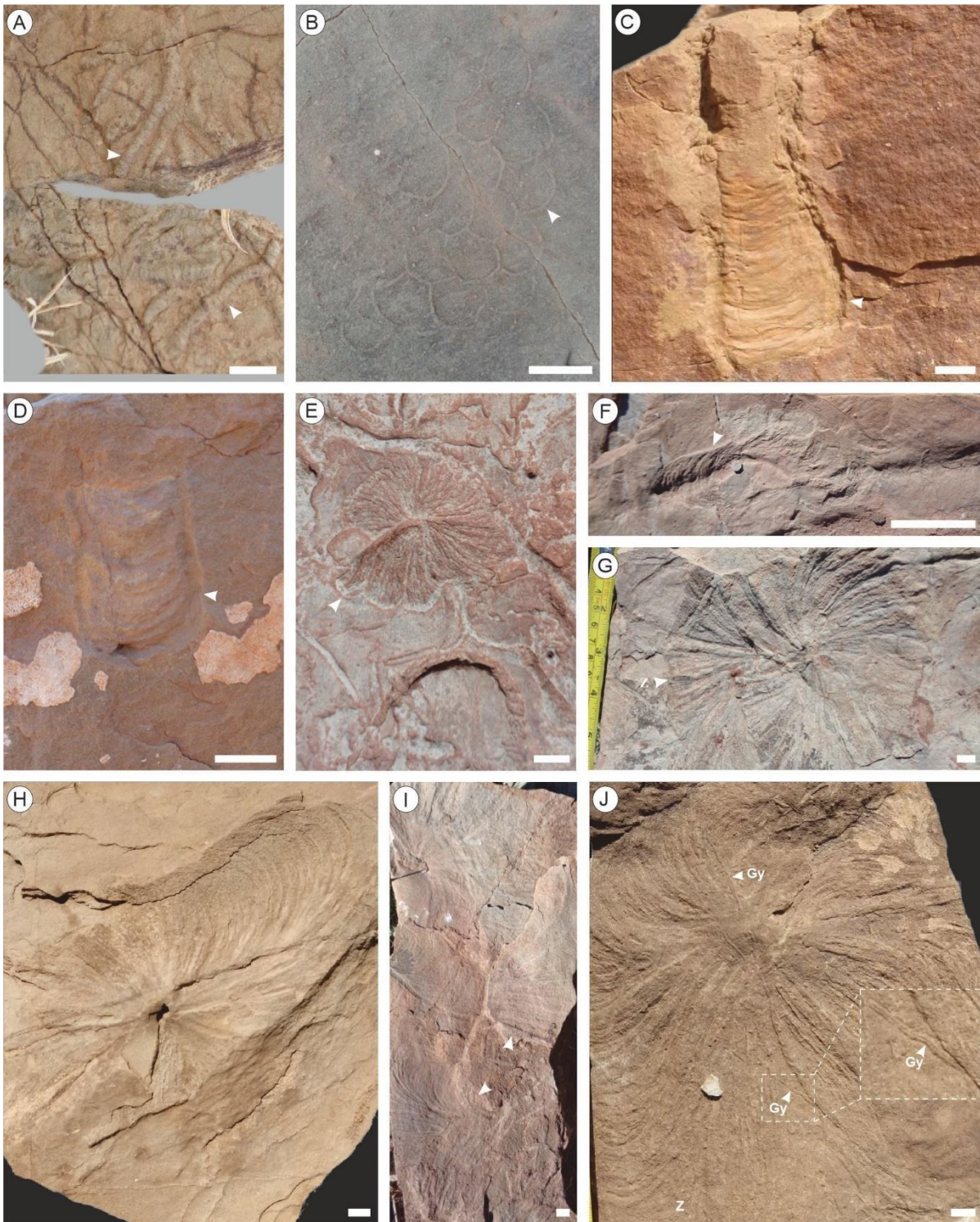


Fig. 35. Spreite, network, branched, and meandering structures from the Numidian Formation in the Ouarsenis Mountains, NW Algeria. (A) *Rutichnus* isp., hypichnial full relief; (B) *Squamodictyon tectiforme*, hypichnial semi-relief; (C), (D) *Diplocraterion* isp., endichnial full relief; (E), (F), (G) *Zoophycos* isp., small forms; (H), (I), (J) *Zoophycos* isp. (Z), large forms; (J) *Gyrochorte* isp. (Gy), epichnial semi-relief; scale = 1 cm.

4.3. DISTRIBUTION OF TRACE FOSSILS

Table 3

The NF in the Ouarsenis Mountains, Algeria, reveals diverse trace fossils belonging to twenty-two ichnogenera. The Ain Ghanem and Kef Maiz sections have a larger ichnodiversity (35% and 46% of all ichnotaxa, respectively) than the Kef Rzama and the Forêt des Cèdres sections (9% and 10%, respectively).

The ichnodiversity changes significantly among the facies. Facies F4 reveals almost all the trace fossils recorded in the studied sections, primarily in (1) the lower unit of the Ain Ghanem and Kef Maiz sections, (2) the lower part of the upper unit of the Kef Maiz section, and (3) when interbedded with facies F1 in the upper unit of all the studied sections.

The ichnodiversity decreases significantly in facies F2, which yields only *Ophiomorpha rudis* and *Thalassinoides* isp. in the upper unit of the Forêt des Cèdres section and *Thalassinoides* isp. in the lower unit of the Ain Ghanem section. Facies F8 yields very abundant *Tubulichnium mediterraneum* in the lower and upper units of the Ain Ghanem section, and in the lower unit of the Kef Rzama section, where it co-occurs with rare *?Alcyonidiopsis* isp.

Table 3. Distribution of trace fossils and the corresponding facies in the investigated sections of the Numidian Formation in the Ouarsenis Mountains, NW Algeria. Abundance: very rare (VR; 1 ichnotaxon), rare (R; 2–6 ichnotaxa), common (C; 7–9 ichnotaxa), very common (VC; 10–22 ichnotaxa), abundant (A; 23–41 ichnotaxa), very abundant (VA; >42 ichnotaxa).

Ichnotaxon	Forêt des Cèdres section	Kef Rzama section		Ain Ghanem section		Kef Maiz section	
	upper unit	lower unit	upper unit	lower unit	upper unit	lower unit	upper unit
<i>Lockeia</i> isp.							R (F4)
<i>Spirophycus bicornis</i>				R (F4)			
<i>Spirophycus</i> isp.						R (F4)	
<i>Siphonichnus</i> isp.						R (F4)	
<i>?Arthropycus tenuis</i>							C (F4)
<i>Halimedides</i> isp.							R (F4)

<i>Ophiomorpha annulata</i>	R (F4)						
<i>Ophiomorpha rudis</i>	R (F2)			C (F4)			
<i>Oravaichnium</i> isp.						R (F4)	R (F4)
<i>Palaeophycus tubularis</i>							R (F4)
<i>Palaeophycus striatus</i>		R (F4)					
<i>Palaeophycus</i> isp.						R (F4)	R (F4)
<i>Planolites beverleyensis</i>						R (F4)	R (F4)
<i>Planolites montanus</i>				R (F4)		C (F4)	C (F4)
? <i>Planolites</i> isp.	R (F4)		C (F4)	R (F4)		C (F4)	VC (F4)
? <i>Parataenidium</i> isp.				R (F4)			
<i>Phycodes</i> isp.						VR (F4)	
<i>Thalassinoides</i> isp.	R (F2, F4)			R (F2, F4)			
<i>Thorichnus</i> isp.						VC (F4)	VC (F4)
? <i>Alcyonidiopsis</i> isp.		R (F8)					
<i>Tubulichnium mediterraneum</i>		VA (F8)		VA (F8)	C(F7)		
<i>Tubulichnium rectum</i>				C (F4)			
<i>Cosmorhapse lobata</i>				R (F4)			
<i>Cosmorhapse sinuosa</i>				R (F4)			
<i>Gordia arcuata</i>	A (F4)						
<i>Helminthoidichnites</i> isp.	R (F4)	R (F4)		VC (F4)		C (F4)	VC (F4)
<i>Helminthopsis</i> isp.				R (F4)			VR (F4)
<i>Nereites</i> isp.				R (F4)		R (F4)	

<i>?Scolicia vertebralis</i>						R (F4)	
<i>Scolicia strozzii</i>				R (F4)			
<i>Gyrochorte</i> isp.				VC (F4)			
<i>Taenidium</i> isp.						R (F4)	R (F4)
<i>Phycosiphon incertum</i>						R (F4)	
<i>Chondrites</i> isp.				C (F4)		C (F4)	R (F4)
<i>Megagraption irregulare</i>							VR (F4)
<i>Paleomeandron rude</i>				VR (F4)			
<i>Rutichnus</i> isp.						C (F4)	
<i>Paleodictyon strozzii</i>				C (F4)		R (F4)	
<i>Squamodictyon tectiforme</i>							R (F4)
<i>Diplocraterion</i> isp.							R (F4)
<i>Lophoctenium</i> isp.				VC (F4)			
<i>Zoophycos</i> isp.				C (F4)			R (F4)

4.4. DISCUSSION

4.4.1. ICHNOFACIES AND DEPOSITIONAL SYSTEM

Figs. 36, 37

Some data on the palaeoenvironment of the NF in Algeria were given by [Moretti et al. \(1991\)](#), who suggested a submarine slope setting for the NF strata in the Constantine Mountains based on sedimentological data, but no such interpretations were given for the study area. The described trace fossil assemblages and ichnofacies based on them along with the presented sedimentary features allow for a more precise interpretation of the NF palaeoenvironment. The trace fossil assemblage, in general, belongs to the deep-sea *Nereites* ichnofacies. This is indicated by the presence of graphoglyptids (*Paleodictyon*, *Paleomeandron*, *Megagraption*, *Cosmorhaphe*) and other trace fossils ([Table 4](#)), which are common in this ichnofacies (see [Uchman and Wetzel, 2012](#)). The distribution of trace fossils, and differences in their composition and diversity permit to distinguish the three main ichnosubfacies of the *Nereites* ichnofacies ([Table 4](#)).

The deep-sea interpretation is supported by agglutinated foraminifers, which are recorded (preliminary data) from the varicoloured marly mudstone (facies F8) in the studied sections and previously reported from the same facies in the Constantine Mountains (Hoyez, 1989; Moretti et al., 1991). The foraminifers include representatives of *Ammodiscus* isp., *Bathysiphon* isp., *Cyclammina* isp., *Hyperammina* isp., *Kalamopsis* isp., *Glomospira* isp., *Glomospirella* isp., *Haplophragmoides* isp., *Recurvoides* isp., *Trochammina* isp., and *Trochamminoides* isp. They are very similar to those recorded in the NF from Morocco (Kaminski et al., 1996) and Tunisia (Riahi et al., 2014), and in the Eocene Variegated Shale in the Carpathian Flysch in Poland (Kender et al., 2005), and correspond to lower bathyal to abyssal depths (Kaminski et al., 1996).

The *Ophiomorpha rudis* ichnosubfacies is recorded in the medium- to very thick-bedded sandstones (FA1), interbedded with thinner beds of facies F2 and F4 in the upper unit of the Forêt des Cèdres and Kef Maiz sections. This ichnofacies contains abundant *Ophiomorpha rudis*, *O. annulata*, and *Thalassinoides* isp., which may co-occur with *Planolites* isp., *P. montanus*, *Gordia arcuata*, and *Helminthoidichnites* isp. Deposits representing this ichnosubfacies accumulated probably in channel and channel-levee-overbank settings. A more distal variant of the *Ophiomorpha rudis* ichnosubfacies occurs in the thick- to thin-bedded sandstones of facies F2 and F4 in the lower unit of the Ain Ghanem section. They yield *O. rudis*, *Thalassinoides* isp., *Zoophycos* isp., *Lophoctenium* isp., *Scolicia strozzii*, *Tubulichnium rectum*, *Planolites* isp., and *P. montanus*. These deposits probably accumulated in crevasse splays generated from nearby isolated narrow channels within the mud-dominated part of the depositional system, which were occasionally fed with sandy turbiditic sediments. The channels were subjected to avulsion.

The *Paleodictyon* ichnosubfacies occurs in thin- to medium-bedded sandstones of facies F4 in the lower unit of the Ain Ghanem and Kef Maiz sections and the lowest part of the upper unit in the Kef Maiz section. These deposits were probably deposited in channel-margin or channel-levee-overbank settings. Trace fossils representing this ichnosubfacies include *Paleodictyon strozzii*, *Paleomeandron rude*, *Megagraption irregulare*, *Squamodictyon tectiforme*, *Chondrites* isp., *Taenidium* isp., *Helminthopsis* isp., *Helminthoidichnites* isp., *Zoophycos* isp., *Cosmorhaphé sinuosa*, *C. lobata*, *Planolites montanus*, *Planolites* isp., *P. beverleyensis*, *Oravaichnium* isp., *Halimedes* isp., *Rutichnus* isp., *Thorichnus* isp., *Siphonichnus* isp., and *Arthropycus tenuis*.

The *Nereites* ichnosubfacies is recorded from thin-bedded sandstones of facies F4 in the lower unit of the Kef Maiz and Ain Ghanem sections. The sandstones were deposited on the

basin floor by occasional turbidites in crevasse-splays (spilling over from nearby channels) or small lobes located in the distal parts of vanishing channels or at their terminations. The turbidites interrupted the pelagic and hemipelagic sedimentation. This ichnosubfacies is represented by *Nereites* isp., *Phycosiphon incertum*, ?*Scolicia vertebralis*, *Helminthoidichnites* isp., *Tubulichnium mediterraneum*, ?*Alcyonidiopsis* isp., ?*Planolites* isp., *Spirophycus* isp., and *S. bicornis*.

The vertical distribution of trace fossils shows a general shallowing-up trend resulting mostly from the progradation of the depositional system. The succession of ichnofacies starts with the *Nereites* ichnosubfacies in the lower unit of the studied sections, and is associated with the exclusive occurrence of the *Ophiomorpha rudis* ichnosubfacies in the lower unit of the Ain Ghanem section, followed by the *Paleodictyon* ichnosubfacies in the lower unit of the Ain Ghanem section and the lowest part of the Kef Maiz section. The upper unit of the studied sections is dominated by the *Ophiomorpha rudis* ichnosubfacies, as observed mainly in the Forêt des Cèdres and Kef Maiz sections. *Diplocraterion* isp. occurs at the top of the Kef Maiz section. Generally, this is a shallow-marine trace fossil of the *Skolithos* ichnofacies, but no sedimentological features of a shallow-marine setting have been noted in the studied section. Its occurrence fits to the general shallowing-up trend but is still rather in a deep-sea setting.

The shallowing-up trend recorded by the succession of ichnosubfacies is also associated with a generally decreasing-upward abundance and diversity of the trace fossils in the sections. The high diversity of trace fossils in the lower unit is related to favourable environmental and preservational conditions. A calm environment associated with an occasional turbiditic input rich in nutrients allowed for the proliferation of burrowing organisms. In contrast, the low diversity and low abundance of trace fossils in the upper unit can be caused in general by stress conditions related to high episodic turbulence, erosion of the sea floor and substrate instability (as evidenced by soft-sediment deformation structures), which limited the proliferation of trace makers and caused the erosion of the bioturbated sediments. In the calmer environment of the lower unit, delicate soursing and casting promoted preservation of burrows formed in mud, which are generally more abundant than burrows formed in sand in deep-sea turbiditic systems (Kern, 1980).

Table 4. Distribution of trace fossils according to their ichnosubfacies.

Paleodictyon ichnosubfacies	Ophiomorpha rudis ichnosubfacies	Nereites ichnosubfacies	Non-attributable trace fossils
<i>Squamodictyon tectiforme, Paleodictyon strozzii, Paleomeandron rude, Megagraption irregulare, Chondrites isp., Taenidium isp., Helminthopsis isp., Helminthoidichnites isp., Zoophycos isp., Cosmorhapha sinuosa, Cosmorhapha lobata, Planolites montanus, Planolites beverleyensis, ?Planolites isp., Oravaichnium isp., Halimedides isp., Rutichnus isp., Thorichnus isp., Siphonichnus isp., ?Arthropycus tenuis</i>	<i>Ophiomorpha rudis, Ophiomorpha annulata, Thalassinoides isp., Zoophycos isp., Lophoctenium isp., Scolicia strozzii, Gordia arcuata, Helminthoidichnites isp., Tubulichnium rectum, Planolites montanus, ?Planolites isp.</i>	<i>Nereites isp., Phycosiphon incertum, ?Scolicia vertebralis, Helminthoidichnites isp., Tubulichnium mediterraneum, ?Alcyonidiopsis isp., ?Planolites isp., Spirophycus isp., Spirophycus bicornis</i>	<i>Lockeia isp., Gyrochorte isp., Phycodes isp., Palaeophycus tubularis, Palaeophycus, striatus, Palaeophycus isp., ?Parataenidium isp., Diplocraterion isp.</i>

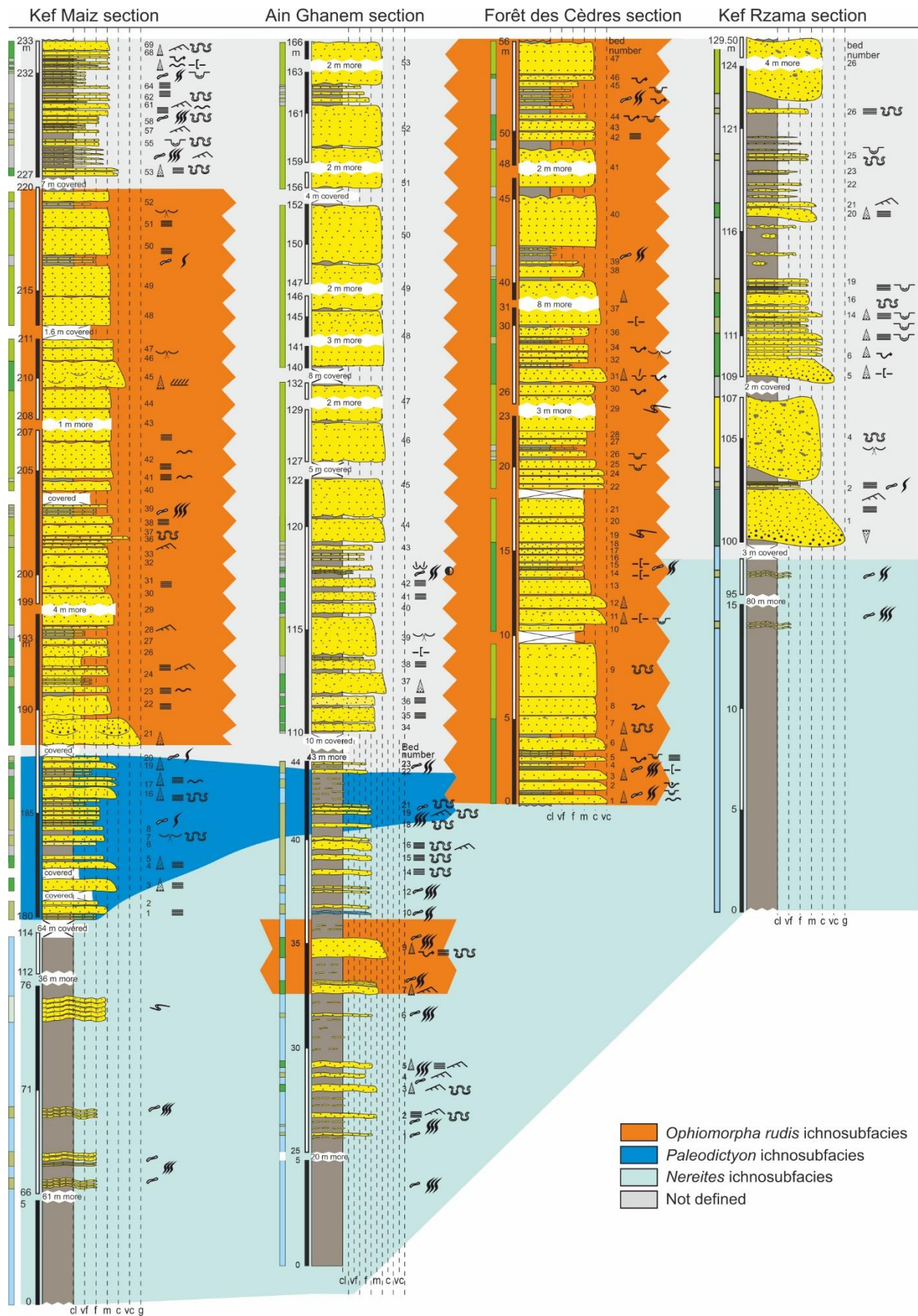


Fig. 36. Vertical distribution of the distinguished ichnofacies in the studied sections with regard to lithostratigraphic subdivision (for explanation of lithofacies see Fig. 7).

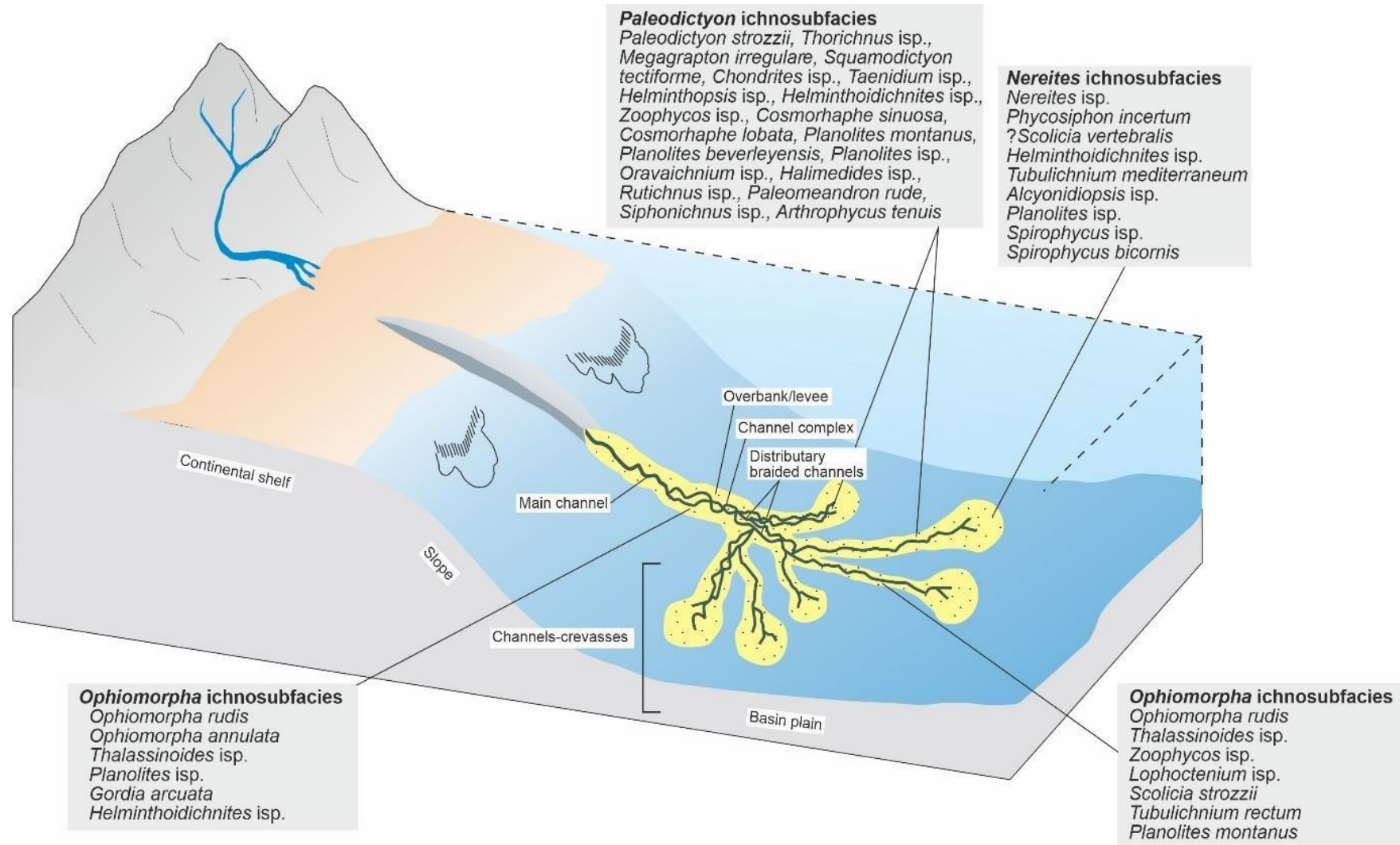


Fig. 37. Simplified schematic block diagram showing the distribution of ichnofacies in the study area.

4.4.2. COMPARISONS

The trace fossil assemblages from the NF in Algeria are similar to those in Tunisia (Riahi et al., 2014) and southern Spain (Rodríguez-Tovar et al., 2016), which represent also the *Nereites* ichnofacies with the *Paleodictyon* and *Ophiomorpha rudis* ichnosubfacies. However, the fossil assemblages from the sections studied in Algeria are less diverse. Data on the ichnology of other parts of the NF (apart from Tunisia and Spain) are not available, except for fragmentary data by Myron (2011), who reported some dispersed trace fossils from Sicily and attributed them to the *Nereites* ichnofacies. Similarly to the Algerian sections studied, the Tunisian and Spanish sections display the highest ichnodiversity in the mudstone/sandstone alternations, which are equivalents of FA2, including the dominance of graphoglyptids in equivalents of facies F4 in this study. The medium- to very thick-bedded sandstones of facies F1 and F2 in Algeria are poorly bioturbated and show lower ichnodiversity. On the contrary, some of their equivalents in Tunisia are characterized by abundant *Ophiomorpha rudis* and *Diplocraterion cf. habichi* (Riahi et al., 2014). Moreover, sections in southern Spain yield abundant *Ophiomorpha* and *Scolicia* (Rodríguez-Tovar et al., 2016). The mudstone or marly mudstone facies (F8) shows abundant to very abundant *Tubulichnium mediterraneum* in almost all compared outcrops in addition to rare *Alcyonidiopsis* isp. in Algeria, and abundant *Diplocraterion cf. habichi*, *Planolites montanus*, and *Chondrites* isp. in Tunisia.

When comparing to other equivalent Oligocene to Miocene turbiditic deposits from the Mediterranean region, the Grès d'Annot Basin deposits from southern France (Phillips et al., 2011) display highly abundant and low diversity trace fossil assemblages, mostly in fine- to medium-grained sandstones (equivalent to facies F4), dominated by *Ophiomorpha*, *Phycosiphon*, *Planolites*, and *Scolicia*. In turn, the thick-bedded sandstones of France (equivalent to facies F1) show low diversity trace fossils, dominated by *Ophiomorpha rudis* with less common *Thalassinoides suevicus*. The foredeep basins of the Northern Apennines in central Italy (Monaco et al., 2010) shows more abundant and diverse trace fossils. The mud-dominated facies (equivalent to facies F8 and F7) reveals less common trace fossils dominated by *Zoophycos*, *Thalassinoides suevicus*, and *Ophiomorpha annulata* in some parts while other places show trace fossils of the *Nereites* ichnosubfacies. The bulk of trace fossils occurs in thin- to medium-bedded sandstones (equivalent to facies F4), such as 1) interturbidites with channelized facies or 2) rhythmic beds within mudstones, including predepositional and postdepositional trace fossils with a general dominance of graphoglyptids. The thick-bedded sandstones (equivalent to facies F1 and F2) reveal scarce trace fossils, dominated by *Ophiomorpha* and *Scolicia*.

In addition to the general similarities, the comparison shows that every depositional system, even if almost of the same age and region, shows some differences in trace fossil composition, abundance, and distribution. This may be caused by differences in depositional processes, food abundance and other local factors, including preservational potential.

4.5. PARTIAL CONCLUSIONS

The presented ichnological study allowed the determination of twenty-two ichnogenera and the distinguishing of eight lithofacies grouped in three main facies associations. The trace fossils are dominated by post-depositional ichnotaxa (62%), including *Planolites montanus*, *P. beverleyensis*, ?*Planolites* isp., *Siphonichnus* isp., *Nereites* isp., *Chondrites* isp., *Phycosiphon incertum*, *Taenidium* isp., *Lophoctenium* isp., ?*Scolicia vertebralis*, *S. strozzii*, *Gyrochorte* isp., *Zoophycos* isp., *Oravaichnium* isp., *Halimedides* isp., *O. annulata*, *Ophiomorpha rudis*, *Palaeophycus tubularis*, *Palaeophycus striatus*, *Palaeophycus* isp., ?*Parataenidium* isp., *Thalassinoides* isp., *Tubulichnium mediterraneum*, ?*Alcyonidiopsis* isp., *Tubulichnium rectum*, *Lockeia* isp., and *Diplocraterion* isp., and pre-depositional ichnotaxa (38%), including *Spirophycus bicornis*, *Spirophycus* isp., *Oravaichnium* isp., *Phycodes* isp., *Thorichnus* isp., *Squamodictyon tectiforme*, *Megagraption irregulare*, ?*Arthropycus tenuis*, *Cosmorhapha lobata*, *C. sinuosa*, *Gordia arcuata*, *Helminthoidichnites* isp., *Helminthopsis* isp., *Paleomeandron rude*, *Rutichnus* isp., and *Paleodictyon strozzii*. They commonly occur in fine grained, thin-bedded sandstones (representing facies F4), mostly in facies associations FA2 and FA3. Ichnological analysis associated with sedimentary data indicate a deep-sea environment with typical trace fossil assemblages attributed to the *Nereites* ichnofacies, including its three main ichnosubfacies, i.e. (1) the *Ophiomorpha rudis* ichnosubfacies recorded in medium- to very thick-bedded sandstones (FA1) interbedded with thinner sandstone beds of facies F2 and F4 in the upper unit of the studied sections. These deposits probably originated in channel and levee-overbank environments. The medium to thin-bedded sandstones (FA2) in the lower units of the Kef Maiz and Ain Ghanem sections were deposited probably in isolated narrow channels in the mud-dominated part of the depositional system, which was occasionally fed with turbiditic sands. (2) The *Paleodictyon* ichnosubfacies occurs in thin- to medium-bedded sandstones (facies F4) deposited probably in channel-margin or channel-levee-overbank settings, which are recorded in the lower units of the Ain Ghanem and Kef Maiz sections, and the lower part of the upper unit in the Kef Maiz section. (3) The *Nereites* ichnosubfacies is recorded in thin-bedded sandstones (FA2), which were deposited probably in

the basin-floor environment, specifically in crevasse splays or small lobes characterized by occasional turbiditic flows associated with pelagic and hemipelagic sedimentation.

CHAPTER 5

SEDIMENT PROVENANCE ANALYSIS

5.1. INTRODUCTION

The provenance of the deposits of the Numidian Formation (NF) was and is still a matter of controversy among Mediterranean geologists whether the source rock of the detrital material that fed the Maghrebian Flysch Basin (MFB) is of European or African origin. Two main perspectives were suggested; (1) a northern source, represented by the European AlKaPeCa domain. This proposition was supported by [Mattauer \(1958, 1973\)](#), [Caire \(1961\)](#), [Caire and Duée \(1971\)](#); [Magné and Raymond, \(1972\)](#); [Ivaldi, \(1977\)](#); [Lahondère et al. \(1979\)](#); [Vila et al., 1995](#); [Van Houten \(1980\)](#), [Parize et al. \(1986, 1999\)](#), [Benomran et al. \(1987\)](#), [Yaïch et al. \(2000\)](#), and recently by [Fildes et al. \(2010\)](#) based on the interpretation of zircon dating carried out from the northern Tunisia and Sicily; (2) the second perspective was a southern provenance, represented by the African craton, and supported by [Durand Delga \(1955, 1980\)](#), [Ogniben \(1960\)](#), [Wezel \(1970a\)](#), [Gaudette et al. \(1995\)](#), [Hoyez \(1975, 1989\)](#), [Lancelot et al. \(1977\)](#), [Moretti et al. \(1991\)](#), [Johansson et al. \(1998\)](#); [Thomas et al. \(2010a, 2010b\)](#), [Guerrera et al... \(1992, 2012\)](#), [Fornelli et al. \(2015\)](#), and [Azdimousa et al. \(2019\)](#). The northern source is represented by the continental basement from mainland Europe or by the terranes rifted from it, including the AlKaPeCa (Alboran, Calabria, Peloritan, Kabylies) microplate, Sardinia, and Corsica. The southern source is represented by the West African craton, the Hoggar and Tibesti massifs, and the east of the African craton.

In this chapter, the zircon geochronology method is applied to constrain the source rock for the NF deposits in the Ouarsenis Mountains. This method is applied for the first time on the NF in Algeria. It is supported by data on orientation of the palaeoflow measured on the basis of sedimentary structures, specifically sole marks.

5.2. METHODS

The detailed procedure for U-Pb detrital zircon geochronology PIG-PIB is explained here step by step.

Two samples of quartz-rich sandstone were processed using the standard method for separating zircons, i.e., crushing, sieving, using heavy liquids and the Frantz isodynamic separator, followed by careful inspection of the heavy fraction that could potentially contain zircon under binocular microscope. No zircon grains were found in the magnetic fraction in either of the two sand samples.

Following the separation of zircons, more than 200 grains from each sample were transferred to a double-sided tape. Transferring the zircons took place without qualitative selection to achieve random grain choice without any preference for size, colour, or shape.

The zircons from two samples together with the chips of Temora-2 standard zircon ($^{206}\text{Pb}/^{238}\text{U}$ age of 416.8 ± 0.3 Ma; Black et al., 2004) and the “91500” standard zircon as a reference for U-content (U = 78 ppm, a $^{207}\text{Pb}/^{206}\text{Pb}$ age of 1065.4 ± 0.3 Ma; Wiedenbeck et al., 1995) were mounted on epoxy disc (~3.5 cm – megamount) and polished until quasi-central sections were reached. The reference zircon Temora-2 was used to control for the stability and accuracy of the instrument.

Subsequently, the grains were photographed in both transmitted light and reflected light modes using a Nikon Eclipse LU100NPol polarizing microscope with NIS Element software. After optical imaging, the mount was vacuum-coated with 5 nm of gold for cathodoluminescence (CL).

The internal zircon textures were imaged using a HITACHI SU 3500 scanning electron microscope located at PGI-NRI. On the basis of SEM CL, the area of U-Pb analysis was pre-selected. Before isotopic measurement, the gold film was removed and the mount re-cleaned, prior to being recoated with about 15 nm of high purity gold for SHRIMP analysis. All U-Pb isotopic results were collected on the SHRIMP IIe/MC instrument (the sensitive high-resolution ion microprobe) using a duoplasmatron as the primary ion source, according to the general procedure described by Williams (1998).

The isotopic ratios were analysed using a ~20–23 μm -diameter primary beam consisting of ionized oxygen molecules (O_2^+), purified by a Wien filter. Before each analysis, the surface of the site was cleaned by rastering of the primary beam for 2 min, to reduce the amount of common Pb on the mount surface. Secondary ions were collected on a single electron multiplier by cycling the magnet through six scans on nine masses: $^{196}\text{Zr}_2\text{O}$, ^{204}Pb , 204.1 (as a background), ^{206}Pb , ^{207}Pb , ^{208}Pb , ^{238}U , ^{248}ThO , and ^{254}UO . The measurements were carried out with a mass resolution of approximately 5400 (at 1% peak height) for about ~16 min.

The analyses were collected in a sequence consisting of one analysis of a Temora-2 reference zircon measurement after every fourth unknown sample analysis. SHRIMP U-Pb data were processed using open-source SQUID-2 software from Geoscience Australia and plotted using Isoplot (Ludwig, 2009) and IsoplotR (Vermeesh, 2018) software. Common-Pb corrections for unknown samples were based on measured ^{204}Pb . The isotopic composition was calculated using the Pb isotopic evolution model of Stacey and Kramers (1975), and the time corresponding to the preliminary $^{206}\text{Pb}/^{238}\text{U}$ age was calculated using the default common-Pb compositions.

The ages are $^{206}\text{Pb}/^{238}\text{U}$ for zircon grains < 1000 Ma, and $^{207}\text{Pb}/^{206}\text{Pb}$ for those > 1000 Ma, as a consequence of the relatively short half-life of the ^{235}U parent, making $^{207}\text{Pb}/^{206}\text{Pb}$

ages less precise than $^{206}\text{Pb}/^{238}\text{U}$ ages for relatively young zircons (Black et al., 2003). For detrital grains > 1000 Ma, the $^{206}\text{Pb}/^{207}\text{Pb}$ age is used in the cumulative probability plot, but for data < 1000 Ma, the $^{206}\text{Pb}/^{238}\text{U}$ age is preferred because $^{206}\text{Pb}/^{238}\text{U}$ ages are generally more precise for younger ages, whereas $^{206}\text{Pb}/^{207}\text{Pb}$ ages are more precise for older ages (Gehrels, 2011).

5.3. SAMPLING LOCALITIES AND DESCRIPTION OF SAMPLES

The sample KMS-B29 (N36°3.716', E1°15.784') was carried out from very thick-bedded sandstone (5–7 m) belonging to facies F1 (structureless sandstone) (Figs. 38A, B, 39). The sample KRS-B01 (N35°50.190'; E2°2.061') was carried out from very coarse, coarse to medium-grained with dispersed granules, very thick bedded sandstone belonging to facies F3 (inversely-graded pebbly sandstone to parallel stratified sandstone) (Figs. 38C, D, 39).



Fig. 38. Photographs of the beds analysed for zircon dating. (A), (B) Photographs of the sample KMS-bed 29, the Kef Maiz section; (A), (B) Photographs of the sample KRS-bed-01, the Kef Rzama section.

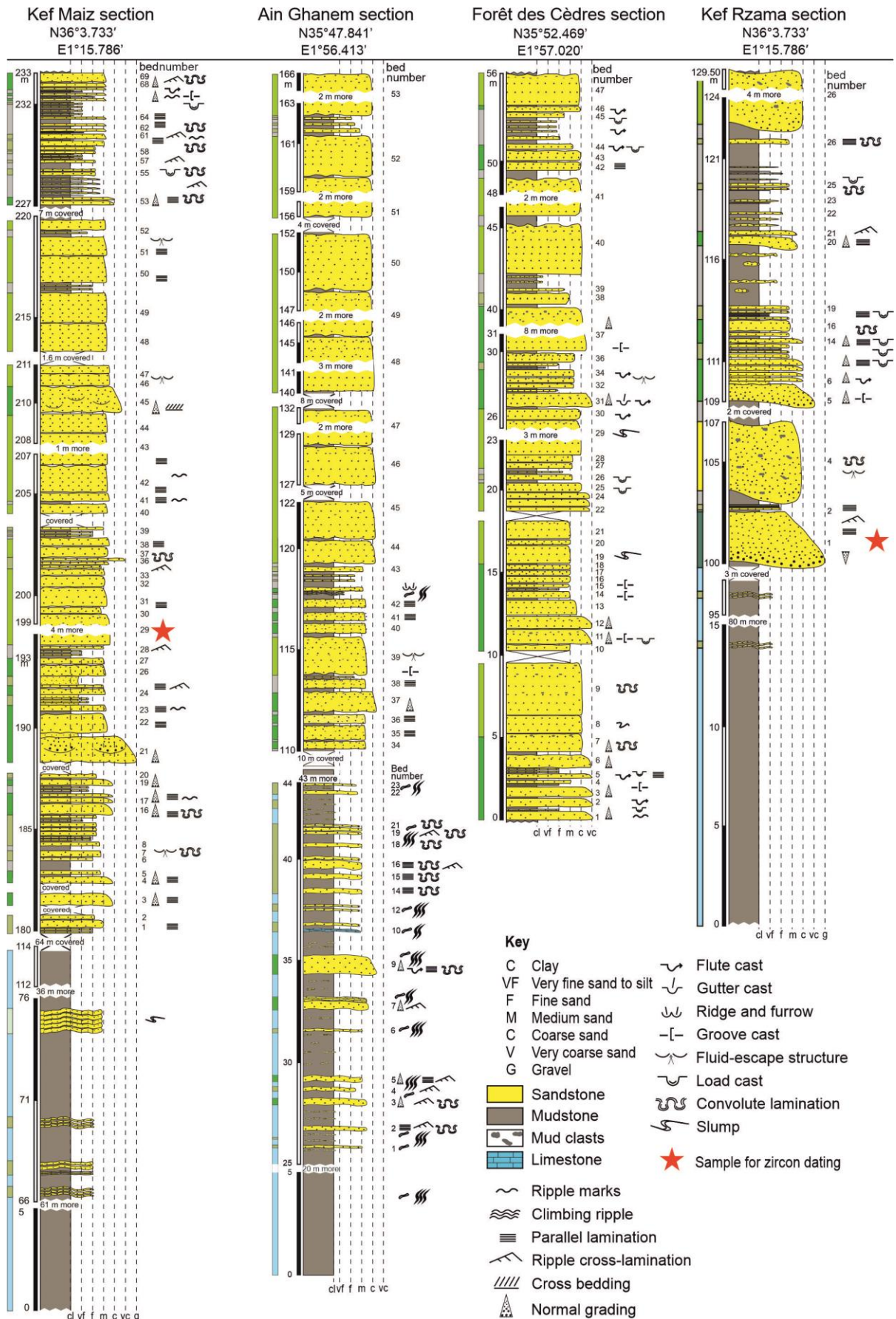


Fig. 39. Lithological columns with indication of sedimentary structures and the analysed samples for the U-Pb zircon dating.

5.4. RESULTS

5.4.1. PALAEOCURRENT DATA

Table 4, Fig. 40

In order to know the palaeoslope dip direction and eventually the possible source of sediment, sedimentary structures that indicate palaeocurrent direction mostly sole marks are analysed here from the study area, including groove casts, frondescient marks, flute casts, longitudinal scour. Fifty-six (56) measurements are taken from the Forêt des Cèdres section, twenty-seven (27) from the Ain Ghanem section, and five (5) from the kef Rzama section.

Table 5. Detail data of palaeoflow measurement in the study area

Section	Class	Number of measurements	Sedimentary structures
Forêt des Cèdres section	30-60	15	Groove casts
	60-90	11	Groove casts / frondescient marks
	90-120	5	FronDESCENT casts
	120-150	18	Flute casts
	150-180	7	Flute casts / longitudinal scour
Ain Ghanem section	140-150	3	Groove casts
	230-240	3	Flute casts
	240-250	10	Flute casts
	250-260	6	Flute casts
	260-270	5	Flute casts
Kef Rzama section	60-90	5	Groove casts

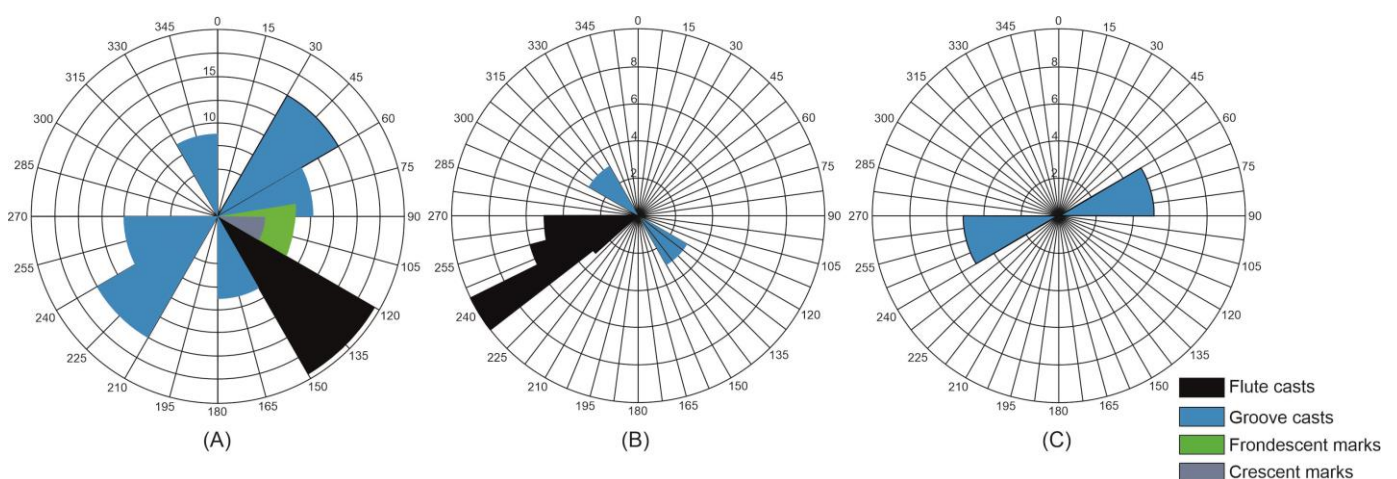


Fig. 40. Palaeocurrent rose diagrams from the study area. (A) Data measured from the Forêt des Cèdres section; (B) Data measured from the Ain Ghanem section; (C) Data measured from the Kef Rzama section.

5.4.1.1. INTERPRETATION

In the Forêt des Cèdres section, flute casts and frondescant casts indicate a south-eastern orientation; however, groove casts show SW-NE directions with a major south-east orientation. In the Ain Ghanem section, flute casts indicate an eastern-to-north-eastern orientation, and the groove casts indicate a close direction-oriented SE–NW. A few data on groove casts from the Kef Rzama section indicate mostly the E-W direction.

The presented palaeoflow data do not show a single orientation of the palaeocurrent but the major orientation given by flute casts ranges from the south-east to the east. Previous studies from the Numidian Formation in the Mediterranean concluded that there is no single dominant orientation of the palaeoflow orientation in Algeria (Hoyez, 1975; Moretti et al., 1991; Laval, 1992; Vila et al., 1995), Tunisia (Hoyez, 1975; Parize et al., 1986; Parize and Beaudoin, 1987; Yaich, 1992a), and Italy (Wezel, 1969; Wezel, 1970b; Parize et al., 1986; Fornelli, 1998; Parize et al., 1999).

The tectonic complications related to the emplacement of the NF in the study area (overturned sections) can justify in some way the discordance of the palaeoflow orientation between different sections. Palaeomagnetic studies from Italy, Tunisia, Spain, and Morocco have demonstrated a structural rotation of the NF thrust sheets of about 55° to 76°, which weakens the reliability of the use of the palaeoflow method to constrain the provenance of the NF sediments (Thomas et al., 2010b and references therein), no such studies were performed on the NF in Algeria.

5.4.2. ZIRCON DATA

5.4.2.1. ZIRCON TEXTURES

Zircon crystals are generally rounded, subrounded, and columnar in shape, occasionally fractured and broken. The original external morphology is generally not preserved as a result of transport (Fig. 41). Their size ranges from 50 to 270 µm. The CL images of zircon grains show a variety of morphological pattern, including (1) zircons with regular not perturbed oscillatory zoning (Fig. 41A, B) indicating that the crystals crystallized in one single magmatic event (Corfu et al., 2003); (2) zircons with xenocrystic cores showing oscillatory zoning discordant with a rim showing subsequent oscillatory zoning of magmatic overgrowth (Fig. 41C, F); (3) zircons showing oscillatory zoning on the core and no zoning on the rim (Fig. 41D, E) which is interpreted as the cores is of magmatic origin overprinted by metamorphism

(Corfu et al., 2003); (4) zircon without zoning showing irregular and complex texture (Fig. 41G, H) indicating a metamorphic origin (Corfu et al., 2003).

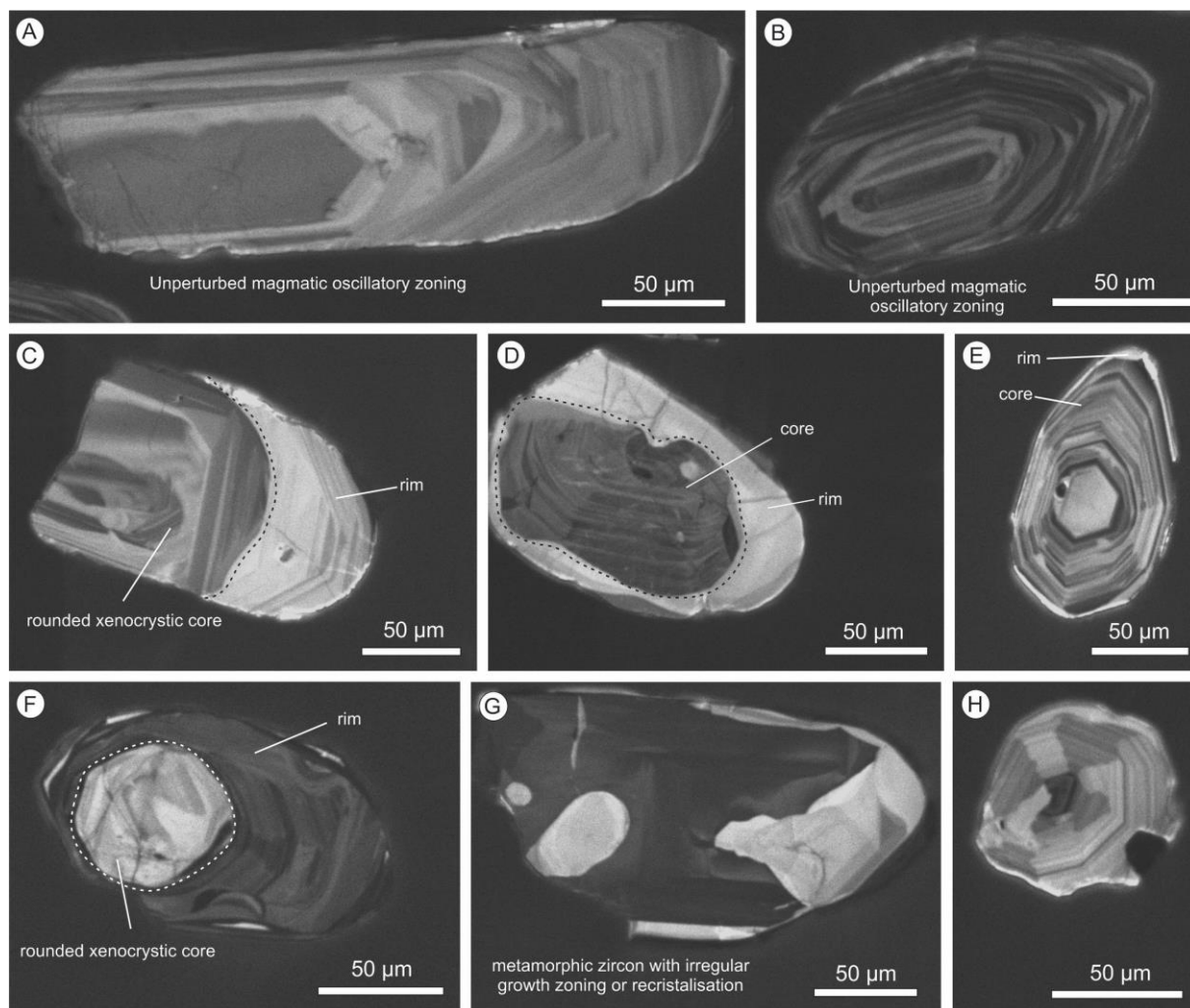


Fig. 41. CL images showing the main zircon textures in the study area. (A), (B) zircons with unperturbed zoning, sample KMS-B29; (C), (F), sample KRS B01; (D), (E), (H), sample KRS B01; (G), sample KMS-B29.

5.4.2.2. U-Pb ZIRCON AGES

Figs. 42–44

The results of the U-Pb zircon ages are illustrated in Figures 42, 43, and 44. Data with a high discordance of U-Pb age (>10%) were discarded.

One hundred and two zircon grains from sample KMS-B29 (the Kef Maiz section) were selected for U-Pb isotopic dating. Oscillatory zoning is common within these grains, which indicates a magmatic origin (Corfu et al., 2003). The Th/U ratio in this sample show 47% > 0.5, indicating a magmatic origin, and 53% between 0.01 and 0.5, indicating an intermediate

origin. The latter generally represent zircon grains of magmatic origin that are affected by medium to high-grade metamorphism (Fig. 44). U-Pb analysis shows a wide range of concordant zircon ages, grouped into four main populations, including (1) twenty-two zircon grains giving ages from 551 to 992 Ma, indicating the Neoproterozoic; (2) twenty-four zircon grains giving ages from 1002 to 1527 Ma, indicating the Mesoproterozoic; (3) twenty zircon grains giving ages from 1670 to 2205 Ma, indicating the Paleoproterozoic; (4) four zircon grains giving ages from 2624 to 2728 Ma, indicating the Neoproterozoic. A single zircon grain indicating the Mesoarchean was discarded (Fig. 42).

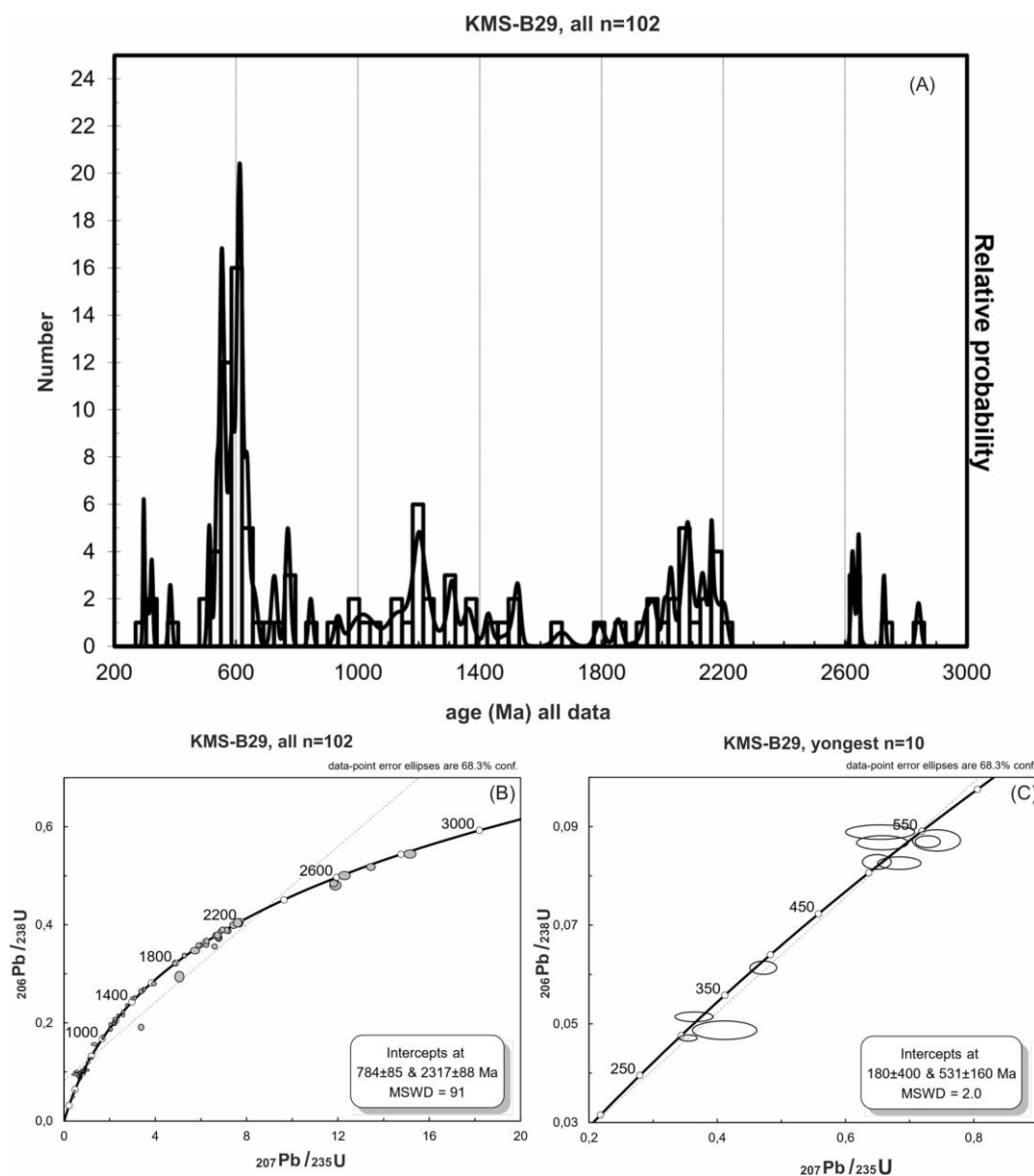


Fig. 42. U-Pb concordia and probability diagrams of zircon ages from the sample KMS-B29, the Kef Maiz section. (A) Histogram of probability density plots of zircon ages; (B) U-Pb concordia diagram showing all data, and (C) showing only youngest ages.

One hundred and three zircon grains from sample KRS-B01 (the Kef Rzama section) were selected for U-Pb isotopic dating. This sample also shows abundance oscillatory zoning pointing to a magmatic origin (Corfu et al., 2003). The Th/U ratio in this sample show 41.74% > 0.5, indicating a magmatic origin, and 56.31% between 0.01 and 0.5 indicating intermediate origin, and only 2% < 0.01, suggesting a metamorphic origin (Fig. 44).

The U-Pb analysis shows a high number of concordant zircon ages, grouped into three main populations, including (1) twenty-six zircon grains giving ages from 563 to 987 Ma, indicating the Neoproterozoic; (2) ten zircon grains giving ages from 1007 to 1328 Ma, indicating the Mesoproterozoic; (3) twenty-three zircon grains giving ages from 1684 to 2470 Ma, indicating the Paleoproterozoic. A few zircon grains indicating the Ordovician, the Cambrian, the Neoproterozoic and the Mesoarchean were discarded (Fig. 43).

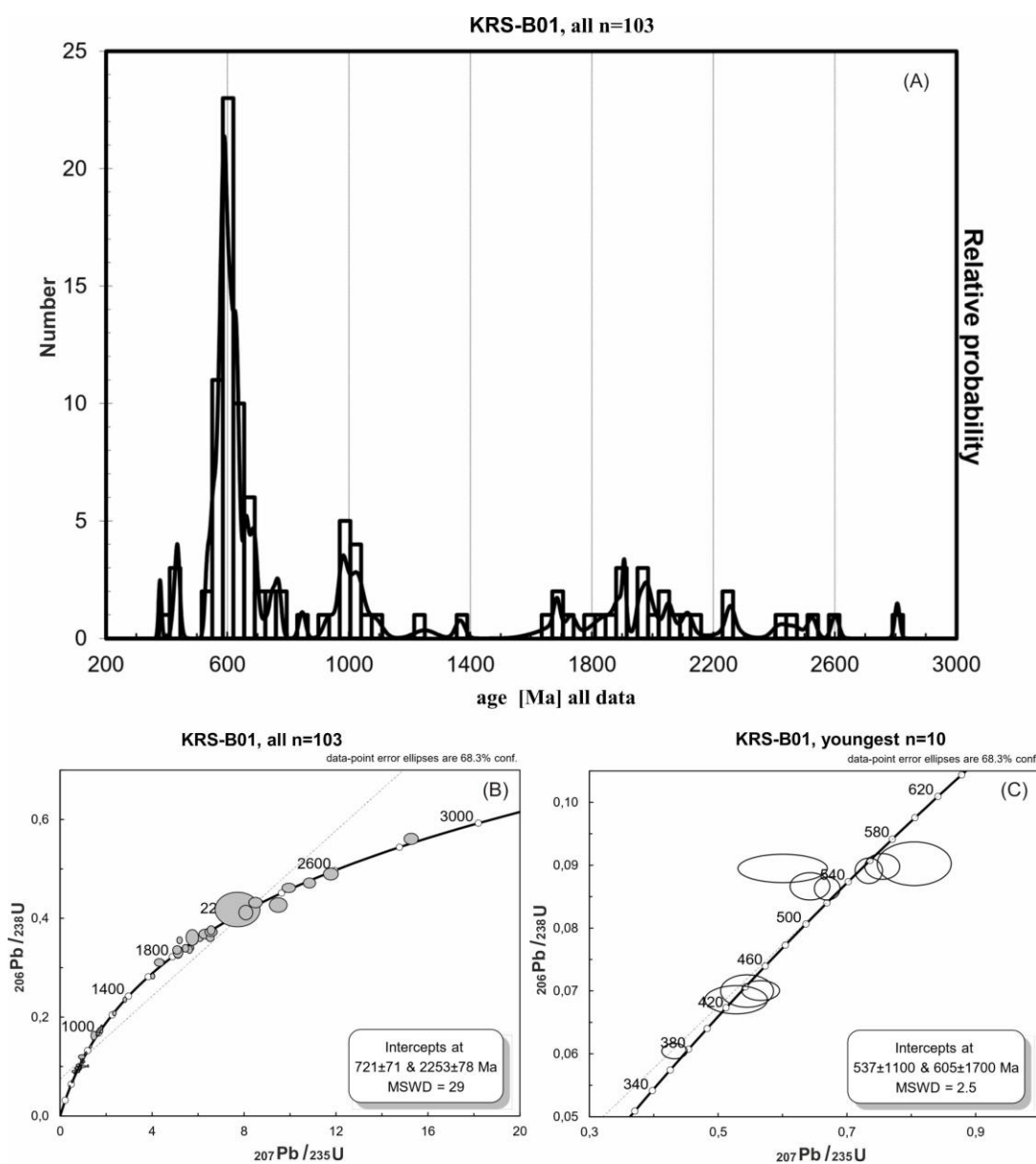


Fig. 43. U-Pb concordia and probability diagrams of zircon ages from the sample KRS-B01, the Kef Rzama section. (A) Histogram of probability density plots of zircon ages; (B) U-Pb concordia diagram showing all data; (C) data showing only youngest ages.

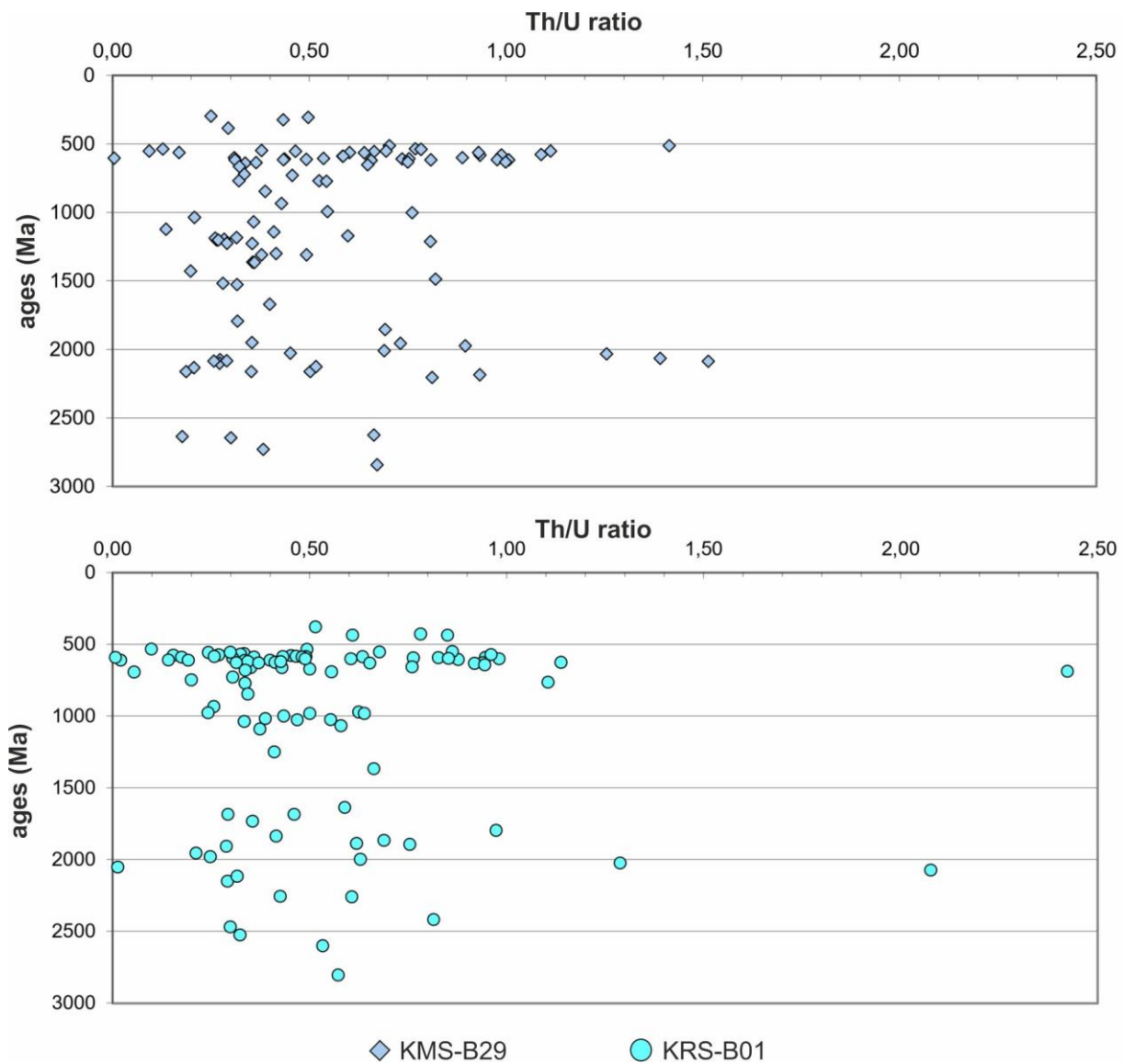


Fig. 44. Diagrams showing the Th/U ratio within the samples KMS-B29 from the Kef Maiz section, and KRS-B01 from the Kef Rzama section.

5.4.2.3. DISCUSSION

The zircon analysed from the two samples KMS-b29 and KRS-b01 yielded similar cluster ages, including three main groups: (1) 563–992 Ma; (2) 1007–1527 Ma; (3) 1684–2470 Ma, with a few zircon grains that indicate the Neoproterozoic and the Mesoproterozoic. A few zircon grains from the sample KRS-b01 indicate younger ages (538 to 470 Ma).

The histogram of the probability density of ages from the two samples KMS-b29 and KRS-b01 (Fig. 42A, Fig. 43A) shows similar peaks with abundant zircon grains, indicating the Paleoproterozoic, the Mesoproterozoic and the Neoproterozoic, the ages characterising the Eburnean and the Panafrican orogenies, respectively, without evidence for the Hercynian and Alpine orogenies.

The zircon ages between 470 and 650, representing the end of the Panafrican orogeny (550–650 Ma) can be found in either in the European terranes (Peucat et al., 1996; Hammor et al., 2006) or the African basement within the Hoggar and Tibesti massifs, and the East African craton (Bertrand et al., 1986; Paquette et al., 1997; Walsh et al., 2002; Inglis et al., 2004; Kuster et al., 2008). However, the zircon ages older than 600 Ma including those indicating the Eburnean orogeny (~2 Ga) are exclusively represented in the African cratons (Walsh et al., 2002; Peucat et al., 2005; 19) Peucat et al., 2003; Suayah et al., 2006; Kuster et al., 2008).

The above-mentioned characteristics of the analysed zircons from the study area, including textures roundness, and the abundance of o zircons referred to the Eubrunean and Panafrican orogenies, with the absence of ages indicating the Hercynian and the Alpine orogenies, point toward an African provenance of the studies deposits. These deposits were affected by polycyclic reworking within the Continental Intercalaire (Cretaceous) (Moretti et al., 1991) or the Nubian Sandstone in Libya (Cretaceous) (Wezel, 1970a; Johansson et al., 1998). The Moroccan Anti-Atlas can also provide zircons with the found ages (Thomas et al., 2010b and references therein).

Similar zircon age populations were found in the NF in the Rif Chain, Morocco (Azdimousa et al., 2019), and in the NF in the Southern Apennines, Italy (Fornelli et al., 2015). Zircon ages from the NF in Gibraltar and Sicily (Lancelot et al., 1976, 1977) deliver only two populations (1830 and 1350 Ma), whereas those analysed from the NF in Tunisia by Gaudette et al. (1975) and Gaudette et al. (1979) deliver one population dated to about 1750 Ma. All these mentioned zircon ages were interpreted as sourced from the African Craton, in contrast to the interpretation given by Fildes et al. (2010) based on the results of zircon ages from the NF in Tunisia and Sicily giving around 514 to 550 Ma, interpreted as sourced from an European source. The review by Thomas (2010b) from the NF in the Mediterranean gives very strong arguments favouring the southern provenance.

5.5. PARTIAL CONCLUSIONS

The method of provenance analysis is applied here in conjunction with data on palaeocurrent orientation to constrain the source rock of the Numidian Formation deposits in the Ouarsenis Mountains. The analysis of the palaeoflow data based on measurements of sole marks does not show a single orientation of the palaeocurrent. However, the major orientation based on orientation of flute casts and frondescant marks is more consistent and ranges from the south-east to the south-west.

A representative number of 205 zircon grains were separated from two samples KMS-b29 and KRS-b01 to perform U/Pb geochronology and morphological description. CL images of zircon grains show a variety of morphological patterns characterized by (1) abundant grains showing oscillatory zoning indicative of magmatic origin associated and (2) zircon grains with oscillatory zoning at the core and no zoning at the rim, indicating magmatic origin overprinted by metamorphism. Structureless zircon grains indicative of metamorphic origin are rare.

The zircons analysed yielded similar cluster ages, including three main groups: (1) 563–992 Ma indicating the Neoproterozoic; (2) 1007–1527 Ma indicating the Mesoproterozoic; (3) 1684–2470 Ma indicating the Paleoproterozoic, with a few zircon grains indicating the Neoproterozoic and Mesoproterozoic. A few zircon grains from sample KRS-b01 indicate younger ages (538–470 Ma). These zircon ages indicate the Eburnean and the Pan-African orogenies without evidence for the Hercynian and Alpine orogenies.

The above-mentioned characteristics of the zircon grains, including roundness, palaeoflow data, and the abundance of grains showing Eburnean and Pan-African ages, with absence of ages indicating the Hercynian and the Alpine orogenies, point toward an African origin of the studied deposits.

CHAPTER 6

GENERAL CONCLUSIONS

6. GENERAL CONCLUSIONS

The main objectives planned for this doctoral thesis on the Numidian Formation of the Ouarsenis Mountains, NW Algeria were achieved, including sedimentological and ichnological studies, and determination of the provenance of detrital material. Biostratigraphic analysis did not provide valuable results, permitting a detailed dating of the studied deposits. More work is needed to deal with this last problem.

The Numidian Formation in the Ouarsenis Mountains is represented by siliciclastic deposits with intercalated hemipelagic mudstones in the four sections studied. The latter are subdivided into two main informal lithostratigraphic units: (1) the lower unit (mud-dominated) made up of varicoloured mudstones (greenish to dark brown) with abundant full relief trace fossil *Tubulichnium mediterraneum* and rare ?*Alcyonidiopsis* sp., including isolated bodies of sandstone and mudstone alternations or discontinuous thin-bedded, fine grained-sandstone; (2) the upper unit (sand-dominated) consists of beige to pale grey/white, fine- to very coarse-grained, conglomeratic in some parts, medium- to very thick-bedded sandstones, alternating with greenish to grey, thin silty mudstone. The two upper and lower aforementioned units are present in three of the four sections; the Forêt des Cèdres section comprises only the sand-dominated upper unit. The lower unit is dated to the Upper Oligocene and the upper unit to the Lower Miocene, based on correlation with the NF of Great Kabylia and on biostratigraphic data from previous studies on the study area.

Investigations of calcareous nannoplankton and foraminifers by the author of the thesis gave some results but only from the lower unit, including rare agglutinated foraminifers, such as *Glomospira* sp., *Ammodiscus* sp., *Paratrochamminoides* sp., *Haplophragmoides* sp., *Trochamminoides* sp., and *Recurvoides* sp. In contrast to calcareous nannoplankton and foraminifers, investigations for dinoflagellate cysts from the lower and upper units of the studied sections gave positive results. Both units yielded rich although taxonomically impoverished dinoflagellate cyst assemblages associated by other aquatic palynomorphs. Biostratigraphic interpretation of the assemblages from the interval studied is difficult and imprecise so far, but it suggests a time span from the late Paleogene to early Miocene.

The sedimentological study permits characterizing eight lithofacies including structureless sandstone (F1), normally-graded, medium- to very coarse-grained sandstone (F2), inversely-graded pebbly sandstone to parallel stratified sandstone (F3), medium- to fine-grained sandstone (F4), and mudclast conglomerates (F5), soft-sediment deformed sandstone/siltstone (F6), mudstone with siltstone and sandstone (F7), and varicoloured marly mudstone (F8). The association of these lithofacies yielded three main facies associations,

GENERAL CONCLUSIONS

corresponding to the depositional subenvironment setting, including (1) FA1 sand-rich facies association deposited in the channel-fill setting. It occurs in the upper part of all the studied sections; (2) FA2 mudstone and sandstone alternations facies association, corresponding to channel margin, channel-levee-overbank, crevasse-splays and lobes. This facies association occurs occasionally in the lower and the upper units of the studied sections; (3) FA3 mud-rich facies association deposited on the basin-floor or slope-apron settings, which were cut by, narrow, sparse channels, occurring in the lower unit of all the studied sections except for the Forêt des Cèdres section.

Ichnological study coupled with lithofacies allowed the determination of twenty-two ichnogenera. Trace fossils are dominated by post-depositional ichnotaxa (62%), including *Planolites montanus*, *P. beverleyensis*, ?*Planolites* isp., *Siphonichnus* isp., *Nereites* isp., *Chondrites* isp., *Phycosiphon incertum*, *Taenidium* isp., *Lophoctenium* isp., ?*Scolicia vertebralis*, *S. strozzii*, *Gyrochorte* isp., *Zoophycos* isp., *Oravaichnium* isp., *Halimedides* isp., *O. annulata*, *Ophiomorpha rudis*, *Palaeophycus tubularis*, *Palaeophycus striatus*, *Palaeophycus* isp., ?*Parataenidium* isp., *Thalassinoides* isp., *Tubulichnium mediterraneum*, ?*Alcyonidiopsis* isp., *Tubulichnium rectum*, *Lockeia* isp., and *Diplocraterion* isp., and predepositional ichnotaxa (38%), including *Spirophycus bicornis*, *Spirophycus* isp., *Oravaichnium* isp., *Phycodes* isp., *Thorichnus* isp., *Squamodictyon tectiforme*, *Megagraption irregulare*, ?*Arthropycus tenuis*, *Cosmorhapse lobata*, *C. sinuosa*, *Gordia arcuata*, *Helminthoidichnites* isp., *Helminthopsis* isp., *Paleomeandron rude*, *Rutichnus* isp., and *Paleodictyon strozzii*. They commonly occur in fine-grained, thin-bedded sandstones (representing facies F4), mostly in facies associations FA2 and FA3. Ichnological analysis associated with sedimentary data indicate a deep-sea environment with typical trace fossil assemblages attributed to the *Nereites* ichnofacies, including its three main ichnosubfacies, i.e. (1) the *Ophiomorpha rudis* ichnosubfacies recoded in medium- to very thick-bedded sandstones (FA1) interbedded with thinner sandstone beds of facies F2 and F4 in the upper unit of the sections studied. These deposits probably originated in channel and levee-overbank environments. Medium- to thin-bedded sandstones (FA2) in the lower units of the Kef Maiz and Ain Ghanem sections were probably deposited in isolated narrow channels in the mud-dominated part of the depositional system, which was occasionally fed with turbiditic sands. (2) The *Paleodictyon* ichnosubfacies occurs in thin- to medium-bedded sandstones (facies F4) deposited probably in channel-margin or channel-levee-overbank settings, which are recorded in the lower units of the Ain Ghanem and Kef Maiz sections, and the lower part of the upper unit in the Kef Maiz section. (3) The *Nereites* ichnosubfacies is recorded in thin-bedded sandstones (FA2), which were probably deposited in the basin-floor environment, specifically

GENERAL CONCLUSIONS

in crevasse splays or small lobes characterized by occasional turbiditic flows associated with pelagic and hemipelagic sedimentation.

The method of provenance analysis is applied here in conjunction with data on palaeocurrent orientation to constrain the source rock of the Numidian Formation deposits in the Ouarsenis Mountains. The analysis of the palaeoflow data based on measurements of sole marks does not show a single orientation of the palaeocurrent. However, the major orientation based on orientation of flute casts and frondescant marks is more consistent and ranges from the south-east to the east.

A representative number of 205 zircon grains were separated from two samples KMS-b29 and KRS-b01 to perform U/Pb geochronology and morphological description. CL images of zircon grains show a variety of morphological patterns characterized by (1) abundant grains showing oscillatory zoning indicative of magmatic origin and (2) zircon grains with oscillatory zoning at the core and no zoning at the rim, indicating magmatic origin overprinted by metamorphism. Structureless zircon grains indicative of metamorphic origin are rare.

The zircons analysed yielded similar cluster ages, including three main groups: (1) 563–992 Ma indicating the Neoproterozoic; (2) 1007–1527 Ma indicating the Mesoproterozoic; (3) 1684–2470 Ma indicating the Paleoproterozoic, with a few zircon grains indicating the Neoproterozoic and Mesoproterozoic. A few zircon grains from sample KRS-b01 indicate younger ages (538–470 Ma). These zircon ages indicate the Eburnean and the Panafrikan orogenies without evidence for the Hercynian and Alpine orogenies.

The above-mentioned characteristics of the zircon grains, including roundness, palaeoflow data, and the abundance of grains showing Eburnean and Panafrikan ages, with absence of ages indicating the Hercynian and the Alpine orogenies, point toward an African origin of the studied deposits.

CHAPTER 7

REFERENCES

7. REFERENCES

- Aceñolaza, G.F., Alonso, R.N., 2001.** Ichno-asociaciones de la transición Precámbrico-Cámbrico en el noroeste de Argentina. *Journal of Iberian Geology*, **27**: 11–22.
- Alexandrescu, G., Brustur, T., 1981.** The *Sabularia* ichnofacies in Vinețisu Beds from the north part of East Carpathians. *Dări de Seamăale Institutului de Geologieși Geofizică*, **68** (3): 17–22. [In Romanian.]
- Algarra, A.M., 1987.** *Evolución geológica alpina del contacto entre las zonas internas y las zonas externas de la cordillera Bética (sector centro-occidental)*. Doctoral dissertation, Universidad de Granada, Granada, 1171 pp.
- Allen, J.R.L. (Ed.), 1982.** *Sedimentary Structures: Their Character and Physical Basis*, Volume II. Developments in Sedimentology, **30**: 663 pp.
- Alpert, S.P., 1977.** Trace fossils and the basal Cambrian boundary. *Geological Journal Special Issue 9*: 1–8.
- Archer, A.W., Maples, C.G., 1984.** Trace fossil distribution across a marine-to-non marine gradient in the Pennsylvanian of southwestern Indiana. *Journal of Paleontology*, **58**: 448–466.
- Arkell, W.J., 1939.** U-shaped burrows in the Corallian Beds of Dorset. *Geological Magazine*, **76**: 455–460.
- Arnott, R.W.C., Hand, B.M., 1989.** Bedforms, primary structures and grain fabric in the presence of suspended sediment plain. *Journal of Sedimentary Petrology*, **59**: 1062–1069.
- Aubert, F., 1891.** Note sur la géologie de l'extrême Sud de la Tunisie. *Bull. Soc. Géol. Fr*, **3**(19), 408-413.
- Azdimousa, A., Jabaloy-Sánchez, A., Talavera, C., Asebriy, L., González-Lodeiro, F., & Evans, N. J., 2019.** Detrital zircon U-Pb ages in the Rif Belt (northern Morocco): Paleogeographic implications. *Gondwana Research*, **70**, 133-150.
- Azpeitia Moros, F., 1933.** Datos para el estudio paleontológico del Flysch de la Costa Cantábrica y de algunos otros puntos de España. *Boletín del Instituto Geológico y Minero de España*, **53**: 1–65.

REFERENCES

- Benhamou, M., 1996.** *Evolution tectono-eustatique d'un bassin de la Téthys Maghrébine : l'Ouarsenis (Algérie) pendant le Jurassique inférieur et moyen.* Thèse Doct. d'Etat, Univ. Oran, 434 p. 139 fig., 27 pl.
- Benomran, O., Nairn, A.E.M., Schamel, S., 1987.** Sources and dispersal of mid-Cenozoic clastic sediments in the central Mediterranean region. *Memorie della Societa Geologica Italiana* 36, 47–68.
- Bertrand, J.M., Michard, A., Boulier, A.-M., Dautel, D., 1986.** Structure and U/Pb geochronology of central Hoggar (Algeria); a reappraisal of its Pan-African evolution. *Tectonics* 5 (7), 955–972.
- Billings, E., 1862.** New species of fossils from different parts of the Lower, Middle and Upper Silurian rocks of Canada. In *Palaeozoic Fossils, Volume 1, 1861–1865. Geological Survey of Canada Advance Sheets*, pp. 96–168.
- Bischoff, B., 1968.** *Zoophycos*, a polychaete annelid, Eocene of Greece. *Journal of Paleontology*, 42: 1439–1443.
- Bizon, G., Hoyez, B., 1979.** Données stratigraphiques sur les formations sous-numidiennes en Algérie. *Compte Rendus de l'Académie des Sciences, Série D – Sciences Naturelles*, 289: 655–658.
- Black, L.P., Kamo, S.L., Allen, C.M., Davis, D.W., Aleinikoff, J.N., Valley, M.J.W., Mundil, R., Campbell, I.H., Korsch, R.J., Williams, I.S., Foudoulis, C., 2004.** Improved 206Pb/238U microprobe geochronology by the monitoring of a trace-element-related matrix effect: SHRIMP, ID-TIMS, ELA-ICP-MS and oxygen isotope documentation for a series of zircon standards. *Chemical Geology* 205, 115–140.
- Bouillin, J.P., 1977.** *Géologie Alpine de la petite Kabylie dans les régions de Collo et d'El Milia.* Thèse Doctorat d'Etat, Université Paris VI, 511 pp.
- Bouillin, J.P., 1986.** Le bassin maghrébin: une ancienne limite entre l'Europe et l'Afrique à l'ouest des Alpes. *Bulletin de la Société Géologique de France, Série 8, 2*: 547–558.
- Bouillin, J.P., 1992.** La répartition des affleurements de la dorsale Kabyle: héritage d'une segmentation Mésozoïque de la marge Nord-Téthysienne. *Compte Rendus de l'Académie des Sciences*, 315: 1127–1132.
- Bouma, A.H., 1962.** *Sedimentology of Some Flysch Deposits: A Graphic Approach to Facies Interpretation.* Elsevier, Amsterdam, 168 pp.

REFERENCES

- Bromley, R.G., 1996.** *Trace Fossils: Biology, Taphonomy and Applications*, 2nd Edition. Chapman and Hall, London, 361 pp.
- Bromley, R.G., Asgaard, U., 1979.** Triassic freshwater ichnocoenoses from Carlsberg Fjord, East Greenland. *Palaeogeography, Palaeoclimatology, Palaeoecology*, **28**: 39–80.
- Bromley, R.G., Hanken, N.-M., 1991.** The growth vector in trace fossils: examples from the Lower Cambrian of Norway. *Ichnos*, **1**: 261–276.
- Bromley, R.G., Uchman, A., Gregory, M., Martin, A.J., 2003.** *Hillichnus lobosensis* igen. et isp. nov., a complex trace fossil produced by tellinacean bivalves, Paleocene, Monterey, California, U.S.A. *Palaeogeography, Palaeoclimatology, Palaeoecology*, **192**: 157–186.
- Broquet, P., 1968.** *Etude géologique de la région des Madonies (Sicile)*. Ph.D. Thesis, Université de Lille. Faculté des Sciences, 797 pp.
- Buatois, L.A., Mángano, M.G., 1993.** The ichnotaxonomic status of *Plangtichnus* and *Treptichnus*. *Ichnos*, **2**: 217–224.
- Buatois, L.A., Mángano, M.G., 2011.** *Ichnology: Organisms–Substrate Interactions in Space and Time*. Cambridge University Press, Cambridge, (358 pp.).
- Buckman, J.O., 2001.** *Parataenidium*, a new *Taenidium*-like ichnogenus from the Carboniferous of Ireland. *Ichnos*, **8**: 83–97.
- Butler, R. W., Pinter, P. R., Maniscalco, R., Hartley, A. J., 2020.** Deep-water sand-fairway mapping as a tool for tectonic restoration: decoding Miocene central Mediterranean palaeogeography using the Numidian turbidites of southern Italy. *Journal of the Geological Society*, **177**: 766–783.
- Caire, A., 1951.** Structure et évolution de la zone sub-bibanique dans la région de Mansourah-les-Biban (département de Constantine). *Bulletin de la Société Géologique de France*, **6**(8), 721-734.
- Callow, R.H., McIlroy, D., Kneller, B., Dykstra, M., 2013.** Integrated ichnological and sedimentological analysis of a Late Cretaceous submarine channel-levee system: the Rosario Formation, Baja California, Mexico. *Marine and Petroleum Geology*, **41**: 277–294.
- Calver, M.A., 1968a.** Coal measures invertebrate faunas. In: Murchison, D.G., Westoll, T.S. (Eds), *Coal and Coal Bearing Strata*. Oliver & Boyd, London, pp. 147–177.

REFERENCES

- Calver, M.A., 1968b. Distribution of Westphalian marine faunas in northern England and adjoining areas. *Proceedings of the Yorkshire Geological Society*, **37**: 1–72.
- Chalouan, A., Michard, A., El Kadiri, K., Negro, F., Frizon de Lamotte, D., Soto, J.I., Sadiqi, O., 2008. The Rif Belt. *Lecture Notes in Earth Sciences*, **116**: 203–302.
- Chamberlain, C.K., 1971. Morphology and ethology of trace fossils from the Quachita Mountains, southeast Oklahoma. *Journal of Paleontology*, **45**: 212–246.
- Chamberlain, C.K., 1977. Ordovician and Devonian trace fossils from Nevada. *Nevada Bureau of Mines and Geology, Bulletin* **90**: 1–24.
- Corfu, F., Hanchar, J.M., Hoskin, P.W.O., Kinny, P., 2003. Atlas of zircon textures. In: Hanchar, J.M., Hoskin, P.W.O. (Eds.), *Zircon. Reviews in Mineralogy and Geochemistry* **53**, pp. 469–500.
- Collinson, J., Mountney, N., Thompson, D., 2006. *Sedimentary Structures*, Third Edition. Dunedin Academic Press Ltd, Terra Publishing, Harpenden, 304 pp.
- Corner, G.D., Fjalstad, A., 1993. Spreite trace fossils (*Teichichnus*) in a raised Holocene fjord-delta, Breidvikeidet, Norway. *Ichnos*, **2**: 155–164.
- Cornish, F.G., 1986. The trace fossil *Diplocraterion*: evidence of animal-sediment interactions in Cambrian tidal deposits. *Palaios*, **1**: 478–491.
- Crimes, T.P., 1987. Trace fossils and correlation of late Precambrian and early Cambrian strata. *Geological Magazine*, **124**: 97–119.
- Crimes, T.P., 1992. Changes in the trace fossil biota across the Proterozoic-Phanerozoic boundary. *Journal of the Geological Society*, **149**: 637–646.
- Crimes, T.P., Anderson, M.M., 1985. Trace fossils from Late Precambrian-Early Cambrian strata of southeastern Newfoundland (Canada): temporal and environmental implications. *Journal of Paleontology*, **52**: 310–343.
- Crimes, T.P., Crossley, J.D., 1991. A diverse ichnofauna from Silurian flysch of the Aberystwyth Grits Formation, Wales. *Geological Journal*, **26**: 27–64.
- Crimes, T.P., Goldring, R., Homewood, P., Stuijvenberg, J., van, Winkler, W., 1981. Trace fossil assemblages of deep-sea fan deposits, Gurnigel and Schlieren flysch (Cretaceous–Eocene). *Eclogae Geologicae Helvetiae*, **74**: 953–995.

REFERENCES

- D'Alessandro, A., 1982.** Processi tafonomici e distribuzione delle tracce fossili nel Flysch di Gorgolione (Appennino Meridionale). *Rivista Italiana di Paleontologia e Stratigrafia*, **87**: 511–560.
- D'Alessandro, A., Bromley, R.G., Stemmerik, L., 1987.** *Rutichnus*: a new ichnogenus for branched, walled, meniscate trace fossils. *Journal of Paleontology*, **61**: 1112–1119.
- Dashtgard, S.E., 2011.** Neoichnology of the lower delta plain: Fraser River Delta, British Columbia, Canada: Implications for the ichnology of deltas. *Palaeogeography, Palaeoclimatology, Palaeoecology*, **307**: 98–108.
- Dashtgard, S.E., Gingras, M.K., 2012.** Marine invertebrate neoichnology. *Developments in Sedimentology*, **64**: 273–295.
- De La Chavanne, J. D., 1910.** Recherches géologiques et paléontologiques dans la région de Guelma (Algérie), par J. Daresté de La Chavanne. A. Jourdan.
- Demircan, H., Uchman, A., 2016.** Ichnology of prodelta deposits of the Mezardere Formation (late Eocene–early Oligocene) in the Gökçeada island, western Turkey. *Geodinamica Acta*, **28**: 86–100.
- Didon, H., Durand Delga, M., Esteras, M., Feinberg, J., Sutter, G., 1984.** La formation des grès numidiens de l'arc de Gibraltar s'intercale stratigraphiquement entre des argiles oligocène et des marnes burdigaliennes. *Comptes Rendus de l'Académie des Sciences de Paris*, **299**: 121–128.
- Durand Delga, M., 1969.** Mise au point sur la structure du Nord-Est de la Berbérie. *Publications du service géologique de l'Algérie, Bulletin* **39**: 89–131.
- Durand Delga, M., Fonbote, J.M., 1980.** Le cadre structural de la méditerranée occidentale. In: 26ème congrès géologique international, Paris, Colloque C5. *Mémoires du Bureau de Recherches Géologiques et Minières*, **115**: 67–85.
- Durand Delga, M., Magné, J., 1958.** Données stratigraphiques et micropaléontologiques nouvelles sur le Numilitique de l'Est de Cordières bétiques. *Revus de Micropaléontologie*, **1**: 155–175.
- Durand Delga, M., 1955.** Etude géologique de l'Ouest de la chaîne numidique. *Bulletin du Service de la Carte géologique de l'Algérie, 2^{ème} série*, **24**: 533 pp.
- Dżułyński, S., 1965.** New data on experimental production of sedimentary structures. *J. Sed. Petrol.*, **35**, 196–212.

REFERENCES

- Ehrenberg, K., 1944.** Ergänzende Bemerkungen zu den seinerzeit aus dem Miozän von Burgschleinitz beschriebenen Gangkernen und Bauten dekapoder Krebse. *Paläontologische Zeitschrift*, **2**: 354–359.
- Ekdale, A. A., 1980.** Graphoglyptid burrows in modern deep-sea sediment. *Science*, **207**: 304–306.
- Ekdale, A.A., Berger, W.H., 1978.** Deep-sea ichnofacies: modern organism traces on and in pelagic carbonates of the western equatorial Pacific. *Palaeogeography, Palaeoclimatology, Palaeoecology*, **23**: 268–171.
- Ekdale, A.A., Bromley, R.G., 2001.** A day and night in the life of a cleft-foot clam: *Protovirgularia-Lockeia-Lophoctenium. Lethaia*, **34**: 119–124.
- Ekdale, A.A., Lewis, D.W., 1991.** The New Zealand *Zoophycos* revisited: morphology, ethology and paleoecology. *Ichnos*, **1**: 183–194.
- Emmons, E., 1844.** The Taconic System; Based on Observations in New York, Massachusetts, Maine, Vermont, and Rhode-Island. *Caroll and Cook*, Albany, 68 pp.
- Esteras, M., Feinberg, H., Durand-Delga, M., 1995.** Nouveaux éléments sur l'âge des grès Numidiens de la nappe de l'Aljibe (Sud-Ouest de l'Andalousie. Espagne). In: IV Coloquio Internacional Sobre el Enlace Fijo del Estrecho de Gibraltar, Sevilla. *Asociación Española de Estudios para la Comunicación Fija a Través del Estrecho de Gibraltar, Madrid*, pp. 205–215.
- Fallot, P., 1937.** Essai sur la géologie du Rif septentrional. *Notes Mém. Serv. Géol. Maroc*, **40**, 553 pp.
- Feinberg, H., Hoyez, B., Lahondère, J.C., 1981.** Nouvelles données biostratigraphiques sur le Numidien de l'Algérie et du Maroc. *Cahiers de Micropaléontologie*, **3**: 93–99.
- Ficheur, E., 1890.** Description géologique de la Kabylie du Djurdjura. *Étude spéciale des terrains Tertiaires*. Pierre Fontana et C^{ie}, Alger, 479 pp.
- Fildes, C., Stow, D.A.V., Riahi, S., Soussi, M., Patel, U., Milton, A.J., Marsh, S., 2010.** European provenance of the Numidian Flysch in northern Tunisia. *Terra Nova* **22**, 94–102.
- Fillion, D., Pickerill, R.K., 1990.** Ichnology of the Upper Cambrian? to Lower Ordovician Bell Island and Wabana groups of eastern Newfoundland. Canada. *Palaeontographica Canadiana*, **7**: 119 pp.

REFERENCES

- Fischer-Ooster, C., 1858.** Die fossilen Fucoiden der Schweizer Alpen, nebst Erörterungen über deren geologisches Alter. *Huber, Bern*, 74 pp.
- Fitch, A., 1850.** A historical, topographical and agricultural survey of the County of Washington. Parts 2–5. *New York Agricultural Society Transactions*, **9**: 753–944.
- Flandrin, J., 1948.** Contribution à l'étude stratigraphique du Nummulitique algérien. *Bulletin du Service de la Carte géologique de l'Algérie*, 2^{ème} série, **19**: 334 pp.
- Fornelli A, Micheletti F, Langone A and Perrone V., 2015.** First U-Pb detrital zircon ages from Numidian sandstones in Southern Apennines (Italy): evidences of African provenance. *Sedimentary Geology* **320**, 19–29.
- Frey, R.W., Howard, J.D., Pryor, W.A., 1978.** *Ophiomorpha*: its morphologic, taxonomic, and environmental significance. *Palaeogeography, Palaeoclimatology, Palaeoecology*, **23**: 199–229.
- Frey, R.W., Pemberton, S.G., 1984.** Trace fossil facies model. *Geoscience Canada, Reprint Series 1*: 189–207.
- Frizon De Lamotte, D., Saint Bézar, B., Bracène, R., Mercier, E., 2000.** The two main steps of the Atlas building and geodynamics of the western Mediterranean. *Tectonics*, **19**: 740–761.
- Fu, S., Werner, F., 2000.** Distribution, ecology and taphonomy of the organism trace, *Scolicia*, in northeast Atlantic deep-sea sediments. *Palaeogeography, Palaeoclimatology, Palaeoecology*, **156**: 289–300.
- Fürsich, F.T., Alberti, M., Pandey, D.K., 2017.** Behavioural variants of the trace fossil *Gyrochorte*. *Zitteliana*, **89**: 13–22.
- Fürsich, F.T., Taheri, J., Wilmsen, M., 2007.** New occurrences of the trace fossil *Paleodictyon* in shallow marine environments: examples from the Triassic–Jurassic of Iran. *Palaios*, **22**: 408–416.
- Gaillard, C., 1991.** Recent organism traces and ichnofacies on the deep-sea floor off New Caledonia, Southwestern Pacific. *Palaios*, **6**: 302–315.
- Gaillard, C., Olivero, D., 2009.** The ichnofossil *Halimedes* in Cretaceous pelagic deposits from the Alps: Environmental and ethological significance. *Palaios*, **24**: 257–270.
- García-Ramos, J.C., Mángano, M.G., Piñuela, L., Buatois, L.A., Rodríguez-Tovar, F.J., 2014.** The ichnogenus *Tubotomaculum*: an enigmatic pellet-filled structure from Upper

REFERENCES

- Cretaceous to Miocene deep-marine deposits of southern Spain. *Journal of Paleontology*, **88**: 1189–1198.
- Gaudette, H.E., Hurley, P.M., Lajmi, T., 1975.** Source area of the Numidian flych of Tunisia as suggested by detrital zircon ages. *The Geological Society of America Annual Meetings*, **7**, September 1975, Boulder Colorado, pp. 1083–1084.
- Gaudette, H.E., Hurle, P.M., Lajmi, T., 1979.** Provenance studies in Tunisia by U–Pb ages of detrital zircons. *American Association of Petroleum Geologists Bulletin* **63**, 456.
- Gavala y Laborde, J., 1924.** Mapa Geológico de la Provincia de Cádiz a escala 1:100.000. Madrid. *Instituto Geológico de España*.
- Gehres, G., 2012.** Detrital Zircon U-Pb Geochronology: Current Methods and New Opportunities. In Busby C, Azor A (eds) *2012 Blackwell Publishing Ltd Tectonics of Sedimentary Basins*: 45–62.
- Gevers, T.W., Frakes, L.A., Edwards, L.N., Marzolf, J.E., 1971.** Trace fossils in the lower Beacon sediments (Devonian), Darwin mountains, southern Victoria Land, Antarctica. *Journal of Paleontology*, **45**: 81–94.
- Gibert, J., Malard, F., Turquin, M.J., Laurent, R., 2000.** Karst ecosystems in the Rhone River basin. *Ecosystems of the World*, **30**: 533–558.
- Gibert, J.M. de, Benner, J.S., 2002.** The trace fossil *Gyrochorte*: ethology and paleoecology. *Revista Española de Paleontología*, **17**: 1–12.
- Gingras, M.K., Bann, K.L., 2006.** The bend justifies the leans: interpreting recumbent ichnofabrics. *Journal of Sedimentary Research*, **76**: 483–492.
- Gingras, M.K., Dashtgard, S.E., MacEachern, J.A., Pemberton, S.G., 2008.** Biology of shallow-marine ichnology: a modern perspective. *Aquatic Biology*, **2**: 255–268.
- Glacon, G., Rouvier, H., 1967.** Précisions lithologiques et stratigraphiques sur le 'Numidien' de Kroumirie (Tunisie septentrionale). *Bulletin de la Société géologique de France*, **7**(3), 410–417.
- Glangeaud, L., 1932.** Étude géologique de la région littorale de la Province l'Alger (Thèse de doctorat, Sciences naturelles, Muséum d'histoire naturelle). *Bulletin du Service de la carte géologique de l'Algérie*, Série 2, Stratigraphie, **8**: 627 pp.
- Goldring, R., 1962.** The trace fossils of the Baggy Beds (Upper Devonian) of North Devon, England. *Paläontologische Zeitschrift*, **36**: 232–251.

REFERENCES

- Goldring, R., Pollard, J.E., Taylor, A.M., 1991.** *Anconichnus horizontalis*: a pervasive ichnofabric-forming trace fossil in post-Paleozoic offshore siliciclastic facies. *Palaios*, **6**: 250–263.
- Guerrera, F., Loicono, F., Pulisi, D., Moretti, E., 1992.** The Numidian Nappe in the Maghreb Chain: state of the art. *Bolletino Bollettino della Società Geologica Italiana*, **111**: 217–253.
- Guerrera, F., Martín-Algarra, A., Perrone, V., 1993.** Late Oligocene-Miocene syn-/late-orogenic successions in western and central Mediterranean chains from the Betic Cordillera to the southern Apennines. *Terra Nova*, **5**: 525–544.
- Guerrera, F., Martín-Algarra, A., Martín-Martín, M., 2012.** Tectono-sedimentary evolution of the ‘Numidian Formation’ and Lateral Facies (southern branch of the western Tethys): constraints for central-western Mediterranean geodynamics. *Terra Nova*, **24**: 34–41.
- Guerrera, F., Martín-Martín, M., Perrone, V., Tramontana, M., 2005.** Tectonosedimentary evolution of the southern branch of the Western Tethys (Maghreb Flysch Basin and Lucanian Ocean) on the basis of the stratigraphic record. *Terra Nova*, **24**: 34–41.
- Hakes, W. G., 1985.** Trace fossils from brackish-marine shales, Upper Pennsylvanian of Kansas, USA. In: Curran, H.A. (Ed.), *Biogenic Structures: Their Use in Interpreting Depositional Environments*. *The Society of Economic Paleontologists and Mineralogists*, Special Publication, **35**: 21–35.
- Hall, J., 1847.** *Palaeontology of New York*, Volume 1. C. Van Benthuysen, Albany, 338 pp.
- Hall, J., 1852.** *Palaeontology of New York*, Volume 2. C. Van Benthuysen, Albany, 362 pp.
- Hammor, D., Bosch, D., Caby, R., Bruguier, O., 2006.** A two-stage exhumation of the Variscan crust: U–Pb LA-ICP-MS and Rb–Sr ages from Greater Kabylia, Maghrebides. *Terra Nova* **18** (5), 299–307.
- Han, Y., Pickerill, R.K., 1994.** *Phycodes templus* isp. nov. from the Lower Devonian of northwestern New Brunswick, eastern Canada. *Atlantic Geology*, **30**: 37–46.
- Hand, B.M., Ellison, J.B., 1985.** Inverse grading in density-current deposits. SEPM, 1985 Midyear Meeting, Abstracts with Programs. *SEPM, Golden, Colorado*, p. 39.
- Hanken, N.-M., Uchman, A., Nielsen, J.K., Olausen, S., Eggebø, T., Steinsland, R., 2016.** Late Ordovician trace fossils from offshore to shallow water mixed clastic and carbonate facies in the Ringerike area, Oslo Region, Norway. *Ichnos*, **23**: 189–221.

REFERENCES

- Häntzschel, W., 1962.** Trace fossils and problematica. In: Moore, R.C. (Ed.), Treatise on Invertebrate Paleontology, Part W, Miscellanea. *Geological Society of America/University of Kansas*, New York/Lawrence, pp. W177–W245.
- Häntzschel, W., 1975.** Trace fossils and problematica. In: Teichert, C. (Ed.), Treatise on Invertebrate Paleontology, Part W, Miscellanea Supplement 1. *Geological Society of America/University of Kansas Press*, Boulder/Lawrence, pp. W1–W269.
- Heer, O., 1865.** Die Urwelt der Schweiz. *Friedrich Schultze*, Zurich, 662 pp.
- Heer, O., 1877.** Flora Fossils Helvetiae: Die vorweltliche Flora der Schweiz. *J. Wurster & Comp.*, Zürich, 182 pp.
- Hendry, H.E., 1978.** Cap des Rosiers Formation at Grosses Roches, Quebec – deposits in the mid-fan region on an Ordovician submarine fan. *Canadian Journal of Earth Sciences*, **15**: 1472–1488.
- Hiscott, R.N., 1994.** Traction-carpet stratification in turbidites—fact or fiction? *Journal of Sedimentary Research*, **A64**: 204–208.
- Hiscott, R.N., Middleton, G.V., 1979.** Depositional mechanics of thick-bedded sandstones at the base of a submarine slope, Tourelle Formation (Lower Ordovician), Quebec, Canada. *SEPM Special Publication*, **27**: 307–326.
- Hoyez B., 1975.** Dispersion du matériel quartzueux dans les formations aquitaniennes de Tunisie septentrionale et d'Algérie nord-orientale. *Bull.Soc.géol.France*, (7), XVII, n°6, p.1147-1156.
- Hoyez, B., 1989.** *Le Numidien et les Flyschs oligo-miocènes de la bordure sud de la Méditerranée occidentale*. Ph.D. Thesis, Université Lille 1, France, 459 pp.
- Hubbard, S.M., Romans, B.W., Graham, S.A., 2008.** Deep-water foreland basin deposits of the Cerro Toro Formation, Magallanes basin, Chile: architectural elements of a sinuous basin axial channel belt. *Sedimentology*, **55**: 1333–1359.
- Huneke, H., Mulder, T., eds, 2010.** *Deep-sea sediments*. Developments in Sedimentology, **63**: 849 pp. Elsevier.
- Inglis, J.D., MacLean, J.S., Samson, S.D., D'Lemos, R.S., Admou, H., Hefferan, K., 2004.** A precise U–Pb zircon age for the Bleid granodiorite, Anti-Atlas, Morocco: implications for the timing of deformation and terrane assembly in the eastern Anti-Atlas. *Journal of African Earth Sciences* **39**, 277–283.

REFERENCES

- Ingram, R.L., 1954.** Terminology for the thickness of stratification and parting units in sedimentary rocks. A landmark paper from which of present terminology flows. *GSA Bulletin*, **65**: 937–938.
- Izumi, K., 2014.** Utility of geochemical analysis of trace fossils: case studies using *Phycosiphon incertum* from the Lower Jurassic shallow-marine (Higashinagano Formation, southwest Japan) and Pliocene deep-marine deposits (Shiramazu Formation, central Japan). *Ichnos*, **21**: 62–72.
- Jackson, A.M., Hasiotis, S.T., Flaig, P.P., 2016.** Ichnology of a paleopolar, river-dominated, shallow marine deltaic succession in the Mackellar Sea: The Mackellar Formation (Lower Permian), Central Transantarctic Mountains, Antarctica. *Palaeogeography, Palaeoclimatology, Palaeoecology*, **441**: 266–291.
- James, U.P., 1879.** Descriptions of new species of fossils and remarks on some others from the Lower and Upper Silurian rocks of Ohio. *The Paleontologist*, **3**: 17–24.
- Jenkins, R.J.F., 1995.** The problems and potential of using animal fossils and trace fossils in terminal Proterozoic biostratigraphy. *Precambrian Research*, **73**: 51–69.
- Jensen, S., 1997.** Trace fossils from the Lower Cambrian Mickwitzia sandstone, south-central Sweden. *Fossils and Strata*, **42**: 1–111.
- Johansson, M., Braakenberg, N.E., Stow, D.A.V., Faugères, J.C., 1998.** Deep-water massive sands: facies, processes and channel geometry in the Numidian Flysch, N Sicily. *Sedimentary Geology*, **115**: 233–266.
- Kaminski, M.A., Kuhnt, W., Radley, J.D., 1996.** Palaeocene-Eocene deep water agglutinated foraminifera from the Numidian Flysch (Rif, northern Morocco): their significance for the palaeoceanography of the Gibraltar gateway. *Journal of Micropalaeontology*, **15**: 1–19.
- Keighley, D.G., Pickerill, R.K., 1995.** The ichnotaxa *Palaeophycus* and *Planolites*: Historical perspectives and recommendations. *Ichnos*, **3**: 301–309.
- Keighley, D.G., Pickerill, R.K., 1994.** The ichnogenus *Beaconites* and its distinction from *Ancorichnus* and *Taenidium*. *Palaeontology*, **37**: 305–338.
- Kender, S., Kaminski, M. A., Cieszkowski, M., 2005.** Foraminifera from the Eocene variegated shales near Barwinek (Magura Unit, Outer Carpathians), the type locality of Noth (1912) revisited. *Annales Societatis Geologorum Poloniae*, **75**: 249–271.
- Kern, J.P., 1980.** Origin of trace fossils in Polish Carpathian flysch. *Lethaia*, **13**: 347–362.

REFERENCES

- Kim, J.-Y., Paik, I.S., 1997.** Nonmarine *Diplocraterion luniforme* (Blanckenhorn 1916) from the Hasandong Formation (Cretaceous) of the Jinju area, Korea. *Ichnos*, **5**: 131–138.
- Knaust, D., 2009.** Complex behavioural pattern as an aid to identify the producer of *Zoophycos* from the Middle Permian of Oman. *Lethaia*, **42**: 146–154.
- Knaust, D., 2015.** *Siphonichnidae* (new ichnofamily) attributed to the burrowing activity of bivalves: Ichnotaxonomy, behaviour and palaeoenvironmental implications. *Earth-Science Reviews*, **150**: 497–519.
- Knaust, D., 2017.** *Atlas of Trace Fossils in Well Core: Appearance, Taxonomy and Interpretation*. Springer, Cham, 271 pp.
- Kneller, B.C., Branney, M.J., 1995.** Sustained high-density turbidity currents and the deposition of thick massive sands. *Sedimentology*, **42**: 607–616.
- Kotake, N., 1991.** Non-selective surface deposit feeding by the *Zoophycos* producers. *Lethaia*, **24**: 379–385.
- Krobicki, M., Tyszka, J., Uchman, A., Bąk, M., 2006.** Stop A2 – Flaki Range (Fig. A12B) – Branisko Succession (Bajocian-Oxfordian). In: Wierzbowski, A., Aubrecht, R., Golonka, J., Gutowski, J., Krobicki, M., Matyja, B.A., Pieńkowski, G., Uchman, A. (Eds), *Jurassic of Poland and Adjacent Slovakian Carpathians, Field Trip Guide Book of 7th International Congress on the Jurassic System*, Poland, Kraków, September 6–18, 2006. *Polish Geological Institute, Warsaw*, pp. 29–34.
- Książkiewicz, M., 1968.** On some problematic organic traces from the Flysch of the Polish Carpathians. Part 3 (In Polish with English summary). *Annales Societatis Geologorum Poloniae*, **38**: 3–17.
- Książkiewicz, M., 1977.** Trace fossils in the Flysch of the Polish Carpathians. *Palaeontologia Polonica*, **36**: 1–208.
- Kuster, D., Liegeois, J.P., Matukov, D., Sergeev, S., Lucassen, F., 2008.** Zircon geochronology and Sr, Nd, Pb isotope geochemistry of granitoids from Bayuda Desert and Sabaloka (Sudan): evidence for a Bayudian event (920–900 Ma) preceding the Pan-African orogenic cycle (860–590 Ma) at the eastern boundary of the Saharan Metacraton. *Precambrian Research* 164 (1–2), 16–39.

REFERENCES

- La Manna, F., Grasso, M., Romeo, M., Maniscalco, R., Di Stefano, A., 1995.** Evoluzione tettonico-sedimentaria Neogenica del bordo Terrinico del Monti Nebrodi (Sicilia settentrionale). *Studi Geologici Camerti*, **2**: 293–305.
- Lahondère, J.C., Feibreg, H., Hag, B.V., 1979.** Datation des grès numidiens d'Algérie orientale: conséquences structurales. *Comptes Rendus de l'Académie des Sciences de Paris, Série D* **299**: 383–386.
- Late Alpine activity on North African cratonic margin. *American Journal of Science* **280**, 1051–1062.
- Lancelot, J., Reille, J.L., Broquet, P., Mattauer, M., 1976.** Datation U – Pb des zircons detritiques du flysch numidien d'Espagne et de Sicile; conséquences paleogeographiques (U–Pb dating of detrital zircons in the Numidian flysch of Spain and Sicily; paleogeographic consequences). *Reunion Annuelle des Sciences de la Terre* (**4**), *Société Géologique de France*.
- Lancelot, J., Reille, J.L., Wezel, F.C., 1977.** Etude morphologique et radiochronologique de zircons détritiques des flyschs “numidien” et “gréso-micacé”. *Bulletin De La Société Géologique De France* **7** (19), 773–780.
- Laval, F., 1992.** Gravity depositional systems and sedimentary megasequence of the Numidian Flysch Formation, North and East of the Grande Kabylie Massif (Algeria). *Geodinamica Acta* **5** (4), 217–233.
- Leaman, M., McIlroy, D., 2016.** Three-dimensional morphological permeability modelling of *Diplocraterion*. *Ichnos*, **24**: 51–63.
- Leprêtre R, Frizon de Lamotte D, Combier V, Gimeno-Vives O, Mohn G, Eschard R. 2018.** The Tell-Rif orogenic system (Morocco, Algeria, Tunisia) and the structural heritage of the southern Tethys margin, *BSGF - Earth Sciences Bulletin* 189: 10.
- Leszczyński, S., Uchman, A., Bromley, R.G., 1996.** Trace fossils indicating bottom aeration changes: Folsz Limestone, Oligocene, Outer Carpathians, Poland. *Palaeogeography, Palaeoclimatology, Palaeoecology*, **121**: 79–87.
- Lorenz von Liburnau, J.R., 1902.** Ergänzung zur Beschreibung der fossilen *Halimeda fuggeri*. *Sitzungsberichte der kaiserlich-königlichen Akademie der Wissenschaften, Mathematisch-Naturwissenschaftliche Klasse*, **111**: 685–712.

REFERENCES

- Lowe, D. R., 1982.** Sediment gravity flows: II. Depositional models with special reference to the deposits of high-density turbidity currents. *Journal of Sedimentary Petrology*, **52**: 279–297.
- Ludwig KR 2009.** SQUID 1.02, a user's manual. *Berkeley Geochronology Center, CA*, special publication no. 2
- Lukeneder, A., Uchman, A., Gaillard, C., Olivero, D., 2012.** The late Barremian *Halimedes* horizon of the Dolomites (Southern Alps, Italy). *Cretaceous Research*, **35**: 199–207.
- Lundgren, B., 1891.** Studierovverfossilforande Iosa block (in Swedish). *Geologiska Föreningen i Stockholm Förhandlingar*, **13**: 111–121.
- MacLeay, W.S., 1839.** Note on the Annelida. In: Murchison, R.I. (Ed.), *The Silurian System, Part II, Organic Remains*. *J. Murray*, London, pp. 699–701.
- Magné, J., Raymond, D., 1972.** Dans le Nord de la Grande Kabylie (Algérie), le Numidien a un âge compris entre l'Oligocène moyen et le Burdigalien inférieur. *Comptes Rendus de l'Académie des Sciences de Paris*, **274**: 3052–3055.
- Mángano, M.G., Buatois, L.A., 1991.** Discontinuity surfaces in the Lower Cretaceous of the High Andes (Mendoza, Argentina): trace fossils and environmental implications. *Journal of South American Earth Sciences*, **4**: 215–299.
- Mángano, M.G., Buatois, L.A., 2016.** The Cambrian Explosion. In: Mángano, M., Buatois, L. (Eds), *The Trace-Fossil Record of Major Evolutionary Events*. *Topics in Geobiology*, **1** **39**: 73–126.
- Mángano, M.G., Buatois, L.A., Maples, C.G. West, R.R., 2000.** A new ichnospecies of *Nereites* from Carboniferous tidal-flat facies of eastern Kansas, USA: implications for the *Nereites-Neonereites* debate. *Journal of Paleontology*, **74**: 149–157.
- Mángano, M.G., Carmona, N.B., Buatois, L.A., Guinea, F.M., 2005.** A new ichnospecies of *Arthropycus* from the Upper Cambrian-Lower Tremadocian of Northwest Argentina: Implications for the arthropycid lineage and potential in ichnostratigraphy. *Ichnos*, **12**: 179–190.
- Martin, A.J., Rindsberg, A.K., 2007.** Arthropod trace makers of *Nereites*? Neoichnological observations of juvenile limulids and their paleoichnological applications. In: Miller, W.M., III (Ed.), *Trace Fossils: Concepts, Problems, Prospects*. *Elsevier, Amsterdam*, pp. 478–491.

REFERENCES

- Massalongo, A., 1855.** *Zoophycos*, novum genus plantarum fossilium: monographia. *Antonelli, Verona*, 52 pp.
- Massalongo, A., 1856.** Studi Paleontologici. *Antonelli, Verona*, 53 pp.
- Mattauer, M., 1958.** Étude géologique de l'Ouarsenis oriental (Algérie). *Publications du Service de la carte géologique de l'Algérie* (nouvelle série), Bulletin, 17.
- McCann, T., Pickerill, R.K., 1988.** Flysch trace fossils from the Cretaceous Kodiak Formation of Alaska. *Journal of Paleontology*, **62**: 330–347.
- Melvin, J., 1986.** Upper Carboniferous fine-grained turbiditic sandstones from southwest England: a model for growth in an ancient, delta-fed subsea fan. *Journal of Sedimentary Petrology*, **56**: 19–34.
- Menzoul, B., Stow, D.A.V., Adaci, M., Benhamou, M., Mahdjoub Araibi, H., Bensalah, M., Benyoucef, M., 2019.** Deepwater sediment facies and sole marks of the Numidian Flysch, Algeria. In: Boughdiri, M., Bádenas, B., Selden, P., Jaillard, E., Bengtson, P., Granier, B. (Eds), *Paleobiodiversity and Tectono-Sedimentary Records in the Mediterranean Tethys and Related Eastern Areas. Advances in Science, Technology & Innovation (IEREK Interdisciplinary Series for Sustainable Development)*. *Springer, Cham*, pp. 241–243.
- Menzoul, B., Uchman, A., Adaci, M., & Bensalah, M., 2022.** Deep-sea trace fossils from the Numidian Formation (Upper Oligocene–Lower Miocene) in the Ouarsenis Mountains, northwestern Algeria. *Geological Quarterly*, **66**(2).
- Middleton, G.V., 1970.** Experimental studies related to problems of flysch sedimentation. *Geological Association of Canada Special Paper*, **7**: 253–272.
- Miller, M.F., 1991.** Morphology and paleoenvironmental distribution of Paleozoic *Spirophyton* and *Zoophycos*: implications for the *Zoophycos* ichnofacies. *Palaios*, **6**: 410–425.
- Monaco, P., 2011.** Morphologic variations of the trace fossil *Rutichnus* in cm-thick turbidites from the Verghereto Formation (Northern Apennines, Italy). *Rivista Italiana di Paleontologia e Stratigrafia*, **117**: 161–172.
- Monaco, P., Milighetti, M., Checconi, A., 2010.** Ichnocoenoses in the Oligocene to Miocene foredeep basins (Northern Apennines, central Italy) and their relation to turbidite deposition. *Acta Geologica Polonica*, **60**: 53–70.

REFERENCES

- Moretti, E., Coccioni, R., Guerrera, F., Lahondère, J.C., Loiacono, F., Puglisi, D., 1988.** Numidian Flysch of the Constantine Mountains (Tell-Orientale, Algeria). *AAPG Bulletin*, **72**: 1015.
- Moretti, E., Coccioni, R., Guerrera, F., Lahondère, J.C., Loiacono, F., Puglisi, D., 1991.** Numidian sequence between Guelma and Constantine (Eastern Tell, Algeria). *Terra Nova*, **3**: 153–165.
- Mutti, E., 1992.** Turbidite Sandstones. *AGIP, Istituto di Geologia, Universita di Parma, San Donato Milanese*, 275 pp.
- Mutti, E., Lucchi, F.R., 1975.** Turbidite facies and facies associations. In: Mutti, E. et al. (eds), Examples of Turbidite Facies and Facies Associations from Selected Formations of Northern Apennines. *International Association of Sedimentologists, IX International Congress*, Nice, Excursion Guidebook A-11, pp. 21–36.
- Myron, F.H.T., 2011.** *Sedimentology and Basin Context of the Numidian Flysch Formation; Sicily and Tunisia*. Ph.D. Thesis, University of Manchester, 278 pp.
- Narbonne, G.M., Aitken, J.D., 1990.** Ediacaran fossils from the Sekwi Brook and Mackenzie Mountains, Yukon, Canada. *Palaeontology*, **33**: 945–980.
- Neto de Carvalho, C., Baucon, A., 2010.** *Nereites* trails and other sandflat trace fossils from Portas de Almourão geomonument (Lower Ordovician, Naturtejo Geopark). *e-Terra*, **17**: 1–4.
- Nicholson, H.A., 1873.** Contributions of the study of the errant annelids of the older Paleozoic rock. *Proceeding of the Royal Society of London*, **21**: 288–290.
- Normark, W.R., 1978.** Fan valleys, channels, and depositional lobes on modern submarine fans: characters for recognition of sandy turbidite environments. *AAPG Bulletin*, **62**: 912–931.
- Ogniben, L., 1960.** Nota illustrativa dello schema geologico della Sicilia nord-orientale. *Riv. Min. Sic.*, n 64-65, p. 183-212.
- Ogniben, L., 1964.** Il Flysch Numidico nel quadro della geologia della Sicilia. *Memorie della Societa Geologica Italiana* **4**, 1–18.
- Olivero, D., Gaillard, C., 2007.** A constructional model for *Zoophycos*. In: Miller, W. III (Ed.) Trace Fossils: Concepts, Problems, Prospects. *Elsevier, Amsterdam*, pp. 466–477.
- Owen, G., 1996.** Experimental soft-sediment deformation: structures formed by the liquefaction of unconsolidated sands and some ancient examples. *Sedimentology*, **43**: 279–293.

REFERENCES

- Owen, G., Moretti, M., 2008. Determining the origin of soft-sediment deformation structures: a case study from Upper Carboniferous delta deposits in south-west Wales, UK. *Terra Nova*, **20**: 237–245.
- Palmer, T.J., 1978. Burrows at certain omission surfaces on the Middle Ordovician of the Upper Mississippi Valley. *Journal of Paleontology*, **52**: 109–117.
- Parize, O., Beaudoin, B., Burollet, P.F., Cojan, G.F., Pinault, M., 1986. La provenance du materiel gréseux numidien est septentrionale (Sicile et Tunisie). *Comptes Rendus de l'Academie des Sciences de Paris* 288, 1671–1674.
- Parize, O., Beaudoin, B., Fries, G., 1999. Deep-water massive sands: facies, processes and channel geometry in the Numidian Flysch, Sicily—comment. *Sedimentary Geology* **127**, 111–118.
- Patacca, E., Scandone, P., Bellatalla, M., Perilli, N., Santini, U., 1992. The Numidian-sand event in the Southern Apennines. *Memorie di Scienze Geologiche*, **43**: 297–337.
- Pautot, G., Truillet, R., Hoffert, M., 1975. *Tubotomaculum* et nodules de manganèse. Comparaison d'objets énigmatiques fossiles avec des concrétions marines et lacustres. *Bulletin de la Société Géologique de France*, Série 7, 17: 25–37.
- Pemberton, S.G., Frey, R.W., 1982. Trace fossil nomenclature and the *Planolites-Palaeophycus* dilemma. *Journal of Paleontology*, **56**: 843–881.
- Pemberton, S.G., MacEachern, J.A., Dashtgard, S.E., Bann, K.L., Gingras, M.K., Zonneveld, J.-P., 2012. Shorefaces. *Developments in Sedimentology*, **64**: 563–604.
- Pemberton, S.G., Spila, M., Pulham, A.J., Saunders, T., MacEachern, J.A., Robbins, D., Sinclair, I.K., 2001. Ichnology and sedimentology of shallow to marginal marine systems: Ben Nevis & Avalon Reservoirs, Jeanne d'Arc Basin. *Geological Association of Canada*, Short Course Notes **15**: 343 pp.
- Peucat, J.J., Mahdjoub, Y., Drareni, A., 1996. U–Pb and Rb–Sr geochronological evidence for late Hercynian tectonic and Alpine overthrusting in Kabylean metamorphic basement massifs (northeastern Algeria). *Tectonophysics* **258** (1–4), 195–213.
- Peucat, J.J., Drareni, A., Latouche, L., Deloule, E., Vidal, P., 2003. U–Pb zircon (TIMS and SIMS) and Sm–Nd whole-rock geochronology of the Gour Oumelalen granulitic basement, Hoggar massif, Tuareg shield, Algeria. *Journal of African Earth Sciences* **37** (3–4), 229–239.

REFERENCES

- Peucat, J.J., Capdevila, R., Drareni, A., Mahdjoub, Y., Kahoui, M., 2005.** The Eglab massif in the West African Craton (Algeria), an original segment of the Eburnean orogenic belt: petrology, geochemistry and geochronology. *Precambrian Research* **136** (3–4), 309–352.
- Peruzzi, D. G., 1880.** Osservazioni sui generi *Paleodictyon* e *Paleomeandron* dei terreni cretacei ed eocenici dell'Appennino sett. e centrale. *Atti della Società Toscana di Scienze Naturali Residente in Pisa*, Memorie **5**: 3–8.
- Phillips, C., McIlroy, D., Elliott, T., 2011.** Ichnological characterization of Eocene/Oligocene turbidites from the Grès d'Annot Basin, French Alps, SE France. *Palaeogeography, Palaeoclimatology, Palaeoecology*, **300**: 67–83.
- Pickering, K.T., Hiscott, R.N., 1995.** Foreland basin-floor turbidite system, Cloridorme Formation, Québec, Canada: long-distance correlation in sheet turbidites. In: Pickering, K.T., Hiscott, R.N., Kenyon, N.H., Ricci Lucchi, F., Smith, R.D.A. (Eds), Atlas of Deep Water Environments. *Springer, Dordrecht*, pp. 310–316.
- Pickering, K.T., Hiscott, R.N., 2015.** *Deep Marine Systems: Processes, Deposits, Environments, Tectonics and Sedimentation*. John Wiley & Sons, Chichester, 672 pp.
- Pickering, K.T., Stow, D.A.V., Watson, M.P., Hiscott, R.N., 1986.** Deep water facies, processes and models: a review and classification scheme for modern and ancient sediments. *Earth-Sciences Reviews*, **23**: 75–174.
- Pinter, P. R., Butler, R. W., Hartley, A. J., Maniscalco, R., Baldassini, N., Di Stefano, A., 2018.** Tracking sand-fairways through a deformed turbidite system: The numidian (Miocene) of Central Sicily, Italy. *Basin Research*, **30**: 480–501.
- Paquette, J.L., Caby, R., Djouadi, M.T., Bouchez, J.L., 1997.** U–Pb dating of the end of the Pan-African orogeny in the Tuareg shield: the post-collisional syn-shear Tioueine pluton (Western Hoggar, Algeria), Symposium 55 on Post-Collisional Magmatism. *Strasbourg, France*, pp. 245–253.
- Plaziat, J.-C., Mahmoudi, M., 1988.** Trace fossils attributed to burrowing echinoids: A revision including new ichnogenus and ichnospecies. *Geobios*, **21**: 209–233.
- Plička, M., Uhrová, J., 1990.** New trace fossils from the Outer Carpathian flysch (Czechoslovakia). *Acta Musei Moraviae, Scientiae Naturales*, **75**: 53–59.

REFERENCES

- Pokorný, R., Krmíček, R., Sudo, M., 2017.** An endemic ichnoassemblage from a late Miocene paleolake in SE Iceland. *Palaeogeography, Palaeoclimatology, Palaeoecology*, **485**: 761–773.
- Pollard, J.E., 1988.** Trace fossils in coal-bearing sequences. *Journal of the Geological Society*, **145**: 339–350.
- Polvêche, J., 1960.** Contribution à l'étude géologique de l'Ouarsenis oranais. *Publications du Service de la carte géologique de l'Algérie* (nouvelle série), Bulletin **24**: 577 pp.
- Quatrefages, M.D., 1849.** Note sur la *Scolicia prisca* (A. de Q.), annélide fossile de la craie. *Annales des Sciences Naturelles*, **3**: 265–266.
- Raoult, J.F., 1974.** Géologie du centre de la chaîne numidique (Nord du Constantinois, Algérie). *Mémoires de la Société Géologique de France*, **111 (121)**: 163 pp.
- Raymond, D., 1976.** *Evolution sédimentaire et tectoniques du Nord-Ouest de la Grande Kabylie (Algérie) au cours du cycle alpin*. Thèse d'État, Sciences naturelles, Paris, 152 pp.
- Riahi, S., Patel, U., Soussi, M., Stow, D.A.V., Croudace, I., Fildes, C., Ben Ismaïl Lattrache, K., Boukhalfa, K., 2009.** The onshore Tunisia Numidian Flysch: Petrography, geochemistry and reservoir characteristics. In: *4th North African/Mediterranean Petroleum and Geosciences Conference & Exhibition* Tunis, Tunisia, 2–4 March 2009, *Conference Proceedings*. EAGE Tunisia, Tunis, 6 pp.
- Riahi, S., Soussi, M., Kamel, B., Kmar, B. I. L., Stow, D., Sami, K., Mourad, B., 2010.** Stratigraphy, sedimentology and structure of the Numidian Flysch thrust belt in northern Tunisia. *Journal of African Earth Sciences*, **57**: 109–126.
- Riahi, S., Soussi, M., Lattrache, K. B. I., 2015.** Age, internal stratigraphic architecture and structural style of the Oligocene–Miocene Numidian Formation of northern Tunisia. *Annales Societatis Geologorum Poloniae*, **85**: 345–370.
- Riahi, S., Soussi, M., Stow, D., 2021.** Sedimentological and stratigraphic constraints on Oligo–Miocene deposition in the Mogod Mountains, northern Tunisia: new insights for paleogeographic evolution of North Africa passive margin. *International Journal of Earth Sciences*, **110**: 653–688.
- Riahi, S., Uchman, A., Stow, D.A.V., Soussi, M., Ben Ismail-Lattrache, K., 2014.** Deep-sea trace fossils of the Oligocene–Miocene Numidian Formation, northern Tunisia. *Palaeogeography, Palaeoclimatology, Palaeoecology*, **414**: 155–177.

REFERENCES

- Richter, R., 1850.** Aus der thüringischen Grauwacke. *Zeitschrift der Deutschen Geologischen Gesellschaft*, **2**: 198–206.
- Richter, R., 1937.** Marken und Spuren aus allen Zeiten. I–II. *Senckenbergiana*, **19**: 150–163.
- Rippon, J.H., Spears, D.A., 1989.** The sedimentology and geochemistry of the sub-Clowne cycle (Westphalian B) of north-east Derbyshire, U.K. *Proceedings of the Yorkshire Geological Society*, **47**: 181–198.
- Rodríguez-Tovar, F.J., Miguez-Salas, O., Dorador, J., Duarte, L.V., 2019.** Opportunistic behaviour after the Toarcian Oceanic Anoxic Event: The trace fossil *Halimedides*. *Palaeogeography, Palaeoclimatology, Palaeoecology*, **520**: 240–250.
- Rodríguez-Tovar, F.J., Piñuela, L., García-Ramos, J.C., 2016.** Trace fossils assemblages from the Cenozoic “Flysch Units” of the Campo de Gibraltar Complex (southern Spain). *Ichnos*, **23**: 53–70.
- Rodríguez-Tovar, F.J., Uchman, A., 2004a.** Trace fossils after the K-T boundary event from the Agost section, SE Spain. *Geological Magazine*, **141**: 429–440.
- Rodríguez-Tovar, F.J., Uchman, A., 2004b.** Ichnotaxonomic analysis of the Cretaceous/Palaeogene boundary interval in the Agost section, south-east Spain. *Cretaceous Research*, **25**: 635–647.
- Rona, P.A., Merrill, G.F., 1978.** A benthic invertebrate from the Mid–Atlantic Ridge. *Bulletin of Marine Sciences*, **28**: 371–375.
- Rouvier, H., 1977.** *Géologie de l'Extrême Nord Tunisien: tectoniques et paléogéographies superposées à l'extrémité orientale de la chaîne nord maghrébine*. Ph.D. Thesis, Université Pierre et Marie Curie, Paris VI, 703 pp.
- Sacco, F., 1886.** Impronte organiche dei terreni terziari del Piemonte. *Atti della Reale Accademie delle Scienze di Torino*, **21**: 297–348.
- Savi, P., Meneghini, G., 1850.** Osservazioni stratigraphiche e paleontologiche concerneti la geologia della Toscana e dei paessi limitrofi. Appendix in R.I Murchison, Memoria sulla Struttura Geologica delle Alpi, degli Apennini e dei Carpazi. *Stamperia Grandiducale, Firenze*, 249 pp.
- Savrda, C.E., Krawinkel, H., McCarthy, F.M.G., McHugh, C.M.G., Olson, H.C., Mountain, G., 2001.** Ichnofabrics of a Pleistocene slope succession, New Jersey margin: relations to

REFERENCES

- climate and sea-level dynamics. *Palaeogeography, Palaeoclimatology, Palaeoecology*, **171**: 41–61.
- Schäfer W., 1956.** Wirkungen der Benthos-Organismen auf den jungen Schichtverband. *Senckenb Lethaia* **37**:183–263.
- Schlirf, M., 2000.** Upper Jurassic trace fossils from the Boulonnais (northern France). *Geologica et Palaeontologica*, **34**: 145–213.
- Seilacher, A., 1977.** Pattern analysis of *Paleodictyon* and related trace fossils. In: Crimes, T.P., Harper, J.C. (Eds), Trace fossils 2. *Geological Journal Special Issue*, **9**: 289–334.
- Seilacher, A., 1990.** Paleozoic trace fossils. In: Said, R. (Ed.), *The Geology of Egypt*. A.A. Balkema, Rotterdam, pp. 649–670.
- Seilacher, A., 2007.** Trace Fossil Analysis. Springer, Berlin, 226 pp.
- Seilacher, A., Seilacher-Drexler, E., 1994.** Bivalvian trace fossils: A lesson from actuopaleontology. *Courier Forschungsinstitut Senckenberg*, **169**: 5–15.
- Smith, J.J., Hasiotis, S.T., 2008.** Traces and burrowing behaviors of the cicada nymph *Cicadetta calliope*: Neoichnology and paleoecological significance of extant soil-dwelling insects. *Palaios*, **23**: 503–513.
- Smith, J.J., Hasiotis, S.T., Kraus, M.J., Woody, D.T., 2008.** *Naktodemasis bowni*: new ichnogenus and ichnospecies for adhesive meniscate burrows (AMB), and paleoenvironmental implications, Paleogene Willwood Formation, Bighorn Basin, Wyoming. *Journal of Paleontology*, **82**: 267–278.
- Stacey, J.S., Kramers, J.D., 1975.** Approximation of terrestrial lead evolution by a two stage model. *Earth and Planetary Science Letters* **26**, 207–221.
- Stanistreet, I.G., Le Blanc Smith, G., Cadle, A.B., 1980.** Trace fossils as sedimentological and palaeoenvironmental indices in the Ecca Group (Lower Permian) of the Transvaal. *Transactions of the Geological Society of South Africa*, **83**: 333–344.
- Sternberg, G.K. von., 1833.** Versuch einer geognostisch – botanischen Darstellung der Flora der Vorwelt. IV Heft. C.E. Brenek, Regensburg, 48 pp.
- Stow, D.A.V., Johannson, M., 2000.** Deep-water massive sands: nature, origin and hydrocarbon implications. *Marine and Petroleum Geology*, **17**: 145–174.
- Stow, D.A.V., Piper, D.J.W. (Eds), 1984.** *Fine-Grained Sediments: Deep-Water Processes and Facies*. Geological Society, Oxford, Mass., 659 pp.

REFERENCES

- Stow, D.A.V., Reading, H.G., Collinson, J.D., 1996.** *Deep seas. In: Reading, H.G. (Ed.), Sedimentary Environments: Processes, Facies and Stratigraphy*, 3rd Edition. Wiley-Blackwell, Cambridge, pp. 395–453.
- Stow, D.A.V., Shanmugam, G., 1980.** Sequences of structures in fine-grained turbidites: comparison of recent deep-sea and ancient flysch sediments. *Sedimentary Geology*, **25**: 23–42.
- Stow, D.A.V., Tarrez, A., 1998.** Hemipelagites: facies, processes and models. *Geological Society Special Publications*, **129**: 317–338.
- Suayah, I.B., Miller, J.S., Miller, B.V., Bayer, T.M., Rogers, J.J.W., 2006.** Tectonic significance of Late Neoproterozoic granites from the Tibesti massif in southern Libya inferred from Sr and Nd isotopes and U–Pb zircon data. *Journal of African Earth Sciences* **44** (4–5), 561–570.
- Swinbanks, D. D., Murray, J.W., 1981.** Biosedimentological zonation of boundary Bay tidal flats, Fraser River Delta, British Columbia. *Sedimentology*, **28**: 201–237.
- Swinbanks, D., Luternauer, J., 1987.** Burrow distribution of thalassinidean shrimp on a Fraser Delta tidal flat, British Columbia. *Journal of Paleontology*, **61**: 315–332.
- Talling, P.J., Masson, D.G., Sumner, E.J., Malgesini, G., 2012.** Subaqueous sediment density flows: Depositional processes and deposit types. *Sedimentology*, **59**: 1937–2003.
- Tchoumatchenco, P., Uchman, A., 2001.** The oldest deep-sea *Ophiomorpha* and *Scolicia* and associated trace fossils from the Upper Jurassic-Lower Cretaceous deep-water turbidite deposit of SW Bulgaria. *Palaeogeography, Palaeoclimatology, Palaeoecology*, **169**: 85–99.
- Thomas, M.F.H., Bodin, S., Redfern, J., 2010a.** Comment on: “European provenance of the Numidian Flysch in northern Tunisia” (Fildes et al., 2010). *Terra Nova* **22**, 501–503.
- Thomas, M.F.H., Bodin, S., Redfern, J., Irving, D.H.B., 2010b.** A constrained Africa-craton source for Cenozoic Numidian Flysch: implications for the paleogeography of the western Mediterranean basin. *Earth-Science Reviews* **101**, 1–23.
- Torell, O., 1870.** Petrificata suecana formationis cambricae. *Lunds Universitet, Årsskrift*, **6**: 1–14.
- Trewin, N.H., Thirlwall, M.F., 2002.** Old Red Sandstone. In: Trewin, N.H. (Ed.), *The Geology of Scotland*, 4th Edition. *Geological Society*, London, pp. 213–249.

REFERENCES

- Tucker, M.E., 2003.** *Sedimentary Rocks in the Field*, 3rd Edition. John Wiley & Son, New York, 234 pp.
- Uchman, A., 1995.** Taxonomy and palaeoecology of flysch trace fossils: the Marnoso arenacea Formation and associated facies (Miocene, Northern Apennines, Italy). *Beringeria*, **15**: 3–115.
- Uchman, A., 1998.** Taxonomy and ethology of flysch trace fossils: a revision of the Marian Książkiewicz collection and studies of complementary material. *Annales Societatis Geologorum Poloniae*, **68**: 105–218.
- Uchman, A., 1999.** Ichnology of the Rhenodanubian Flysch (Lower Cretaceous–Eocene) in Austria and Germany. *Beringeria*, **25**: 65–171.
- Uchman, A., 2001.** Eocene flysch trace fossils from the Hecho Group of the Pyrenees, northern Spain. *Beringeria*, **28**: 3–41.
- Uchman, A., 2003.** Trends in diversity, frequency and complexity of graphoglyptid trace fossils: evolutionary and palaeoenvironmental aspects. *Palaeogeography, Palaeoclimatology, Palaeoecology*, **192**: 123–142.
- Uchman, A., 2004.** Phanerozoic history of deep-sea trace fossils. *Geological Society Special Publication*, **228**: 125–139.
- Uchman, A., 2007.** Deep-sea trace fossils from the mixed carbonate-siliciclastic flysch of the Monte Antola Formation (Late Campanian-Maastrichtian), North Apennines, Italy. *Cretaceous Research*, **28**: 980–1004.
- Uchman, A., 2009.** The *Ophiomorpha rudis* ichnosubfacies of the *Nereites* ichnofacies: characteristics and constraints. *Palaeogeography, Palaeoclimatology, Palaeoecology*, **276**: 107–119.
- Uchman, A., Gaździcki, A., 2006.** New trace fossils from the La Meseta Formation (Eocene) of Seymour Island, Antarctica. *Polish Polar Research*, **27**: 153–170.
- Uchman, A., Kazakauskas, V., Gaigalas, A., 2009.** Trace fossils from Late Pleistocene lacustrine varve sediments in eastern Lithuania. *Palaeogeography, Palaeoclimatology, Palaeoecology* **272**: 199–211.
- Uchman, A., Mikuláš, R., Rindsberg, A.K., 2011.** Mollusc trace fossils *Ptychoplasma* Fenton and Fenton, 1937 and *Oravaichnium* Plička and Uhrová, 1990: Their type material and ichnospecies. *Geobios*, **44**: 387–397.

REFERENCES

- Uchman, A., Tchoumatchenco, P., 2003.** A mixed assemblage of deep-sea and shelf trace fossils from the Lower Cretaceous (Valanginian) Kamchia Formation in the Troyan region, central Fore-Balkan, Bulgaria. *Annales Societatis Geologorum Poloniae*, **73**: 27–34.
- Uchman, A., Wetzel, A., 2012.** Deep-sea fans. *Developments in Sedimentology*, **64**: 643–671.
- Uchman, A., Wetzel, A., 2017.** Hidden subsurface garden on own faeces – the trace fossil *Tubulichnium rectum* (Fischer-Ooster, 1858) from the Cretaceous-Palaeogene deep-sea sediments. *Palaeontologia Electronica*, **20.2.40A**: 1–18, palaeo-electronica.org/content/2017/1968-tubulichnium-deep-sea-trace.
- Van Houten, F.B., 1980.** Mid-Cenozoic Fortuna formation, northeastern Tunisia—record of Late Alpine activity on North African cratonic margin. *American Journal of Science* **280**, 1051–1062.
- Vermeesch, P. 2018.** IsoplotR: a free and open toolbox for geochronology. *Geoscience Frontiers* **9**, 1479–1493.
- Vialov, O.S., Golev, B.T., 1960.** A contribution to the taxonomy of *Paleodictyon*. *Doklady Akademii Nauk SSSR*, **134**: 175–178. [In Russian.]
- Vila, J.M., 1980.** *La chaîne alpine d'Algérie orientale et des confins algéro-tunisiens*. Ph.D. Thesis, Université Pierre et Marie Curie, Paris VI Paris, 663 pp.
- Vila, J.M., 1994.** Mise en point des données nouvelles sur les terrains Triasiques des confins Algéro-Tunisiens: Trias Allochtone glacier de sel sous-marin et vrai diapirs. *Mémoires du Service Géologique de l'Algérie*, **5**: 105–152.
- Walsh, G.J., Aleinikoff, J.N., Benziane, F., Yazidi, A., Armstrong, T.R., 2002.** U–Pb zircon geochronology of the Paleoproterozoic Tagragra de Tata inlier and its Neoproterozoic cover, western Anti-Atlas, Morocco. *Precambrian Research* **117** (1–2), 1–20.
- Walker, R.G., 1978.** Deep water sandstone facies and ancient submarine fans: models for exploration for stratigraphic traps. *AAPG Bulletin*, **62**: 932–966.
- Webby, B.D., 1984.** Precambrian-Cambrian trace fossils from western New South Wales. *Australian Journal of Earth Sciences*, **31**: 427–437.
- Weiss, W., 1941.** Entstehung der “Zöpfe” im Schwarzen und Braunen Jura. *Natur und Volk*, **71**: 179–184.

REFERENCES

- Wetzel, A., & Uchman, A., 2001.** Sequential colonization of muddy turbidites in the Eocene Beloveža Formation, Carpathians, Poland. *Palaeogeography, Palaeoclimatology, Palaeoecology*, 168(1-2), 171-186.
- Wetzel, A., 1981.** Ökologische und stratigraphische Bedeutung biogener Gefüge in quartären Sedimenten am NW-afrikanischen Kontinentalrand. *“Meteor” Forschungs-Ergebnisse*, C34: 1–47.
- Wetzel, A., 1983a.** Biogenic structures in modern slope to deep-sea sediments in the Sulu Sea Basin (Philippines). *Palaeogeography, Palaeoclimatology, Palaeoecology*, 42: 285–304.
- Wetzel, A., 1983b.** Biogenic sedimentary structures in a modern upwelling region: northwest African continental margin. In: Thiede, J., Suess, E. (Eds), Coastal Upwelling and its Sediments. Record of Ancient Coastal Upwelling. *Plenum Press*, New York, pp. 123–144.
- Wetzel, A., 2002.** Modern *Nereites* in the South China Sea – ecological association with redox conditions in the sediment. *Palaios*, 17: 507–515.
- Wetzel, A., 2008.** Recent bioturbation in the deep South China Sea: a uniformitarian ichnologic approach. *Palaios*, 23: 601–615.
- Wetzel, A., 2010.** Deep-sea ichnology: observations in modern sediments to interpret fossil counterparts. *Acta Geologica Polonica*, 60: 125–138.
- Wetzel, A., Blechschmidt, I., Uchman, A., Matter, A., 2007.** A highly diverse ichnofauna in Late Triassic deep-sea fan deposits of Oman. *Palaios*, 22: 567–576.
- Wetzel, A., Bromley, R.G., 1996.** Re-evaluation of ichnogenus *Helminthopsis* – a new look at the type material. *Palaeontology*, 39: 1–19.
- Wetzel, A., Uchman, A., 1998.** Deep-sea benthic food content recorded by ichnofabrics; a conceptual model based on observations from Paleogene flysch, Carpathians, Poland. *Palaios*, 13: 533–546.
- Wetzel, A., Werner, F., 1981.** Morphology and ecological significance of *Zoophycos* in deep-sea sediments of NW Africa. *Palaeogeography, Palaeoclimatology, Palaeoecology*, 32: 185–212.
- Wezel, F.C., 1969.** Lineamenti Sedimentologico Del Flysch Numidico Della Sicilia Nord-Orientale. *Memorie Degli Istituti Di Geologia e Mineralogia Del L'Universita Di Padova* 26, 1–32.

REFERENCES

- Wezel, F.C., 1970. Geologia del Flysch Numidico della Sicilia Nord-Orientale. *Memorie della Società Geologica Italiana* 9, 225–280.
- Wezel, F.C., 1968. Osservazioni sui sedimenti dell'Oligocene-Miocene della Tunisia Settentrionale. *Memorie della Società Geologica Italiana*, 7: 417–439.
- Wiedenbeck, M., Hanchar, J.M., Peck, W.H., Sylvester, P., Valley, J., Whitehouse, M., Kronz, A., Morishita, Y., Nasdala, L., Fiebig, J., Franchi, I., Girard, J.P., Greenwood, R.C., Hinton, R., Kita, N., Mason, P.R.D., Norman, M., Ogasawara, M., Piccoli, P.M., Rhede, D., Satoh, H., Schulz-Dobrick, B., Skår, Ø., Spicuzza, M.J., Terada, K., Tindle, A., Togashi, S., Vennemann, T., Xie, Q., Zheng, Y.F., 2004. Further characterisation of the 91500 zircon crystal. *Geostandards and Geoanalytical Research* 28, 9–39.
- Wignall, P.B., 1991. Dysaerobic trace fossils and ichnofabrics in the Upper Jurassic Kimmeridge Clay of southern England. *Palaios*, 6: 264–270.
- Wignall, P.B., Hallam, A., 1991. Biofacies, stratigraphic distribution and depositional models of British onshore Jurassic black shales. *Geological Society Special Publications*, 58: 291–309.
- Williams, I. S. 1998. U-Th-Pb Geochronology by Ion Microprobe. In: McKibben, M. A., Shanks III, W. C., Ridley, W. I. (Eds.), Applications of microanalytical techniques to understanding mineralizing processes. *Reviews in Economic Geology* 7. 1-35.
- Wildi, W., 1983. La chaîne tello-rifaine (Algérie, Maroc, Tunisie): structure, stratigraphie et évolution du Trias au Miocène. *Revue de Géographie Physique et de Géologie Dynamique*, 24: 201–297.
- Yaich, C., Hooyberghs, H. J. F., Durllet, C., & Renard, M., 2000. Stratigraphic correlation between the Numidian formation (North Tunisia) and Oligo-Miocene deposits of central Tunisia. *Comptes Rendus De L Academie Des Sciences Serie Ii Fascicule A Sciences De La Terre Et Des Planetes*, 331(7), 499-506.
- Yaich, C., 1992b. Sedimentologie, tectonique (et variations relatives du niveau marin) dans les formations du Miocène inferieur a moyen, Tunisie centrale et orientale. *Géologie Méditerranéenne* 19 (4), 249–264.
- Yaïch, C., Hooyberghs, H.J.F., Durllet, C., Renard, M., 2000. Corrélation stratigraphique entre

REFERENCES

les unités oligomiocènes de Tunisie centrale et le Numidien. *Comptes Rendus de l'Académie des Sciences de Paris* **331**, 499–506.